UNIVERSITY OF SOUTHAMPTON

The Synthesis and Application of Novel Resins and Solid Supported Reagents

by

Sunil Rana

Doctor of Philosophy

Department of Chemistry
Faculty of Science

January 2001

UNIVERSITY OF SOUTHAMPTON

ABSTRACT

FACULTY OF SCIENCE

CHEMISTRY

Doctor of Philosophy

THE SYNTHESIS AND APPLICATION OF NOVEL RESINS AND SOLID SUPPORTED REAGENTS

By Sunil Rana

The aims of this project were to synthesize new PS-based resins and investigate their properties with respect to cross-linking by application to organic and peptide chemistry, and also to investigate the synthesis of novel resin-bound reagents.

A range of PS-DVB resins was synthesized by suspension polymerization and yields of reaction and swelling properties measured as a function of cross-linking. The first synthesis of the natural product Kawaguchipeptin B was performed on each resin and the relationship between purity and cross-linking investigated. The Suzuki reaction was performed and the rate of formation of a biaryl compound on the resins then investigated. The kinetics of cleavage of a dye under acidic conditions, from each resin was investigated as a function of cross-linking.

The synthesis of a paramagnetic resin by novel suspension polymerisation methods was demonstrated and the resin applied to the field of reaction scavenging.

The synthesis of a novel PS-DVB-imidazole and PS-DVB-isocyanate resin was carried out and their utilities in reaction catalysis and scavenging investigated.

Table of Contents

ACKNOWLEDGEMENTS

I would like to thank my supervisors; Mark for unrivalled enthusiasm and direction and also Peter at NovaBiochem, who has also helped guide this project from its earliest days.

I would like to thank the Bradley Group (both past and present) who have helped make the time so enjoyable and also the departmental staff (Julia, Jill, Sue and Sally), without whom nothing would ever get done. Special thanks to Vin, Neil, Helen, Pat, Butrus and Matt who have all had to endure tedious questioning and also thanks to Jed, for, well – just being Jed.

Many thanks to the new crowd, including David (Sir) Orain (now I AM your colleague), Juergen (who let him out) Kress, and the get rich quick crew: Dave, Iain and James. Thanks also to John, Stifun, Saraj and again Neil, for proof reading; the most universally-unrecognised-most-important-part-of-thesis-writing.

Many thanks to the embryonic crowd, the CCE group members especially Max, Rob Brendan and Marco, who had all unwittingly loaned me equipment and chemicals for the final few weeks.

Thanks to the analytical section: John and Julie for mass spectrometry and Joan and Neil for extensive NMR work and run-time. Thanks also to the Turner group including David and Julien.

I would also like to thank my wife Liz for continued support and proof-reading over the last couple of months, and who has taught me that it can actually be more productive not to put off until tomorrow, what can successfully be achieved today (I'm still learning that one).

Finally, a special note to my family: I will eventually get around to explaining what this project was all about in the first place (and why I wasn't at home for 3½ years).

ABBREVIATIONS

^{13}C	Carbon-13
^{1}H	Proton
aq.	Aqueous
Boc	Tertiary-Butyloxycarbonyl
CD_3OD	Methanol-δ
$CDCl_3$	Chloroform-δ
CMS	Chloromethyl styrene
d	doublet
DCE	1,2 Dichloroethane
DCM	Dichloromethane
DIC	*N,N'*-Diisopropylcarbodiimide
DMF	*N, N'*-Dimethylformamide
DVB	Divinyl Benzene
EA	Ethyl acetate
ES-MS	Electrospray Mass Spectrometry
Et_2O	Diethyl Ether
EtOAc	Ethyl Acetate
EtOH	Ethanol
Fmoc	9-Fluorenylmethyloxycarbonyl
FT-IR	Fourier Transform Infra-Red
HOBt	1-Hydroxybenzotriazole
HRMS	High Resolution Mass Spectrometry
Hz	Hertz
IR	Infra-Red
J	Coupling Constant
m	multiplet
MeCN	Acetonitrile
MeOH	Methanol
$MgSO_4$	Magnesium Sulfate (anhydrous)
mp	Melting Point

MS	Mass Spectrometry
MW	Molecular Weight
NMR	Nuclear Magnetic Resonance
PEG	Poly (Ethylene) Glycol
Pmc	2,2,5,7,8-Pentamethylchroman-6-sulfonyl
PS	Polystyrene
PVA	Poly Vinyl Alcohol
q	quartet
Rink	Rink linker (4-[(R,S)-α-[1-(9H-fluoren-9-yl)-methoxyformido]-2,4-dimethoxybenzyl]-phenoxyacetic acid
RP-HPLC	Reverse-Phase High Performance Liquid Chromatography
RT	Room Temperature
S	Singlet
SPOC	Solid Phase Organic Chemistry
SPOS	Solid Phase Organic Synthesis
SPPS	Solid Phase Peptide Synthesis
^{t}Bu	tertiary butyl
tert-	tertiary-
THF	Tetrahydrofuran
TFA	Trifluoroacetic acid
TLC	Thin Layer Chromatography
UV	Ultra Violet

Standard 3 letter abbreviations for amino acids

All amino acids are configured L unless specifically stated

Poly(styrene-co-DVB)

CHAPTER 1 – SOLID PHASE ORGANIC CHEMISTRY – AN OVERVIEW

1.1 INTRODUCTION

Solid phases have become increasingly important tools in solid phase chemistry.[1] Polymers are having greater impact in the chemistry of today, from the macroporous ion exchange resins used in purification,[2,3,4,5] to the chemically functionalised gel beads used in solid phase organic synthesis[6] and catalysis.[7]

Solid phase organic chemistry (SPOC) has its origins in processes that were discovered over 150 years ago. The first laboratory polymerizations of styrene were performed by Simon[8] in 1839, whilst arguably the first reported example of chemical modification to a polymer was carried out in 1838 with the nitration of cellulose.[9] One of the earliest known examples of a polymer-supported catalyst was reported in the literature by Sarkenstein[10] in 1910, who adsorbed the enzyme amylase onto insoluble starch.

The first co-polymerization of styrene and divinylbenzene was carried out by Staudinger[11] in 1934, proving that the divinylbenzene monomer made the resulting polystyrene insoluble in all solvents.[12] Resins in various forms are now used by large numbers of chemists in organic synthesis, but the most widespread use of resins has been in the area of ion exchange chromatography.

Ion exchange resins were introduced in 1945 after the realization by Adams and Holmes[13] in 1935 that polar groups could be introduced into these polymers. An ion exchange resin allows the replacement of a specific ion, usually contained in the solvent/ elutant, with an ion that is polymer bound. Applications for this technology are numerous, especially in purification, and today this forms the basis for a multi-million pound industry. The two main types of these are the cation **(1)** and anion **(2)** exchange resins shown in figure 1.1.

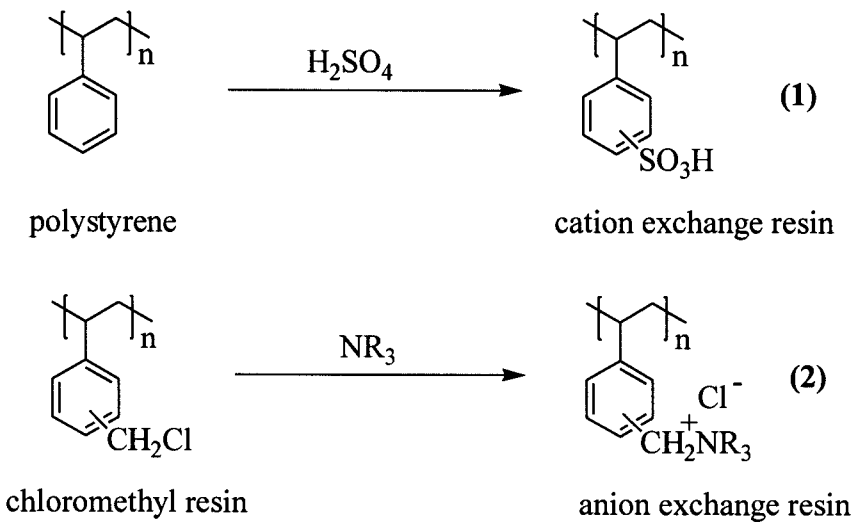

Figure 1.1: The synthesis of simple ion exchange resins.

In a more recent development, Bolton and Jackson[14] reported the preparation and use of thermally regenerable ion exchange resins. These ion exchange resins consist of discrete acidic and basic domains grouped together in a porous 0.3mm to 1.2mm particle. These were synthesized by either polymerization of a mixture of acidic and basic monomers[15] or by encapsulation of microparticles in an inert matrix (the so-called 'plum pudding' model). These ion exchange resins, once 'spent' by the exchange of their counter ions, were regenerated by soaking in a mixture of sodium chloride and sodium hydroxide solution and washing with hot water.[16]

1.2 SOLID PHASE PEPTIDE CHEMISTRY - HISTORICAL OVERVIEW

The concept of using polystyrene resins to perform peptide synthesis, was introduced in 1963 by Bruce Merrifield,[17] who convincingly demonstrated the synthesis of a tetrapeptide. Traditional solution phase synthesis of peptides from amino acids was a laborious process, usually necessitating purification between synthetic steps. When Merrifield showed that this most laborious task could be simplified by the application of the solid phase, he caused a revelation in the scientific community, which subsequently embraced the concept. The Merrifield strategy employed polystyrene beads as the initial *C*-terminal protecting group of the first amino acid, synthesis (elongation) of the growing peptide chain was then possible. Arguably the most

significant achievement in the application of this technology to chemistry was made by Gutte and Merrifield[18] in 1971, in the total solid phase synthesis of the relatively massive naturally occurring 124 amino acid enzyme Ribonuclease A. Ribonuclease A has a high activity against RNA. By specifically cleaving the 5'-ester bond of 3',5'-phosphodiesters the enzymes native function is the cleavage of 'spent RNA'.

1.3 SOLID PHASE TECHNOLOGIES

In the early days of SPOC, many types of solid phase were examined, such as the controlled pore glass[19], silica,[20,21] polyethylene glycol-polyamide (PEGA),[22] and cotton[23,24] supports. A development that occurred in the 1980s in solid phase technology was the functionalisation of the surface of materials by radiation grafting techniques for synthesis. Gamma radiation is often used as the radiation source[25] and results in surface functionalisation of the desired polymer. These surface functionalised polymers have the advantage over traditional solid supports of being easily manipulated, but their main disadvantage is that their chemical loadings are much lower than the traditional gel resins. The Synphase™ crowns[26] are notable commercial examples of these polymers. Crowns tend to be physically larger than resin beads and therefore require large reaction volumes to immerse them completely. In order to drive reactions to completion, high concentrations of substrate are required, which, when coupled to the requirement for high reaction volumes, can be costly compared to traditional beads. Chiron 'lanterns' have been developed as a response to this limitation.

Houghten[27] enclosed a pre-determined mass of PS-DVB beads in porous polypropylene sheeting, forming 'T-Bag' like structures. This system of encasing resin in a membrane combines the chemical properties of the resin with facilitated manipulation protocols in chemical syntheses. In a recent development, CD plugs developed at the University of Southampton also combine these facets effectively.[28] The plugs consist of a short length of a cylindrical polymer containing traditional resin beads inter-meshed with chemically inert polyethylene.

1.4 ADVANTAGES AND DISAGVANTAGES OF SOLID PHASE CHEMISTRY

There are advantages as well as disadvantages to solid phase chemistry compared to traditional solution phase chemistry methods. The main advantages of using the resins are:

- The substrates once tethered to the resins, can be bathed in high concentrations of reactant, thereby allowing reactions to be pushed to completion.
- After synthesis, excess reagents can be washed away from the resin, thereby removing the need for lengthy and costly purification procedures. Convenience is therefore achieved by virtue of simplified purification steps and by more efficient chemical reactions.
- The overall reaction times can be reduced, which in an industrial environment is more economical as more chemical transformation may be carried out per unit time.
- Resins with predictable properties are amenable to automation and since products of chemical reactions can be tethered to the resins, these can be contained and manipulated by robots.

The main disadvantages of solid phase chemistry are:

- Reactions undertaken on the solid phase necessitate the highest possible yields, as resin bound by-products will also remain on the resin and may only be separated from the desired products at the end of the synthesis. During Gutte and Merrifield's synthesis of Ribonuclease A, for example, if the efficiency of each coupling step was 99.5%, then the overall yield of the peptide would have only been 54%. Today, this demand for high individual reaction yields in repetitive SPOC procedures has been partially addressed by the introduction of automated HPLC systems and novel purification media.
- Monitoring of reactions on the solid phase is more difficult on resin than in solution, due to the fact that many commonplace analytical techniques require solvated compounds.

- The solid phase reaction must be designed to be compatible with solvents that are also compatible with the chosen solid phase and in some cases, the products being formed. Failure to ensure this may result in even the most trivial chemical reaction being inefficient or completely non-viable when performed on the solid phase.
- If the substrates or monomers of a repetitive coupling reaction are either difficult to synthesize or are expensive, it can be uneconomical to use the high concentrations of reagents required to drive reactions to completion. This may be prohibitive to the overall chemical process.

1.5 PROPERTIES OF A 'GOOD' SOLID PHASE

The solid phases in section 1.3 represent the culmination of desirable properties into commercial products. In designing these solid phases, the inventors have built in a number of desirable factors, which ensure compatibility with the intended chemistries. The desirable factors may be represented as follows.

1.5.1 *Chemical stability*

In order to perform a diverse range of synthetic steps, a solid support must be chemically stable and not interfere with the intended chemistries. Ramage[29] reported that polystyrene resins may break down in both strongly acidic and strongly basic conditions. He exposed Merrifield resins to TFA in DCM and aminomethyl resins to hydroxylamine in dioxane, and heated them. After concentration of the filtrates, residues of between 7-35% by mass of resin were isolated. Some PEG grafted supports have also been reported to be unstable to TFA,[30] with the problem being the cleavage of the PEG graft from the benzylic carbon atom **(3)** (figure 1.2).

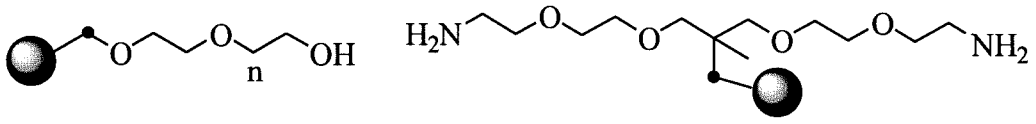

(3) (4)

Figure 1.2: TentaGel and ArgoGel resins.

Researchers at Argonaut Technologies developed a new resin (ArgoGel[31,32]) **(4)**, which experiences reduced cleavage from the benzylic position. They have found though, linear PEGs at <0.5 wt% in the filtrates after exposing their ArgoGel-OH and ArgoGel-NH_2 to a 95:5 mix of TFA:water.[33] Newer PS-PEG resins are continually being developed, which aim to suppress the limitations of the classical PS-PEG systems.[34]

1.5.2 *Mechanical stability*

The resin must be mechanically stable to intended chemical processes. Mechanical breakdown into smaller irregular shaped particles, which although chemically similar to the original parent beads, may cause clogging of filter frits and other normal separation media. Mechanically unstable resin cannot therefore be applied to automated synthesizers, and this would be a liability in an industrial process.

1.5.3 *Definable chemical loading*

It is commonplace for resins to be described in terms of their chemical loading so that syntheses using them can be efficient in terms of the magnitude of the excesses of reagent used. In many chemical reactions, it is necessary to use a precise number of equivalents of reagent; therefore the chemical loading is an essential descriptive parameter.

1.5.4 *Economical synthesis*

It is important to be able to access a wide range of functional groups from the starting resin, without the need for elaborate or costly procedures. For commercial reasons, an ideal resin is one that can be synthesized and disposed of inexpensively with respect to both financial and environmental costs.

1.5.5 *Good swelling properties*

Swelling is a property associated with almost every polymeric material and is related to the cross-linking in the polymer. It occurs when a solvent enters a receptive polymeric matrix and partially solvates it. The limit of this solvation is governed by the cross-linking parameter. Swelling can increase the volume that a resin occupies ten fold and give rise to increased interactions between the solid phase and the solution phase. In the swollen state there is greater space for access and diffusion of substrates to the functional sites, which results in enhancement of chemical reaction rates. Meldal[35] in 1992, reported that a 1% cross-linked PS-DVB resin offered the best compromise between mechanical stability and compatibility of the resin to suitable organic solvents.

There is a relationship between the mechanical stability/ rigidity of a swollen resin and cross-linking parameters.[36,37,38] A lightly cross-linked material will physically, be more solution like once swollen, than a more heavily cross-linked one. A heavily cross-linked resin will tend to be more stable and rigid. Recent developments claim to make the resin 'more organic solvent like',[39] by conferring increased swelling characteristics with respect to the choice of organic solvent used; although this property has been the claim of many longer standing resins for example CLEAR, [40] PEGA[22] and TentaGel[41] (which incidentally can also be swollen in aqueous solvents).

1.6 MODES OF POLYMERIZATION

Four main modes of polymerization have been identified; bulk,[42,43] emulsion,[44,45] dispersion[46,47] and suspension polymerization.[48,49,50]

1.6.1 *Bulk polymerization*

In bulk polymerization, component monomers are allowed to polymerize in the absence of any solvents, resulting in the generation of a very high molecular weight. The monomers are typically poured into a mould and fill this container during the polymerization. A notable example of this process is the large-scale industrial bulk polymerization to produce plastics, for example, in the production of PVCs. In practice, a range of additives, including anti-oxidants, dyes and plasticizers, are included in the initial blend.[51] Bulk polymerization has recently been applied to molecular recognition and molecular imprinted polymers (MIPs).[52]

1.6.2 *Emulsion polymerization*

During emulsion polymerization, an organic phase is suspended in an aqueous phase in the presence of a water-soluble initiator and a surfactant (soap). Even commercial soap, with its assortment of additives and perfumes can be used for this but in practice in the laboratory, the soap's main detergent, sodium lauryl (dodecyl) sulfate (SDS) is preferred. The detergent forms micelles around the organic monomers and polymerization occurs when the radical initiator diffuses through the aqueous phase to make contact with the micelle (figure 1.3).

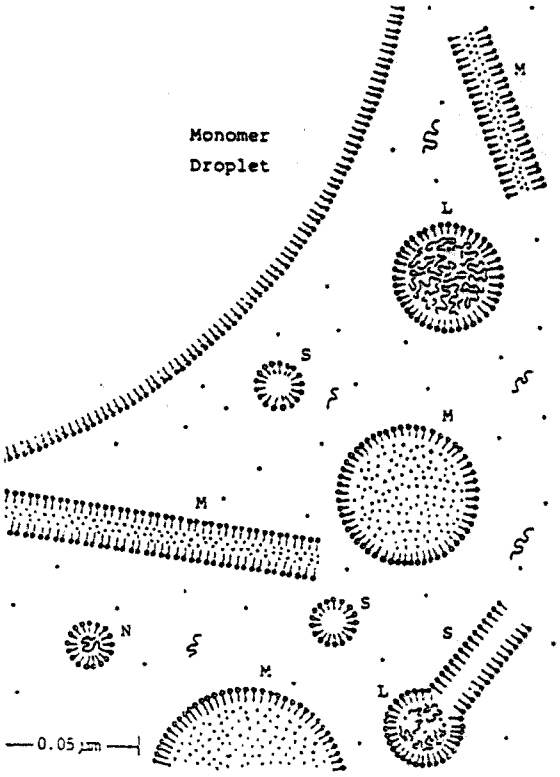

Figure 1.3: Schematic of emulsion polymerization.[53]

Key : . = monomer molecule, M = monomer containing micelle, S = Soap micelle, ℘ = Growing macroradical, N = polymer nucleus, L = Growing latex particle.

Inorganic persulfates can be used as initiators as they are readily soluble in the aqueous phase. This mode of polymerization can be used to produce spherical particles in the size order 0.01 μm –1 μm in diameter and has most commonly been applied to the synthesis of latexes such as paints.

1.6.3 *Dispersion polymerization*

In dispersion polymerization, the monomers have a very low intrinsic solubility in the polymerization medium. For monomers similar in nature to styrene, ethanol can be used. As the polymerization ensues, the growing polymer particles reach the limit of their solubility in the ethanol solution and coalesce to form unstable nuclei in a manner akin to precipitation. Further adsorption occurs until the nuclei become stable and have formed mono-dispersed particles (particles of uniform size distribution).

Dispersion polymerization is an excellent method for the generation of beads of less than 5 μm in diameter.

1.6.4 *Suspension polymerization*

Suspension polymerization is practically similar to emulsion polymerization except that the radical initiator used is not soluble in the aqueous phase, instead it is organic soluble and is present in the droplets in suspension. Surfactant is not used in the same way in this mode of polymerization, but a stabilizer is required. This method produces spherical particles of between 5 μm – 4 mm in diameter and polymerization occurs when the droplets reach a critical temperature and radical initiation occurs. Polymerization in this sense may be thought of as millions of bulk polymerizations proceeding together. As polymerization is an exothermic process the temperature will also rise, and in large-scale industrial polymerization processes, temperature control becomes a major issue. Chain-elongation events compete with chain termination events and a growing polymer chain can be terminated by either impurities in the reaction mixture or by radical quenchers such as oxygen. Thus as a result of a suspension polymerization reaction, a range of bead sizes may be produced making sieving of the beads a necessary post-reaction activity.
The simple polystyrene-based resin remains the main-stay of the solid phase chemist[54] and it is this form of solid phase that was investigated and employed throughout this project.

1.7 SPPS STRATEGIES – RESINS AND SYNTHESIS

1.7.1 *Resin derivatisation*

A number of transformations are available for the preparation of resins for use in SPOC.[i] The readily available Merrifield resin may be converted into aminomethyl resin by treatment with potassium phthalimide and subsequent hydrazinolysis[55] or into

[i] See Chapter 2 for further examples.

hydroxymethyl resin by esterification using potassium acetate and then saponification.[56]

1.7.2 *Coupling onto the solid phase*

To facilitate the reaction of a resin bound amine with an acid in solution to form an amide bond, the acid is activated towards nucleophillic attack by the amine. Various activation strategies exist. Activation to the acid chloride with thionyl chloride,[57] symmetrical anhydride formation with dicyclohexylcarbodiimde (DCC)[58,59] or formation of the unsymmetrical anhydride with isobutyl chloroformate[60] have all been performed. Activation via conversion to the active esters using DCC and HOBt[61,62], pentafluorphenol[63,64] or *p*-nitrophenol[65,66] have also all been reported but probably by far the most successful combination in terms of application to SPPS involves the addition of diisopropylcarbodiimide (DIC) **(5)**[67] or DCC with HOBt[68,69,70] (figure 1.4).

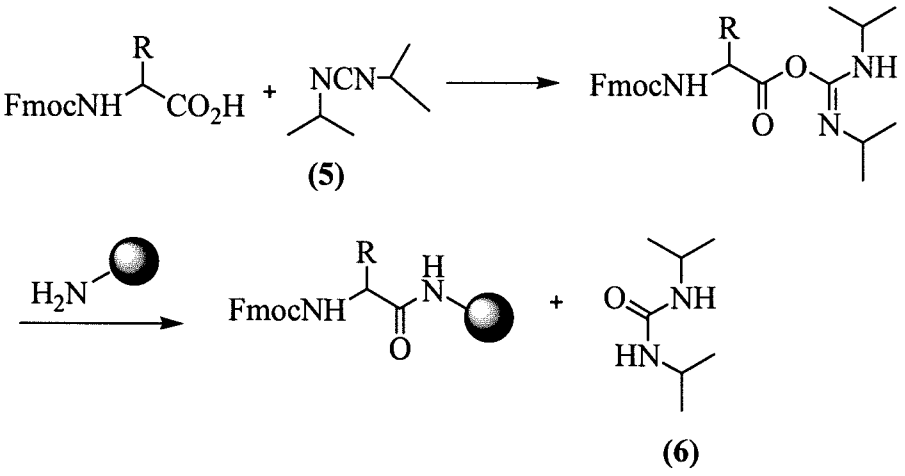

Figure 1.4: Addition of DIC and HOBt to facilitate amide bond formation between an acid and a resin bound amine.

Nucleophillic attack by the incoming amine at the active ester completes the synthesis of the amide bond and also synthesis of the urea **(6)**.

The diisopropyl-urea (DCU) **(6)** is soluble and therefore easily washed out of the resin leaving only resin bound product in the reaction. In solution phase reactions

dicyclohexyl carbodiimide (DCC) is preferred and forms an insoluble urea, which can be filtered from the solution phase products.

Coupling onto the solid phase in the opposite sense, *via* attack of an activated resin bound acid by an amine in solution is also possible, but this method has not been widely accepted in SPPS due to the high levels of racemization incurred at the carbon atom α to the carbon of the activated resin bound acid group.

1.7.3 *Linkers*

In practice it has become commonplace to use linkers to facilitate solid phase synthesis. Linkers were developed to prevent premature cleavage during the TFA deprotection of resin bound protecting groups. Whilst there exist a range of functional groups that can tolerate chemically harsh cleavage conditions ($NaOH$[10], HF[71]), many molecules, for example those being developed as potential drug leads and those containing sensitive functional groups, cannot. Linkers are bi-functional molecules which tether substrates to either spacer molecules or directly to the resin and allow controlled facile cleavage of products from the resin in an attempt to alleviate this problem (figure 1.5).

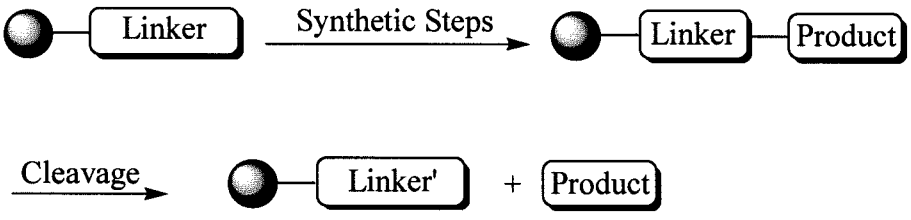

Figure 1.5: Schematic of linkers in SPOC.

Depending on the compound being synthesized and the chemical strategy being employed, linkers can be chosen to release products under acidic, basic or neutral conditions. The number of linkers that have been reported to date is vast, estimated at approximately 600.[72] Notable examples of these are (figure 1.6): the acid cleavable linkers e.g. Wang **(7)**, HMPA **(8)** and Rink amide **(9)**,[73] base cleavable linkers e.g.

REM[74] **(10)**, photolabile **(11)**,[75,76] the Kenner **(12)**[77] safety catch and traceless linkers **(13)**.[78] From these, by far the most popular linkers used today are the Wang and Rink linkers.

a) Acid Cleaved

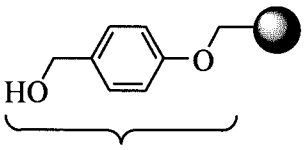

Wang Linker

(7)

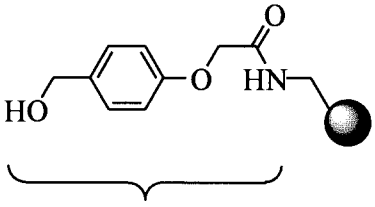

HMPA Linker

(8)

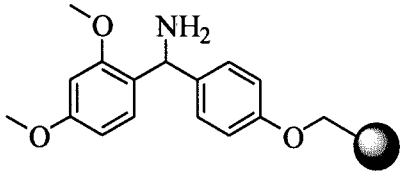

Rink amide linker

(9)

b) Base Cleaved

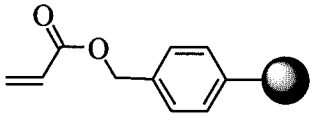

(10)

REM Linker (regenerate resin and Michael addition)

c) Light Cleaved

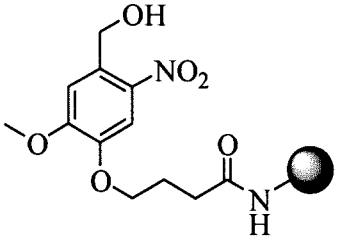

Affymax Research Institute Photolabile Linker

(11)

d) Safety Catch

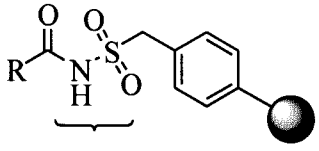

Kenners safety catch linker

(12)

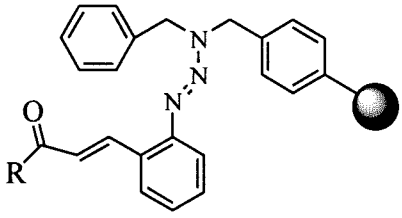

e) Traceless linker for arenes

(13)

Figure 1.6: Examples of linkers from the main classes of linkers in SPOC: a) acid cleavable, b) base cleavable, c) light cleavable, d) safety catch, e) traceless linkers.

1.8 SOLID PHASE ORGANIC CHEMISTRY

1.8.1 *Monitoring reactions*

Solid phase reactions must be driven to completion to maintain the effectiveness of the technique. Previously, the only way to identify the nature of a product on the solid phase was to cleave it from the resin and apply traditional solution phase characterization however it has recently been possible to apply some of these tests more directly to the resin bound product. A number of these methods have been adopted and/ or adapted for use in SPOC as follows.

1.8.1.a *Mass spectrometry*

Mass Spectrometry (MS) has become a prolific analytical tool for solution phase compounds from combinatorial chemistry.[79] The popular MS method (ES-MS)[80] is very amenable to combinatorial chemistry and solid phase peptide synthesis since it has the advantage of short analysis times and automation. This is often combined with high performance liquid chromatography, forming another popular mode of analysis, LC-MS. Resins can also be cleaved *in situ* and MS analysis performed using MALDI-TOF MS.[81,82,83]

1.8.1.b *NMR analysis*

Nuclear magnetic resonance (NMR) analysis of homogenous solution phase compounds is routine but, with only a few modifications and without the use of custom probes, this technique can also been applied to the solid phase.[84] The resin must be swollen, and for this reason the technique when applied to the solid phase is called Gel Phase NMR spectroscopy. In its swollen state the resin bound product has increased molecular movement, which results in narrower line-widths and greater signal resolution compared to the unswollen state.

Even though the bandwidths for a ^{13}C NMR spectrum are broader than for ^{1}H NMR spectra, the overall wider distribution of chemical shifts means that resolution of

signals is usually sufficient for structural information to be determined. A disadvantage of this technique is that it is very insensitive (the relative abundance of ^{13}C is 1%) and in practice, long NMR experiment times coupled with large amounts of sample are necessary for good spectral resolution.

Gel phase ^{1}H NMR spectroscopy has become feasible with the use of a magic angle spinning (MAS) probe. The probe causes the sample to spin at the optimal angle (the magic angle) to the magnetic field, which gives greater spectral line resolution by narrower bandwidths, compared to traditional probes.[85] The technique has been determined to be most effective with resins that contain long PEG chains i.e., resins that contain the most flexible termini.[86]

1.8.1.c *Colourimetric tests*

Colourimetric tests have greatly facilitated monitoring of solid phase reactions. The following tests are widely used in solid phase chemistry for both quantitative and qualitative monitoring of reactions.

1.8.1.c1 *Ninhydrin*

The ninhydrin reaction developed by Moore and Stein[87] in 1948 was adapted for use with solid phase systems by Kaiser,[88] but this test was semi-quantitative. Sarin[89] formulated conditions for the rapid and quantitative determination of free amino groups on the resin. The formation of the complex Ruhemann's purple **(14)** (figure 1.7) is quantified at 570 nm and thus the amount of free primary amine on the resin can be determined.

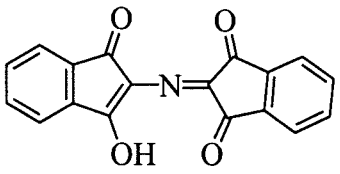

(14)

Figure 1.7: The Ruhemann's Purple Complex.

1.8.1.c2 *Fmoc Test*

During the Fmoc test[23] (figure 1.8) the UV absorbence of a fulvene-piperidyl chromophore **(15)** is measured (monitored at 302 nm) and thus the amount of protected amine determined.[90, 91, 92]

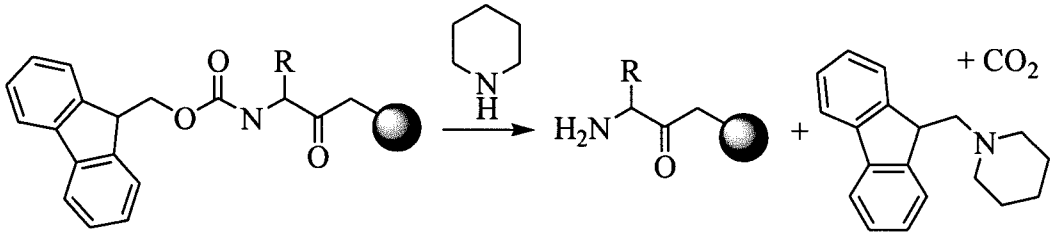

(15)

Figure 1.8: The Fmoc test.

1.8.1.c3 *Bromophenol blue, chloranil tests*

The ninhydrin test is used for the determination of primary amines on the solid phase but cannot be used to determine the amount of secondary amine. Bromophenol blue[93,94,95] can be used to monitor and quantify secondary amine (e.g. proline) on the resin. The bromophenol blue binds to the amine and then is displaced from the resin by acylation. Chloranil[96, 97] also reacts with free amines on the resin to produce a chromogenic compound, which can also be measured spectroscopically.

1.8.1.d *Edman degradation*

Edman degradation[98, 99, 100] using 3-phenyl-2-thiohydantoin (PTH) amino acids can be used to determine the composition of peptide chains on the solid support. The technique is very sensitive and it is possible to obtain complete amino acid analysis of a resin bound peptide from a single resin bead.

1.8.1.e *Infra-red spectroscopy*

Infra-Red spectroscopy can also be applied to the solid phase. Single bead Infra-Red analysis has been used to investigate the course and the kinetics of organic reactions.[ii] In practice however it may be difficult to obtain more than just qualitative data from the IR analysis as the signals from the polymeric matrix often dominates the spectra.

1.8.1.f *Elemental analysis*

Elemental (combustion) analysis may be used in the analysis of solid phase reactions but due to its destructive nature and the fact that the resin itself is included in the analysis, atoms or functional groups specific only to the resin bound molecule are essential for viable interpretation. It is therefore not always applicable to use elemental analysis for routine characterization during solid phase peptide synthesis.

When possible the above on-resin tests are carried out but by far the most common methods of analysis involving cleavage from the resin and traditional solution phase characterization.

1.8.2 *SPOC – Split and Mix*

The generation of compound libraries has played a major part in the drug discovery process, and certainly during the 1980s and '90s, the 'race was on' amongst the pharmaceutical companies to amass the largest collections of libraries for biological

[ii] See chapter 5 for examples.

testing.[101] In 1988 Furka[102] proposed a procedure called 'Split and Mix', which has been used to generate combinatorial libraries of compounds (figure 1.9).

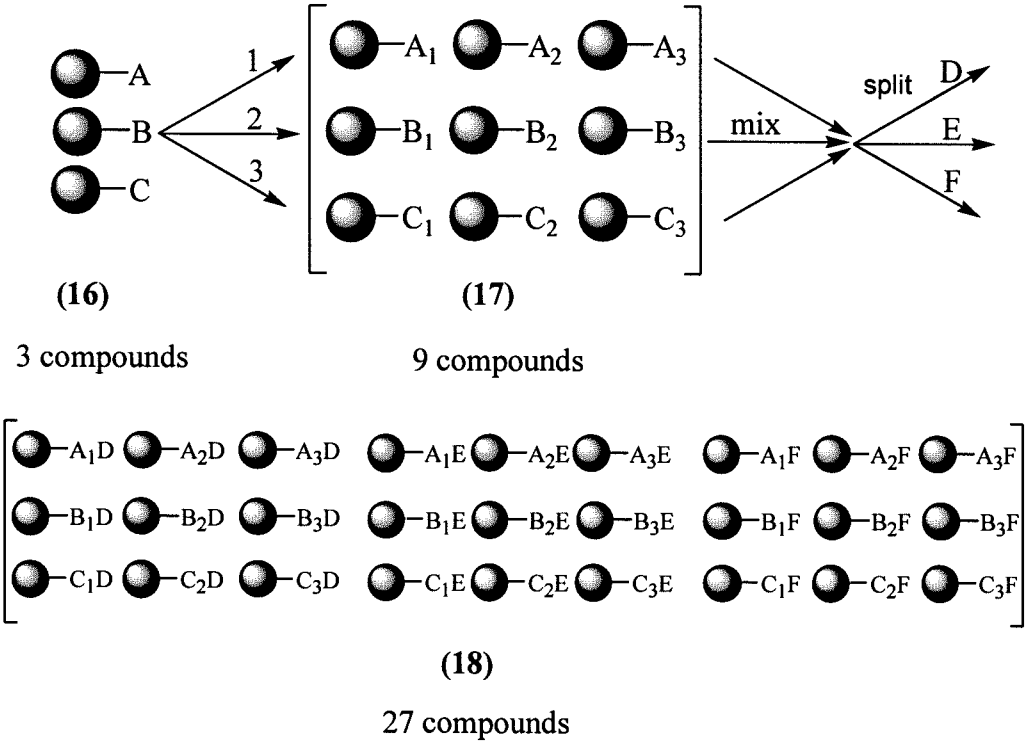

Figure 1.9: The Split and Mix Method developed by Furka.

The resin support is divided into equal portions and these are reacted individually with different reagents. The products **(16)** of these reactions are mixed together and then divided into equal portions. These are then again reacted with different reagents to produce a library of dimers **(17)**. By repeating this process, a library of trimers **(18)** is produced in numbers equal to the number of resin divisions ('pots') raised to the power of the number of times the process is repeated (figure 1.9). Twenty-seven different compounds are generated in three coupling steps. Repetition of the process generates 81 compounds. This process has been successfully applied to the drug discovery process.[101] Though very large, chemically diverse libraries of compounds can be generated. In some companies there has been a trend towards creating more targeted combinatorial libraries, with more defined skeletons and more specifically chosen diversity groups. This has mainly been due to the poor hit rates in biological testing of

combinatorial chemistry libraries, limited repeatability of enzyme screens and poor consistency in resin bound libraries.

1.8.3 *Resins for organic chemistry*

'Solid phase organic chemistry' has shed its 'peptide synthesis' stereotype and has come to indicate facilitation of any chemical reaction by tethering a reagent to an inert polymer matrix. The phrase has also been extended to incorporate facilitation of chemical reactions in solution, by solid phase-immobilized reagents. It has also been applied to organic chemistry[103] in the synthesis of small molecule libraries,[104] in particular the synthesis of oligonucleotides,[105,106] peptoids,[107,108] oligocarbamates[109] and the synthesis of small molecules such as the benzodiazepines,[110] diketopiperazines,[111] tetrahydrofurans[112] and 1,3-diols.[113] SPOC also suits the synthesis of structurally diverse templates, which can be functionalised, tested for biological activity and entered into the drug discovery process.[114,115]

The number of solid phase reagents and supports available to date is vast. A commercial supplier of resins published a table[116] in 1999 containing many resins, reported purely for use in acylation,[117] alkylation,[118] amination,[119] aromatic substitution,[120] Baylis Hillman,[121] condensation,[122,123] cross coupling,[124] cyclisation,[125] electrocyclic [2+3],[126] organometallic,[127] radical,[128] ring opening,[129] transesterification[130] and reduction[131] reactions. This list is by no means exhaustive.

1.8.4 *A comparison between solid phase and solution phase reactions*

Reactions carried out in solution occur within different environments to those carried out on the solid phase due to the chemical characteristics of the polymeric matrix. It would therefore be reasonable to expect the polymeric matrix to exert effects upon a chemical reaction carried out on the solid phase. The size of substrate would also be expected to be relevant in homogeneous/ heterogeneous reaction condition comparisons. The following examples from the literature highlight marked differences

in the outcomes of solution phase (homogeneous) and the solid phase (heterogeneous) reaction analogues.

1.8.4.a *Hydrogenation*

Differences have been reported in 1971 by Grubbs and Kroll,[132] who performed olefin hydrogenation with homogeneous (**19**) and heterogeneous (**20**) (figure 1.10) Rhodium (I) catalyst.

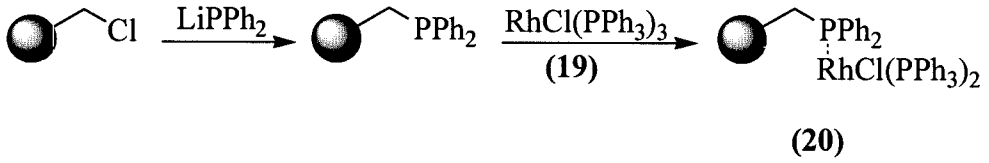

Figure 1.10: Grubbs and Kroll's heterogeneous rhodium catalyst.

Grubbs and Kroll observed that rates of hydrogenation were lower in the heterogeneous system than the homogeneous system and also depended on alkene size. Larger molecules, and also cyclic alkenes compared to acyclic ones, were found to be more subject to diffusional hindrances within the polystyrene beads[iii], resulting in lower rates of hydrogenation.

1.8.4.b *Allylic amination*

The selectivity of a chemical reaction may change in the presence of a solid phase, for example Torst and Keinan[133] demonstrated selectivity in allylic aminations with $Pd(PPh_3)_4$ using a resin bound catalyst compared to the solution phase analogue. Their benzyl-diphenylphosphine palladium catalyst (**21**) supported on a PS-DVB (2%) resin afforded a completely stereospecific amination of both *cis*-(**23**) and *trans*- 3-acetoxy-5-methoxycarbonylcyclohex-1-ene (**24**) with diethylamine, whilst the solution phase catalyst afforded only a mixture of *cis*- (**25**) and *trans*- diethylamino-5-methoxycarbonylcyclohex-1-enes (**26**) (figure 1.11).

[iii] 200-400 mesh PS-DVB (1.8%) chloromethylated on 10% of phenyl rings.

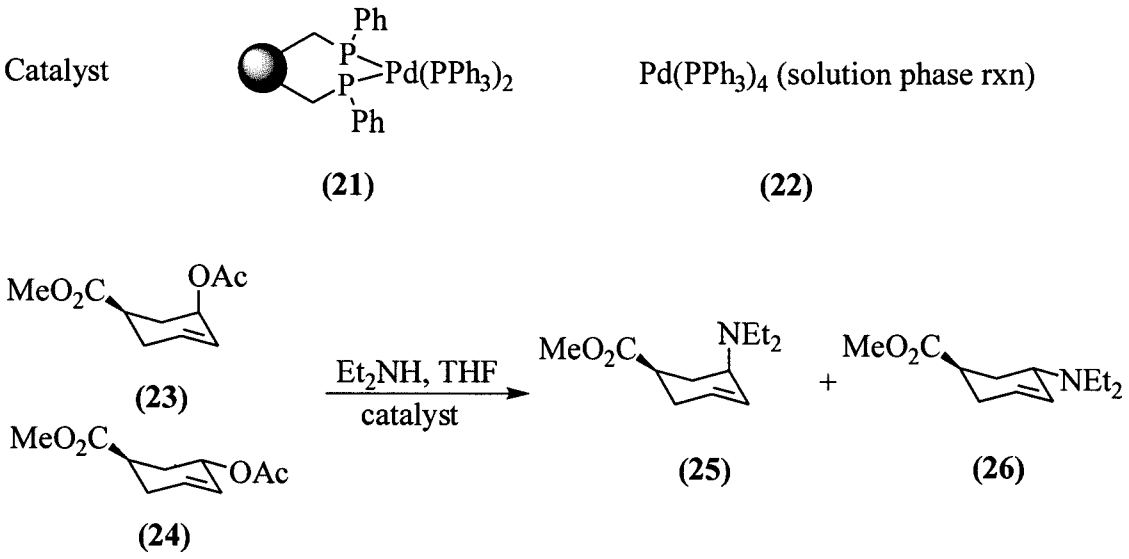

Solid phase reaction			**Solution phase reaction**		
(21) + (23)	**25** (100%)	**26**(0%)	**(22) + (23)**	**25** (67%)	**26** (33%)
(21) + (24)	**25**(0%)	**26**(100%)	**(22) + (24)**	**25**(35%)	**26** (65%)

Figure 1.11: The effect on selectivity of allylic aminations of solid phase and solution phase catalysts.

1.8.4.c *The effect of different solid phases on chemistry*

Examples of non-intuitive outcomes of solid phase reactions are also present in the literature.[7] Some of these are derived from the effect of the polymer support on catalyst stereoselectivity. For example, in the Pd catalyzed hydrogenation of cholesterone and testosterone **(27)** McQuillin, Ord and Simpson[134] showed that the α **(28)**/ β **(29)** ratio of hydrogenation products was influenced by the nature of the Pd catalyst used (figure 1.12).

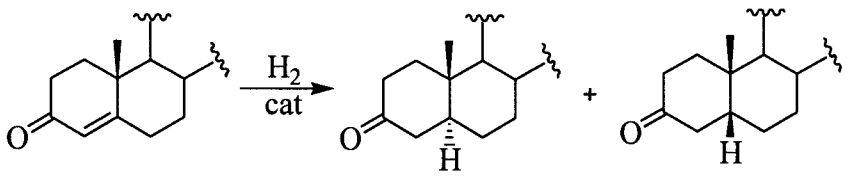

(27) **(28)** **(29)**

alpha *beta*

Figure 1.12: Selectivity in hydrogenation reactions based on the catalyst support.

The alpha/beta ratio was 8.0 using palladium on carbon, 3.8 on Dowex 1 resin and on Dowex 50 resin it was 0.8.

These observations, albeit surprising are considered by many to be insignificant compared to the advantages that can be achieved by the majority of solid phase reactions, hence the current popularity of solid phase chemistry today.

1.8.5 *Resin based scavengers*

The most publicized recent application of immobilized compounds has been in the field of resin bound scavenging/ quenching agents.[135] Reagents containing reactive functional groups have been tethered to inert solid phases to generate a solid phase analogue of the reactive group. The resin can be then applied to a solution phase reaction, to react with unwanted molecules bearing complimentary functional groups in solution (scavenging). The resin bound adduct can be removed from the reaction by filtration (figure 1.13).[136] In its early days the procedure was termed 'quenching'[137] but this has evolved to the currently more popular term of 'scavenging'.

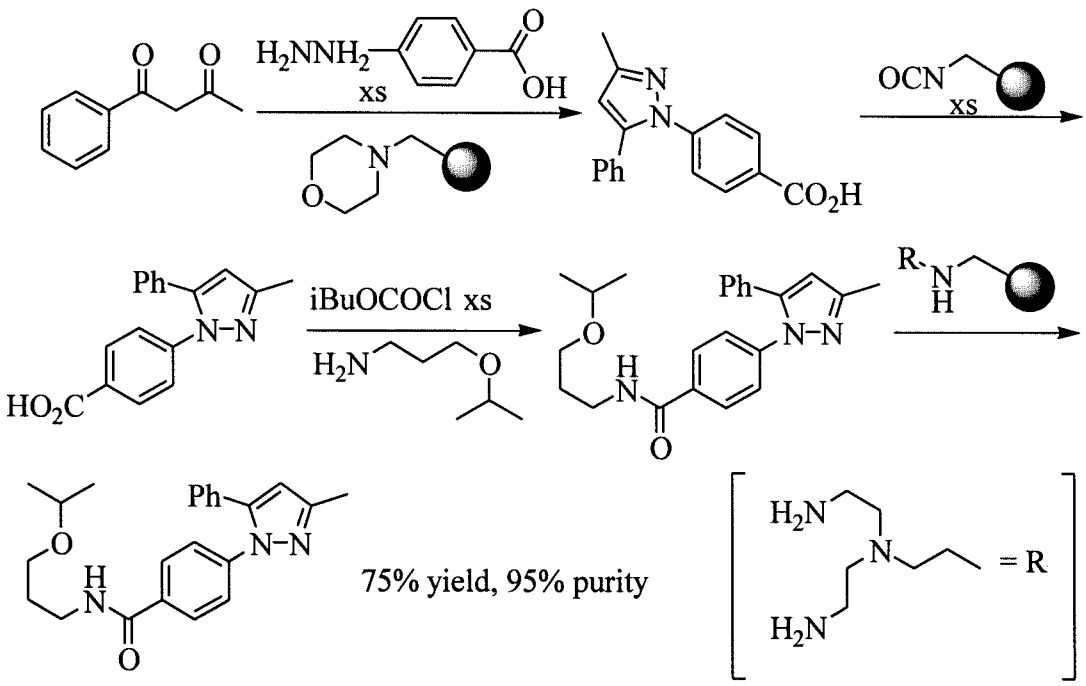

Figure 1.13: Solution phase synthesis of pyrazoles using solid phase scavengers.

To date a large number of scavenger resins have been described; one of the earliest examples being the previously described and widely used ion exchange resins. Diverse chemical groups have been applied to the solid phase, forming the acidic (figure 1.14a), electrophilic (figure 1.14b) and nucleophilic (figure 1.14c) scavenger resins.

a) Acid based scavenger resins

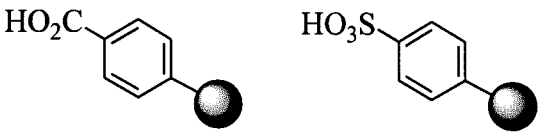

b) Electrophilic scavenger resins

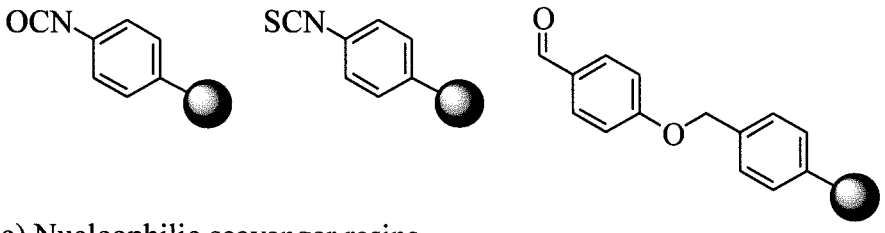

c) Nucleophilic scavenger resins

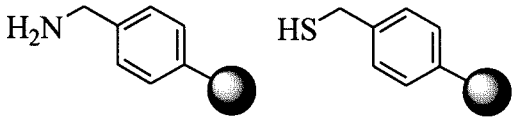

Figure 1.14: Examples of the main classes of scavenger resin.

1.9 CONCLUSION

These examples have highlighted major types of solid phases and demonstrated the advantages and disadvantages of using solid phase systems. As the number of solid phase reactions is extensive, only the most predominant ones were included along with a treatise of the most popular scavenger resins.

CHAPTER 2 - THE CHEMISTRY OF RESIN SYNTHESIS

2.1 INTRODUCTION

Suspension polymerization is a versatile method for bead synthesis, which allows polymers to be prepared by radical polymerization methods.

Polymerization of styrene *via* the anionic route was first described by Schlenk[138] in 1914. This method has since been optimized for industrial utility.[139,140] Sodium and lithium (or the corresponding organo- lithium or sodium compounds, for example butyl lithium or sodium methoxide) have been used to assist in the anionic polymerization of styrene, which can be represented as shown in figure 2.1.

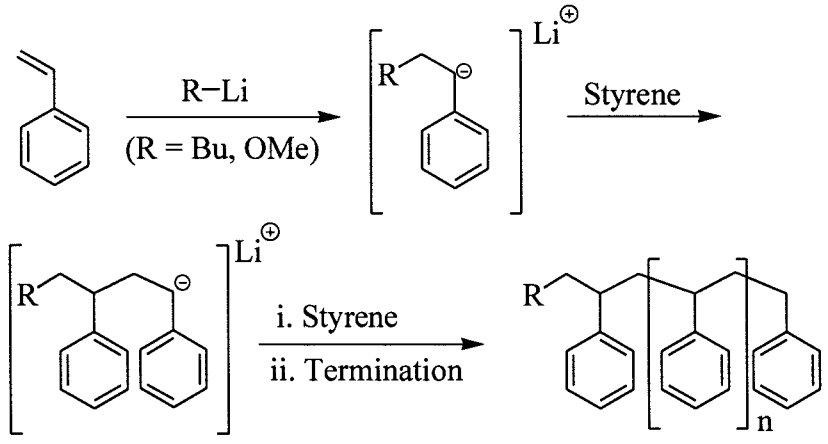

Figure 2.1: Anionic polymerization of styrene.

As this process does not give rise to an inherent chain termination step, it has been termed a 'living' polymerization. Termination is usually induced by the addition of termination agents such as CO_2 or proton donors such as methanol.[141]

Cationic suspension polymerization reactions require acid conditions, either protic (HCl, H_2SO_4) or Lewis acids (BF_3, $AlCl_3$, $SnCl_4$, $SnBr_4$, $TiCl_4$, $ZnCl_2$ etc) to generate cations. Sulfuric acid is most commonly used in this process, and the reactivity of the alkene monomers depends greatly on the stability of the carbonium ion formed.

Whitmore[142] first demonstrated that carbonium ions were the actual intermediates in these acid catalyzed polymerizations of olefins.

The PS-DVB resins in this project were synthesized by a radical initiated suspension co-polymerization process (figure 2.2), which is considered to be one of the most flexible since unlike some of the above[i] modes of polymerization it can be carried out in water. Water acts not only to help suspend the droplets but also as an efficient heat transfer agent for the droplets in suspension.

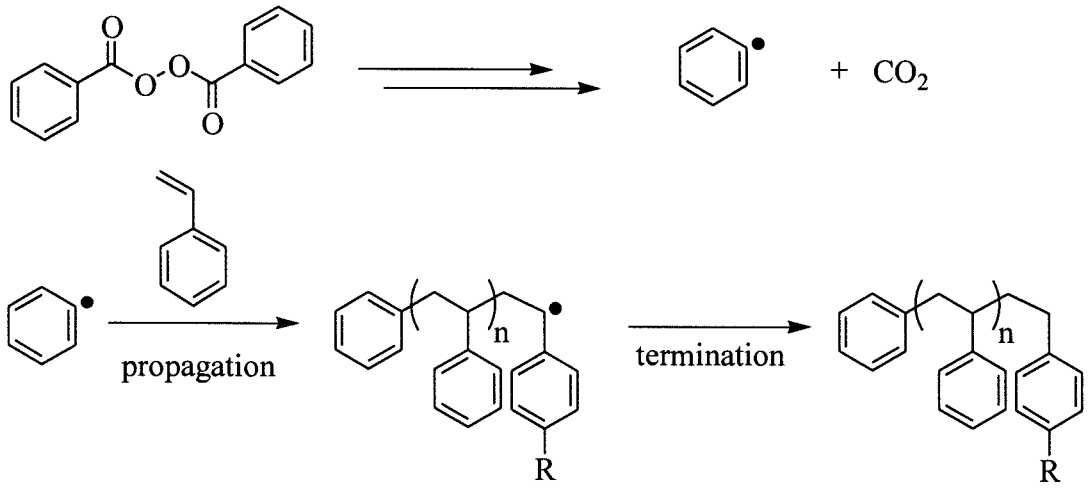

R = Divinyl benzene

= Chloromethyl styrene **(30a)**

= Styrene

Figure 2.2: Synthesis of polystyrene resin via radical induced suspension co-polymerization.

At the critical temperature for O-O bond homolysis[ii], the radical initiator generates the radical species. In the case of benzoyl peroxide, the oxygen-oxygen single bond in the peroxide is homolytically cleaved to form an initial benzoate radical species which rapidly decomposes to carbon dioxide and a phenyl radical (figure 2.2). The phenyl

[i] See Chapter 1 for further examples.

[ii] Bond homolysis of the parent compound into its radical dimer fragments is not triggered by a specific temperature, instead as the temperature increases (and as $\Delta G = -RT\ln K_D$) dissociation of the parent radical compound becomes more favored.

radical attacks the vinyl group, to initiate polymerization. This reaction of the radical with the vinyl group to produce a new species, which is still radical in nature is a called chain/ polymer propagation event. When two radicals quench each other by chemical reaction to produce a non-radical adduct, the result is a chain termination event. A growing polymer can be terminated at any stage of its development by impurities, such as oxygen.[143] Overall, the reaction slows down and stops when the rate of termination exceeds the rate of initiation. When each end of divinylbenzene reacts, cross-linking occurs. When the vinyl group of chloromethyl styrene reacts, the incorporation introduces chemical functionality into the growing polymer. When styrene reacts, chain elongation occurs.

2.1.1 *Phases of reaction*

The radical induced suspension polymerization reaction proceeds through a number of phases before resin beads are eventually formed. Once the organic phase is added to the aqueous phase, and mechanical agitation started, the droplets that form, continually join and separate with other droplets, until an equilibrium droplet size distribution has been attained.[iii] On heating, when 10-20% conversion of monomer has taken place the suspension enters the 'sticky phase'.[144] During the sticky phase, adequate stabilization of the droplets is essential. If the speed of agitation is insufficient, then the droplets will permanently associate in a sticky mass and polymerize as a large number of macroscopic randomly shaped aggregates – or even one large aggregate comprising all of the organic phase. Resizing the droplet equilibrium diameter is not possible once the monomers have entered the sticky phase. When 70-80% conversion of monomer to polymer has taken place and the suspension has passed through the sticky phase, the droplets develop a hard outer surface and harden into the form of resin beads.

[iii] Ascertained following a consultation with Dr. Andrew Coffey, Solid Phase Support Product Manager, Polymer Laboratories, Essex Road, Church Stretton, Shropshire, SY6 6AX, UK.

2.1.2 *Post polymerization functionalisation*

The method of synthesizing the Merrifield (chloromethyl) resin **(30a)** employed during this project (figure 2.2) differs from conventional methods of synthesis in that the functional monomer (chloromethyl styrene) is co-polymerized in the initial suspension polymerization. The post polymerization functionalisation of polystyrene is more popular than co-polymerization of functional monomers[145] and is most often carried out *via* a Friedel Crafts acylation reaction with chloromethyl ether (figure 2.3).

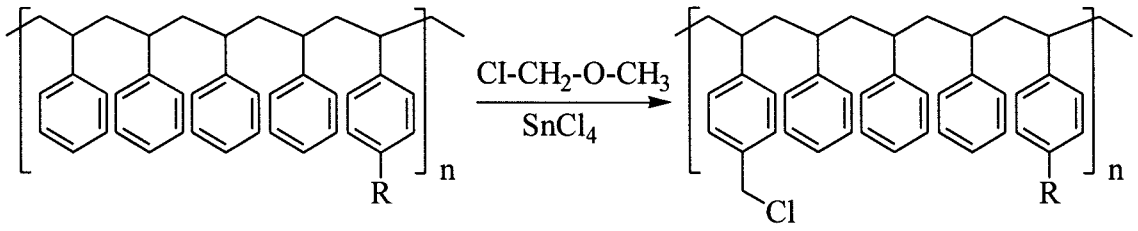

R = divinyl benzene cross-linking agent

Figure 2.3: The synthesis of chloromethyl resin by acylation of polystyrene.

Chloromethyl ether is carcinogenic and not favored for laboratory preparations. It also suffers from the drawback that its main contaminant, the *bis*-chloromethyl ether can also take part in the reaction, which leads to an indefinable increase in cross-linking. The Tscherniac-Einhorn[146] reaction is an alternative method of functionalisation, involving direct amidoalkylation of the unfunctionalised polystyrene (figure 2.4).

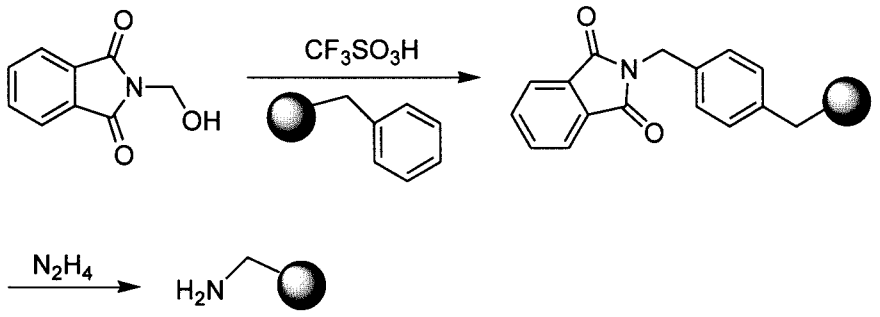

(30)

Figure 2.4: The Tscherniac-Einhorn reaction.

A possible disadvantage of post-polymerization functionalisation is that it occurs at the most chemically accessible sites in the polymeric matrix and is therefore likely to be concentrated near the surface of the PS beads,[147] although conversely autoradiographical studies using functionalised PS beads have actually shown that chemical functionality in post-polymerization functionalised beads is relatively homogeneously distributed throughout the PS beads.[148] Acylation is mainly specific for the *para-* position of the phenyl group with respect to the polymer backbone but there is a possibility that other isomers may be formed during the reaction.

2.1.3 *Suspension polymerization reaction parameters*

The chemical and the physical parameters involved in the suspension polymerization reaction are intimately connected. The choice of monomer and its physical attributes (e.g. hydrophobicity/ hydrophilicity, thermal stability) affect the physical parameters of the reaction as a whole.

When the monomers and the mode of polymerization have been chosen, other physical parameters need to be optimized in the suspension polymerization. Different solutions for successful suspension polymerization of monomers to form resin beads have been proposed and a high proportion of these have been protected by industrial patents, given the obvious commercial potential for resin synthesis.[iv]

2.1.3.a *Reactor geometry*

The shape of the glassware/ or reactor employed during the synthesis has been determined to be an important factor in synthesis. Arshady[149] described the use of a baffled cylindrical glass reactor (figure 2.5a) whilst Erbay[150] used a two-piece round bottomed cylindrical flask (figure 2.5b).

[iv] Examples herein to follow.

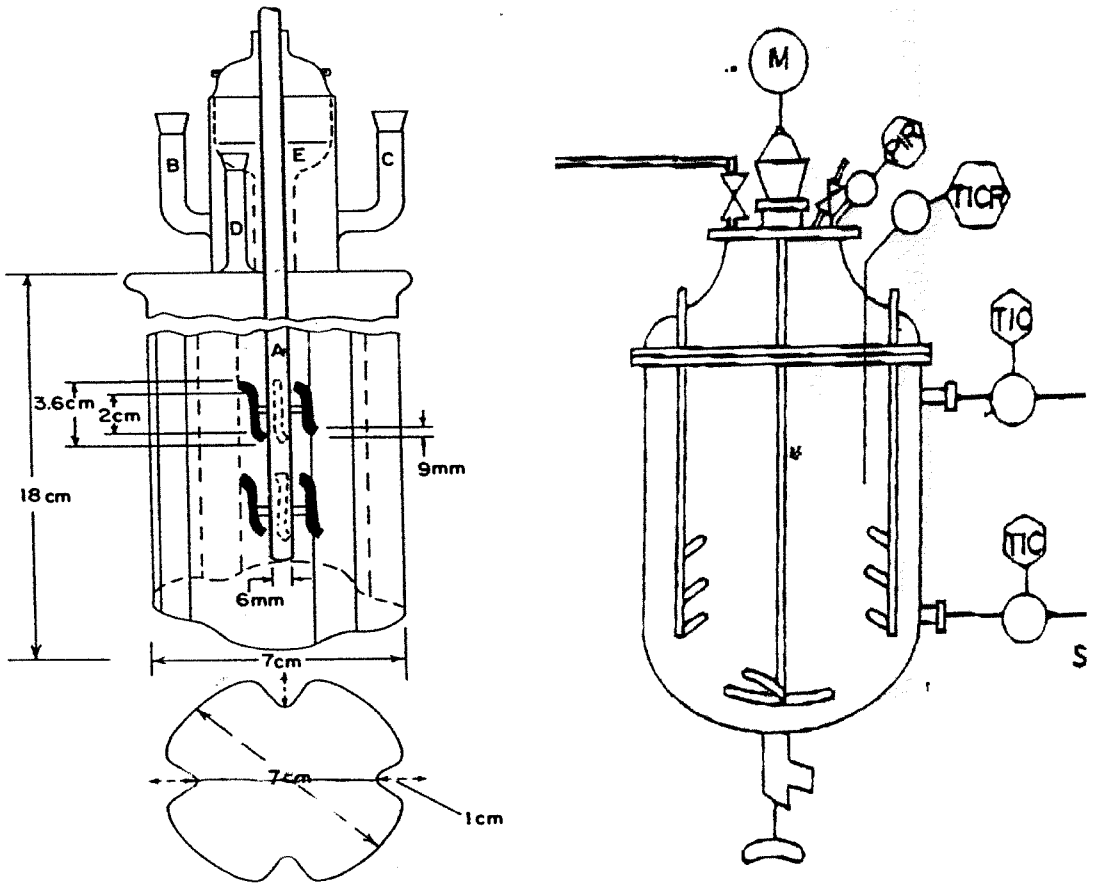

a) b)

Figure 2.5: Two of the vessels employed during the suspension polymerization reaction, a) Arshady's baffled cylindrical glass reactor b) Erbay's 2 piece round bottomed cylindrical flask.

A 1987 European Patent application[151] described the use of a complicated arrangement of a cylindrical reactor with conical upper and lower portions with inlets at the top and bottom of the system, whilst 'goldfish bowls' and simple Morton flasks have also been used to hold various suspension mixtures.[152] Vessel geometry is therefore a significant consideration in the optimization of a suspension polymerization system and once chosen needs to be balanced with respect to other important parameters in the reaction.

2.1.3.b *Stirrer geometry*

The shape and geometry of the impeller/ stirrer used to create and maintain a suspension can also have a marked effect upon the polymerization product. Droplets

must be sufficiently suspended and well stirred in the aqueous medium without exerting too many deforming or coagulation forces on them. Arshady, Kenner and Ledwith[153] used a double sided three-blade system in their baffled conical vessel, whilst commercial laboratory suppliers also supply stirrers of more traditional designs, which are just as useful in optimized polymerization experiments (figure 2.6a+b). Erbay has reported using a three blade curved propeller system (figure 2.6c).

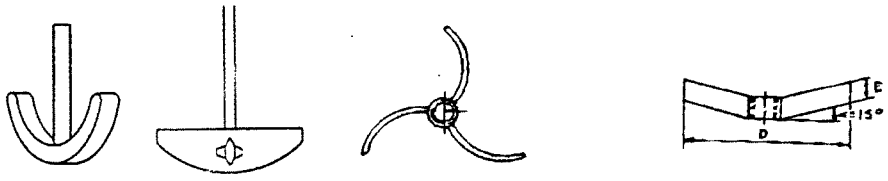

a) b) c)

Figure 2.6: A wide range of stirrers can be used to maintain suspensions, a+b) Traditional designs supplied by the commercial laboratory suppliers, c) Erbay's three blade curved propeller.

Providing local optimization of physical parameters is achieved, any of these stirrers may be employed during the suspension polymerizations with similar levels of success. The materials used in the manufacture of stirrers also vary, and suspensions can be generated and maintained using glass, Teflon coated steel and steel stirrers. Although metallic stirrers are mechanically stronger than the other types, they suffer the drawback that the metal wall can act as a radical quencher during the polymerization.[154] Teflon coated stirrers do not suffer from this drawback although these tend to be more expensive and the stirrer shafts usually require strengthening using steel pins. Practically, glass stirrers are more fragile and suffer the drawback of being more brittle and prone to shattering on vibration and collision.

2.1.3.c *Suspension agent*

When an organic phase is insufficiently suspended in an aqueous phase, the droplets that are formed will have a tendency to coalesce together to form a more continuous organic phase. This effect is especially pronounced when there is a large difference in densities of the organic and aqueous phases. In the case of an insufficiently suspended

styrene, divinylbenzene and chloromethyl styrene system, the organic phase rises and floats at the surface of the aqueous phase. The addition of a water-soluble polymer to the aqueous phase can help stabilize the droplets produced in the suspension. Many stabilizers have been reported for use during suspension polymerizations. Kurth in his synthesis of chlorotrityl functionalised resin used gelatin, but polyvinyl alcohol (PVA), dodecyl benzene sodium sulfonate and tri-calcium phosphate, gum Arabic, polyvinyl pyrrolidone and cellulose ethers are all commercially available alternatives. The choice of stabilizer is usually an empirical one, with many research groups preferring to use only one type of stabilizer throughout their research.[v] PVA is biodegradable, produced by hydrolysis of the cheap starting material polyvinyl acetate and is an industrial favorite. It is available in varying molecular weight ranges with specified degrees of hydrolysis to the alcohol. The amount of suspending agent required for a system is generally determined after much optimization. Too little suspending agent results in droplets, which are not sufficiently stabilized, either during the equilibrium phase or more importantly the sticky phase. Adding too much suspending agent permits stabilization of the micro-droplets, which also form in suspension and lead to the synthesis of beads impracticably small in size. Although smaller beads may be expected to suffer less from the diffusional problems of substrates, expected to be significant in the larger beads, a cut off point must be established because below a certain size, beads become difficult to manipulate. Practically after suspension polymerization reactions, it is very difficult to remove excess suspending agent (which has a low solubility itself) from the large number of very small beads.

2.1.3.d *Stirring speed*

One of the most powerful and practical methods of altering the size distribution of droplets/ beads in suspension is the adjustment of the stirring speed. By increasing the speed of stirring, the mean bead diameter can be reduced, and conversely by reducing the speed of stirring the mean bead size can be increased (conceptualized in figure 2.7). This method of control is subject to other factors though and does have its useful

[v] Kurth has almost solely reported the use of gelatin, whilst Arshady has seldom used any other than PVP, phosphates and sulphates as stabilizers; the author of this thesis and colleagues at Southampton University use PVA.

limits. However the slower the stirring of the suspension and the larger droplets, the more difficult it is to keep the droplets well suspended.

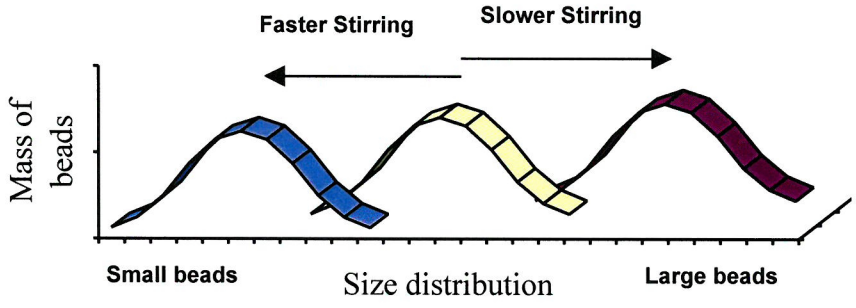

Figure 2.7: The effect of stirring speed on size distribution of beads in suspension

A US Patent describes the addition of 0.0001-0.004% (wt) of polystyrenesulphonate to the suspension in order to narrow the distribution of the beads produced by the reaction. The inventors had intended application of their technology to be made in the industrial synthesis of foams in molds, where consistent particle size is very important. In the laboratory, careful adjustment of speed with the careful control of the suspending agent is the most practical way of achieving a narrow bead size distribution.

Although not well reported in the literature, the position of the stirrer in suspension and its relationship to the vessel can have a marked effect upon the suspension. A typical by-product of a stirring process is the generation of local currents and turbulent forces around the stirrer. Air-flow and fluid dynamic modeling programs on computers may help appreciate these forces and their magnitudes but they can be readily investigated by performing trial polymerizations. If stirring is too rapid a vortex can be generated, and depending on the position of the stirrer in the suspension, and the size of the stirrer in proportion to the rest of the vessel, a positive or detrimental effect can be induced upon the suspension (figure 2.8).

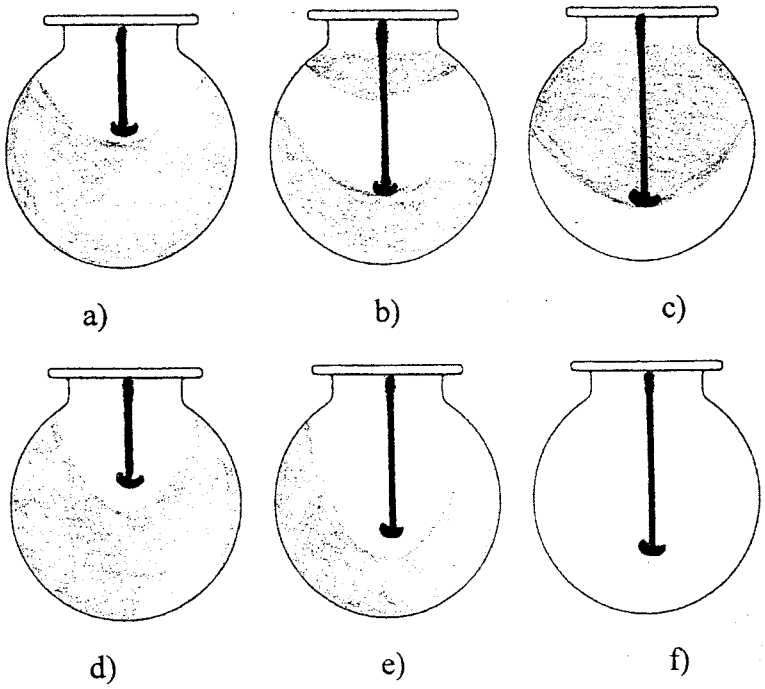

Figure 2.8: The position of the stirrer and the speed of stirring can affect the suspension whilst stirring. The shaded areas show regions of insufficient suspension, which will be different for different shaped stirrers. The examples shown demonstrate the use of an anchor shaped stirrer. Note: a, b, c = slow stirring; d, e, f = faster stirring, at different heights in the vessel

The shaded areas in figure 2.8 indicate regions of insufficient suspension. This can be offset by increasing the speed of stirring (figure 2.8 d, e, f), but this measure also increases the shear forces on the droplets in suspension; eventually destabilizing the system. Thus a compromise between speed/ height and shear-force must be achieved. The shape of the stirrer is also important in this equation.

2.1.3.e *Other variables*

The suspension polymerization reaction is also subject to the more traditional parameters, which influence chemical reactions. If the reaction time is increased, then the yield of polymerization also increases.[155] Increasing the temperature of a reaction also leads to an increase in reaction rate and this will lead to an increase in the number of growing polymer chains. Higher concentrations of initiator result in the synthesis of a greater number of lower molecular weight polymers. This has the effect of reducing

the overall yield of the reaction, as there is a greater chance that the polymeric chains will not be sufficiently cross-linked to be insoluble and will therefore be removed in the post reaction washing process.

The initial phase of the reaction involves the equilibrium of organic phase droplets so polymerization reactions with a relatively low ratio of organic phase: aqueous phase tend to produce very small beads in the suspension because the organic phase is distributed throughout the aqueous phase by stirring. When the ratio of organic: aqueous phase is very high, there is less space between the droplets so droplet equilibrium becomes more rapid. Thus, when the suspension enters the sticky phase it will be more difficult for the suspension to stabilize the droplets, which results in the synthesis of larger non-bead shaped and aggregated material.

The monomers styrene, divinylbenzene and chloromethyl styrene are not soluble in the aqueous phase. There is little doubt that the basic principle of the suspension polymerization is satisfied – that of the organic and aqueous phases being immiscible. Polymers which contain polar or water-soluble groups or monomers are much more difficult to synthesize by suspension co-polymerization. These polymers are sometimes best synthesized by post polymerization functionalisation of the polymer.

2.2 RESULTS AND DISCUSSION

2.2.1 *Perfect beads*

2.2.1.a *Optimization*

After considerable optimization, a system for the synthesis of beads via the suspension polymerization reaction was developed.[vi] By using a gelatin solution as the aqueous phase and employing a 1L 'goldfish' bowl reactor with an anchor stirrer, stirring at 200 rpm beads could be synthesized reproducibly. Using a 2% divinyl benzene cross-linked, chloromethyl styrene and styrene system theoretically loaded at 1.6 mmol functionality/ g of polymer and heating the reaction at 80°C for 16 hours, the yield of

reaction was found to consistently average 70%. It was discovered that even though the product of these reactions was spherical and otherwise 'bead-shaped', there remained the issue that the beads surfaces were not smooth and homogeneous, as viewed using an optical light microscope. There was a clear difference in appearance between these beads (figure 2.9a) and beads of commercial products (figure 2.9b).

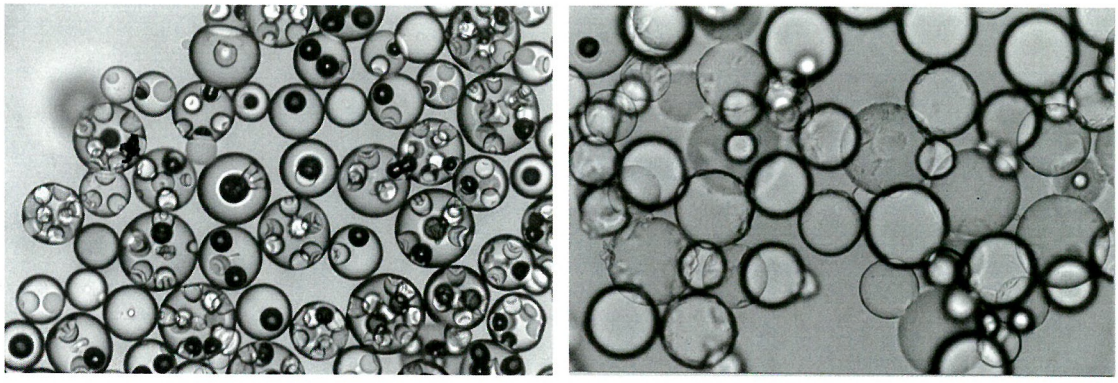

a) *b)*

Figure 2.9: Beads viewed under the optical light microscope. a) These new beads appeared to contain smaller beads inside them, along with the presence of dark spheres. b) Commercial beads (Calbiochem Novabiochem).

The beads, to the naked eye appeared more opaque than the traditional commercial examples of a 2% PS-DVB resin. At first sight, it appears as if there were beads contained within the larger beads. Even when maximally swollen in chloroform and viewed under high power of the optical microscope, it was difficult to obtain additional information regarding the nature and the origin of the light and dark circular areas on the larger beads. However it was possible in some instances to gain different perspectives regarding the phenomenon (figure 2.10).

[vi] For photograph and dimensions, see appendix.

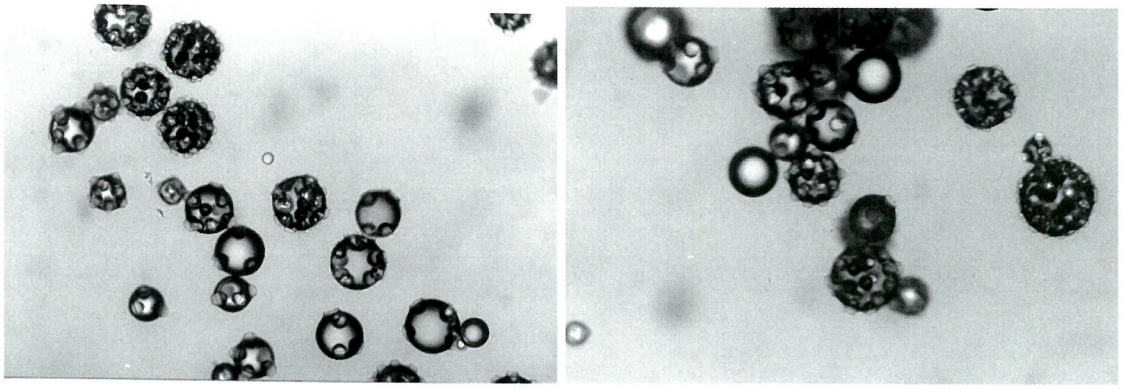

Figure 2.10: Pictures of more irregular beads. Some images revealed the presence of smaller beads associated with the larger beads, not just 'contained' by them.

In order to investigate the nature of the attraction of the smaller beads, a number of qualitative tests were carried out.

2.2.1.a1 *Mechanical agitation.*

By physically shaking the beads in both swelling and non-swelling solvents for 4 hours, it was envisaged that the smaller beads could be removed from the larger ones. This technique remained largely unsuccessful, although a few tiny 'satellite' beads did free themselves from the parents.

2.2.1.a2 *Microscopic manipulation.*

When beads swell, they become less hard and more pliable. It was possible, using tweezers, to physically separate the smaller beads from the larger ones. Whilst it was accepted that this method could never provide a feasible large-scale alternative to the synthesis of beads for SPOC, it was concluded from this study that the 'attraction' described above could be overcome by mechanical forces.

2.2.1.a3 *Coulombic forces*

The addition of a solution of NaCl in various concentrations to a suspension of the beads and performing mechanical agitation to disrupt the attraction between the satellites and the parents, did not result in quantitative separation.

2.2.1.a4 *Sonication*

Immersing the beads in both swelling and non-swelling solvents in an ultrasonic bath for various periods of time (1, 5, 10, 30, 60, 180 minutes) provided the most effective solution in terms of the separation of the satellites from the parent, but the effect was not quantitative and did not completely restore the surface of the perfect beads. It appeared that the surface of the beads had been permanently disrupted, possibly during the polymerization process. Detachment of the satellites was also seen to 'scar' the surface of the beads.

2.2.1.b *Visualization - electron microscopy*

Optical microscopy provided only limited information regarding the surface of the beads, and could not provide any information as to whether there were smaller beads contained within the larger beads. Electron micrographs of the beads were therefore taken.

2.2.1.b1 *The process*

Scanning electron microscopy (SEM) is primarily used for the study of topography in bulk samples.[156] In SEM, an electron gun 'fires' a beam of electrons (which first pass through a condenser lenses and the objective lenses into an aperture) onto a sample. The lens system reduces the beam diameter to give a spot of only a few nanometers on the sample, while a detector monitors energetic emissions from the sample. The most common viewing protocol in SEM is secondary electron image (SEI). Inelastic scattering from the primary electron beam with the sample occurs when valence

electrons are ejected from atoms in the sample. These secondary electrons have energies of up to 50 eV and originate between 5-50 nm below the surface of the specimen. Backscattering occurs when primary electrons undergo elastic collisions with the sample and as a result can have energies of up to 15 KeV. The back scattered electron (BSE) detector records only signals from directly in front of the sample, so the SEI image collected may be described as looking at the sample as if it was being illuminated with a spot light or torch. This image is not well resolved, as the more energetic BSE can originate from up to 500 nm below the surface of the sample. In practice, real time images are obtained because a cathode ray tube (CRT) is scanned with the detector, with the brightness of the image given by the intensity of the image from the detector. The highest magnification is approximately x300000 using a small 3.5nm probe, but in practice, the probe diameter is increased to match the CRT pixel size (thus reducing the available magnification).

2.2.1.b2 *Sample preparation*

Typically the sample is coated in a thin layer of gold to ensure adequate conduction, as build-up of charge on the sample causes distorted and noisy images. Gold clustered onto the samples becomes visible at magnifications of approximately x75000 so for viewing beads coated in this way, magnifications lower than this are optimal for bead visualization.

Resin samples were prepared for SEM analysis by coating the resins with a 20 nm layer of gold (by vacuum gold sputtering) and the following images recorded (figure 2.11).

2.2.1.b3 *Pits and craters/ satellites and parents*

The images shed a great insight into the nature of the surface of the beads (figure 2.11a-d). The increased resolution afforded more information about the interaction between the satellites and the parent beads (figure 2.11e). The transparent circular areas shown in the optical photographs in figure 2.10 corresponded to regions in the

electron micrographs where there were smaller beads adhered to the larger beads. The opaque and darker regions in the optical photographs corresponded to regions on the electron micrographs where there were 'crater-like' scars on the surface of the beads. This evidence suggested that during the suspension, the smaller beads impacted the larger ones and remained together. The presence of the craters suggested that adhesion between the large and small beads had occurred and some of these beads had broken away after significant polymerization had occurred. This theory did implicate an inadequate suspension, but this would only hold true if the pitting effect was not continuous throughout the bead structure.

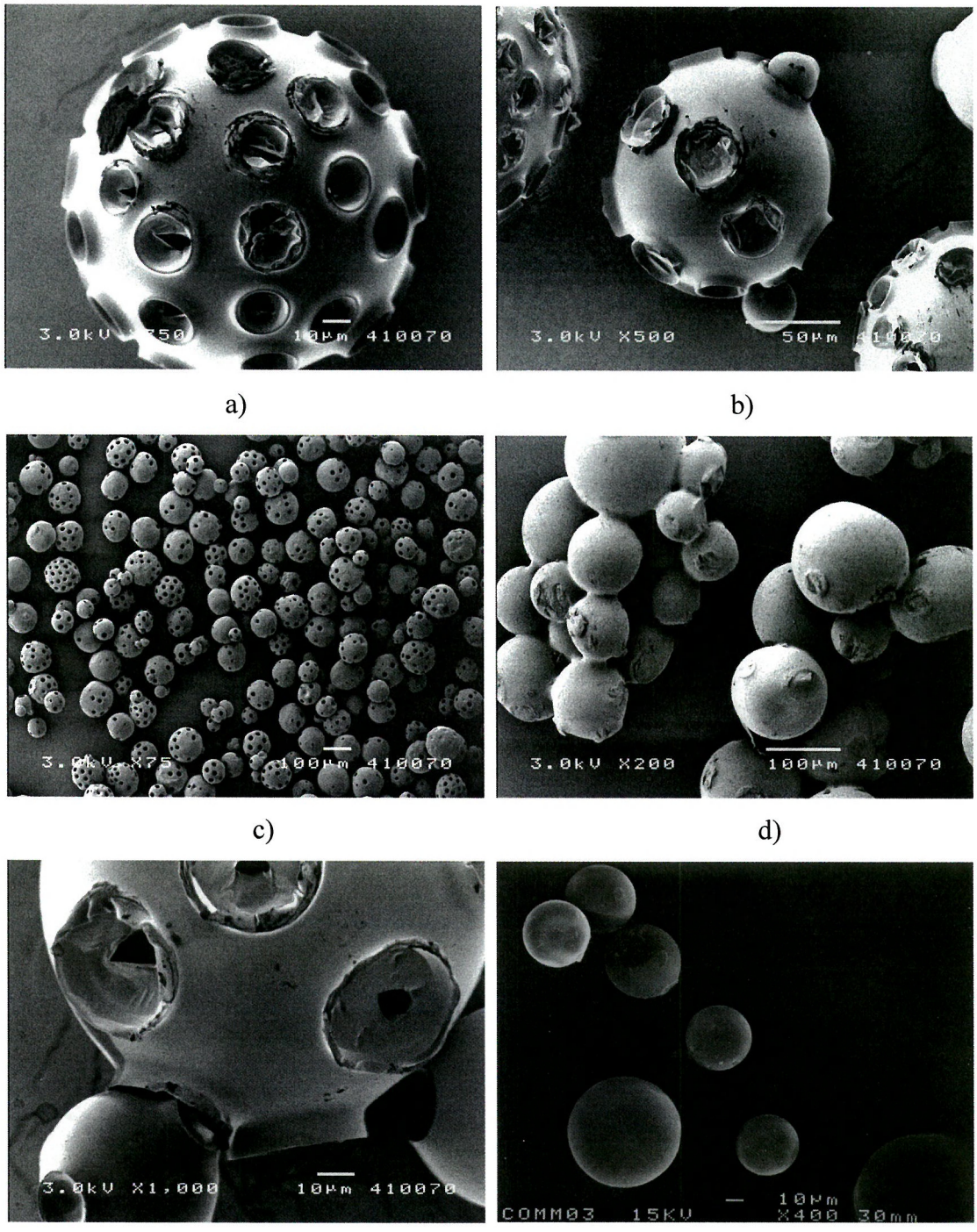

Figure 2.11: a-e) Electron micrographs of the pitted beads, f) micrograph of commercial quality Merrifield resin.

In order to investigate this, SEM SEIs of cross-sections (figure 2.12) and fragments of the pitted beads (figure 2.13) were recorded. Samples for cross-sectional analysis were taken by imbedding the resin beads in the commercially available TAAB resin mixture (used in the setting of biological samples) and heating. Once set, thin samples of the beads were sliced from the resin block using a glass knife in a Cambridge Monotome Rocker. The slices of beads were then prepared for SEM analysis using the gold sputtering method mentioned above.

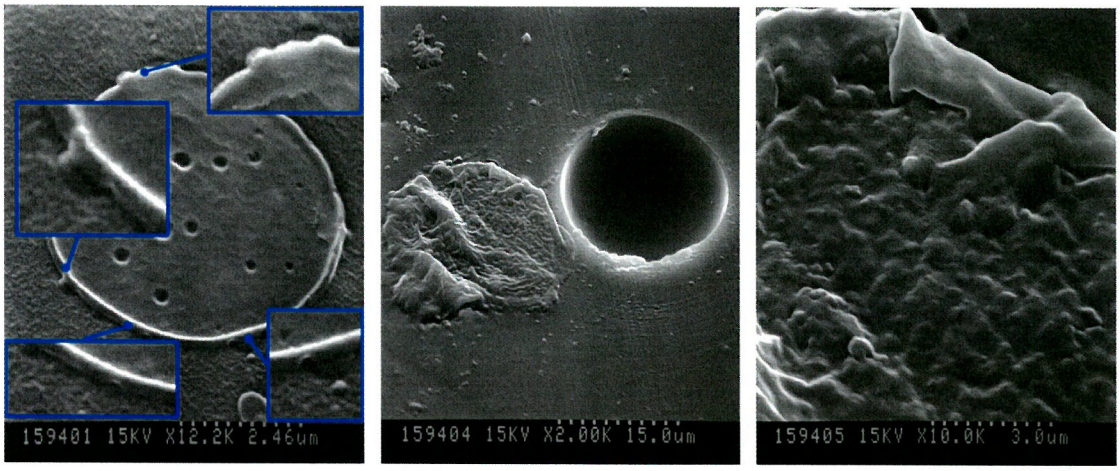

a) *b)* *c)*

Figure 2.12: Electron micrographs of sections of Merrifield resin.

The images show that the craters are localized on the surface of the beads (figure 2.12a), and that the centers of the beads are homogeneous (figures 2.12b + 2.12c). The dark depressions/ indentations visible in figure 2.12a represent air spaces formed within the matrix due to the evaporation of the diluent toluene, added during the polymerization. Diluent is often added to the organic phase to reduce surface tension at the droplet surface during suspension polymerization reactions, which assists in bead formation. The beads in figures 2.12b and 2.12c were synthesized without the aid of a diluent. In figure 2.12b, the 'bead slice' was displaced from the resin during the cutting process, revealing a void. Indentations on the surface of the bead are also visible at the edges of the void and show that even without diluent, these craters and imperfections can occur at the beads surface.

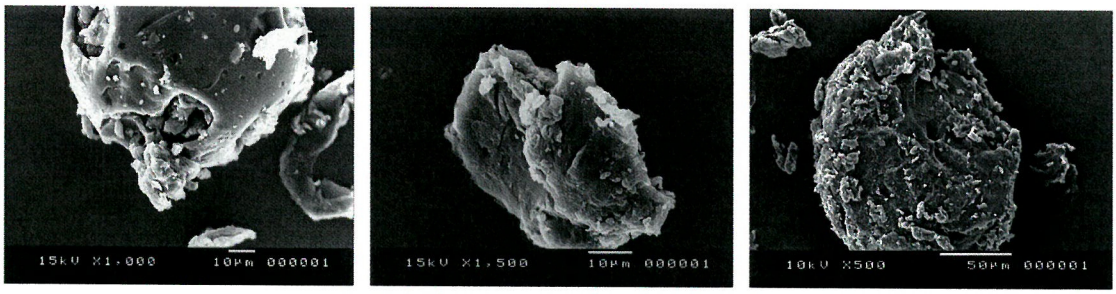

a) *b)* *c)*

Figure 2.13: SEM images of bead fragments.

Cooling a sample of beads in liquid nitrogen and then shattering them with a pestle and mortar afforded bead fragments. These fragments were collected and prepared by SEM analysis using the gold sputtering method described above.

By identifying the surface of the beads in the SEIs, it was possible to see that there were no instances of pitting just below it (figure 2.13b). The pitting present in figure 13a is not visible under the surface of the beads, shown in figures 2.13b and 2.13c.

2.2.1.c *The solution*

During early suspension optimization experiments using a two-component organic monomer system comprising of styrene and divinyl benzene it was noted that beads of commercial quality with homogeneous surfaces were synthesized fairly readily.

The presence of chloromethyl styrene caused the unexpected difference in the surface appearance of the beads (figures 2.10 and 2.11). This observation confirms the belief that the chemical and the physical parameters of the suspension polymerization are related. These effects were observed even when changing from gelatin to the more chemically defined PVA suspension system. It was decided that PVA would be used to minimize the uncertainty in the nature of the suspending agent. Gelatin is a natural product, extracted commercially from a variety of animal sources, with porcine origin being most common. Different combinations of reactor geometry and different stirrer geometries and speeds were utilized in order to create suspension conditions that would alleviate the pitting problem, but they all had varying degrees of success and

were non-repeatable. It seemed as if the factors previously identified and reported in the literature as being crucial in the suspension polymerization reaction actually carried different weightings. Experiments were performed using combinations of un- and pre-washed monomers, which were distilled or not distilled prior to use, with the suspension being both degassed and un-degassed, but again these experiments resulted in non-reproducable successes.

2.2.1.c1 *pH of suspension*

The pH of the suspension was monitored during a suspension polymerization reaction with surprising results. With chloromethyl styrene included in the organic phase, the pH of the suspension fell during the reaction by 5-7 pH units (figure 2.14).

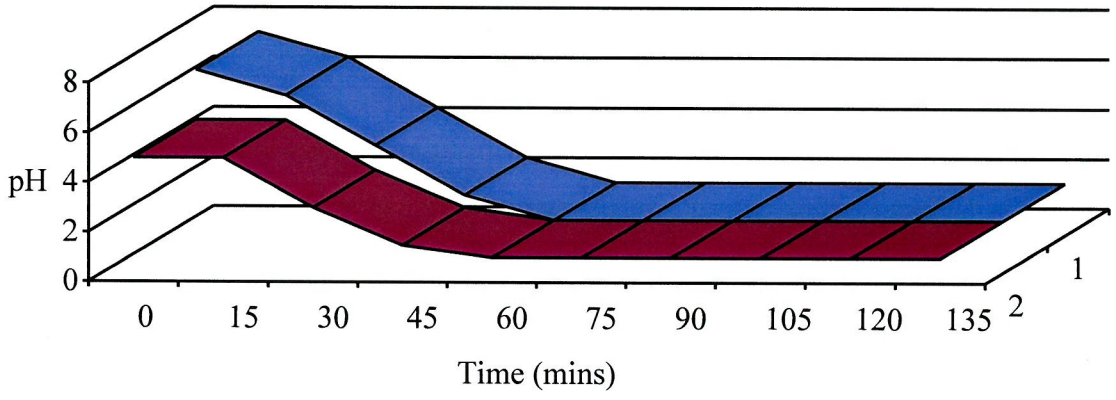

Figure 2.14: The change in pH observed when chloromethyl styrene was included in the suspension polymerization organic phase. Entry 1) Tap water was used in the polymerization. Entry 2) Distilled water was used in the polymerization.

By systematically substituting components of the styrene/ divinyl benzene/ chloromethyl styrene/ benzoyl peroxide/ PVA system and monitoring the pH on heating, critical results regarding the interactions that gave rise to the increase in suspension acidity were revealed.

A solution of PVA, PVA+benzoyl peroxide, PVA+chloromethyl styrene and PVA+benzoyl peroxide+chloromethyl styrene were heated and the resulting pHs of the suspension monitored (figure 2.15).

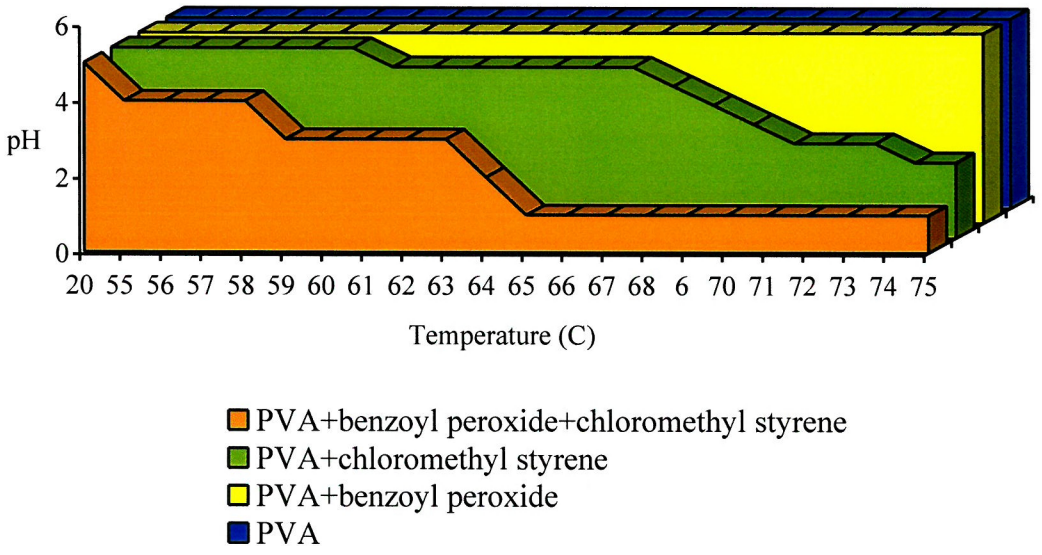

Figure 2.15: The effect on pH of the suspension interactions of chloromethyl styrene, benzoyl peroxide and PVA.

From this data it was possible to determine that an increase in acidity, possibly due to the hydrolysis of chloromethyl styrene in PVA solution occurred, even in the absence of benzoyl peroxide, but in the presence of benzoyl peroxide it is accelerated 10-100 fold. Over the course of a suspension polymerization reaction, this increase in acidity may be significant, especially if it was determined that acidity could affect the surface appearance of a bead. This hypothesis was tested. Suspension polymerization reactions were conducted in the presence and the absence of dibasic sodium phosphate. The pH of the suspension and the nature of the beaded resin product were monitored (figure 2.16).

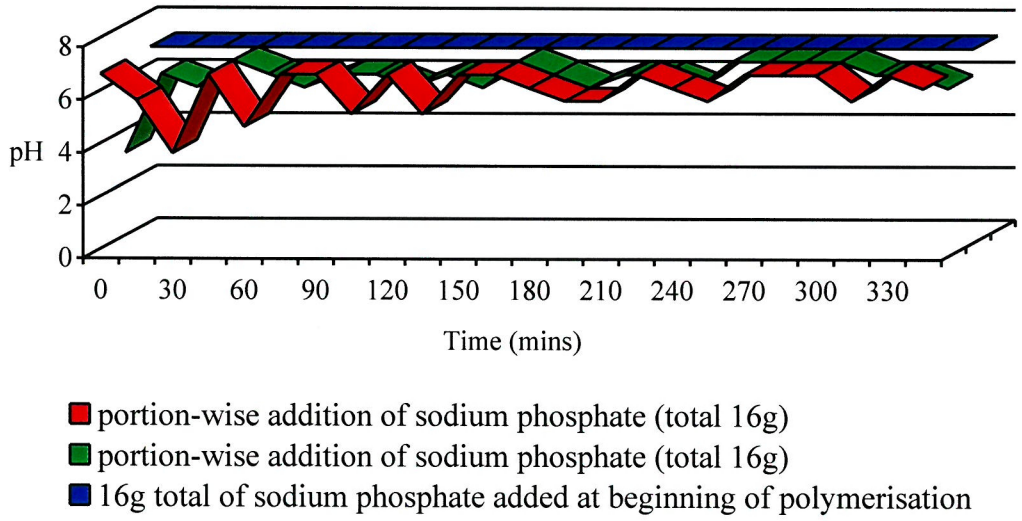

Figure 2.16: The effect of Na_2HPO_4 on the pH of the suspension during polymerization Note: Entries a+b) sodium phosphate added during the polymerization. Entry c) 16g sodium phosphate added at the start and the system left unperturbed for 16 hours.

The beads in each of these experiments were visually perfect (figure 2.17) and had chemical loadings of 0.5 mmol/ g compared to the theoretical loading of 1 mmol/ g. Figure 2.17 shows optical photographs of crude suspension aliquots with undissolved PVA shown as amorphous particles in-between the beads.

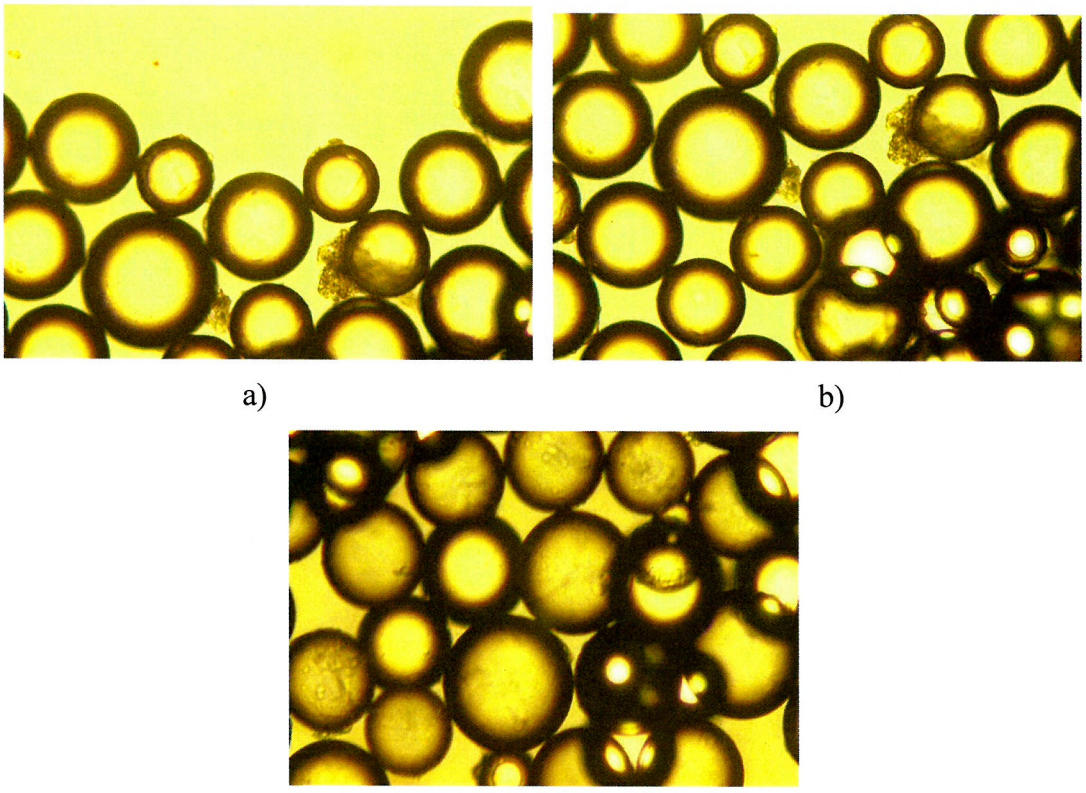

a) b)

c)

Figure 2.17: a-c) Optical photographs of the beads produced by the suspension polymerization reactions described in figure 2.16(a-c).

2.2.2 *Synthesis of a range of cross-linked beads*

Using a styrene/ chloromethyl styrene/ and divinyl benzene system, a range of beads was synthesized by suspension polymerization. The amounts of divinylbenzene were varied with an inverse-proportion relationship to the styrene, to produce 11 batches of PS-DVB beads cross-linked at 0.3%, 0.6%, 0.9%, 1.2%, 1.5%, 1.8%, 2.1%, 2.4%, 2.7%, 3.0% and 6.0%.

2.2.2.a *Yields of reaction*

The chemical yield of the reaction increased with increasing resin cross-linking (figure 2.18).

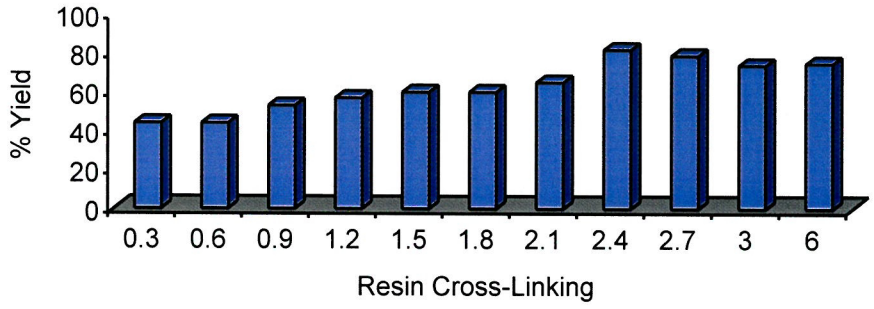

Figure 2.18: The yield of bead product increased with increasing resin cross-linking from 44% in the case of the 0.3% resin to up to 80% in the case of the highest cross-linked resins (2.4-6.0%).

Increasing the amount of divinylbenzene in suspension increases the potential for cross-linking in the developing strands of polymer, thereby increasing their insolubility. It may then be envisaged that lower cross-linked resins, after polymerization, contain a higher proportion of soluble polystyrene than the more highly cross-linked resins. The soluble polystyrene components are washed out of the resin as part of normal post-polymerization processing and cleaning of the beads.

2.2.2.b *Size distribution of beads*

Due to the nature of the polymerization reaction, specifically the random way in which droplets in suspension collide and reform (which is governed by stabilization interactions afforded by the suspending agent), and due to the fact that at any stage during the polymerization, a radical terminator can effect a ceasing of the reaction, the beads synthesized by the suspension polymerization reaction vary in size. Beads of different cross-sectional diameters are produced and it is usual practice after washing to sieve them before performing chemistry on them. Each of the batches of resins represented above (figure 2.18) were sieved using 500 μm, 355 μm, 250 μm, 125 μm, and 45 μm sieves and the size distribution plotted (figure 2.19).

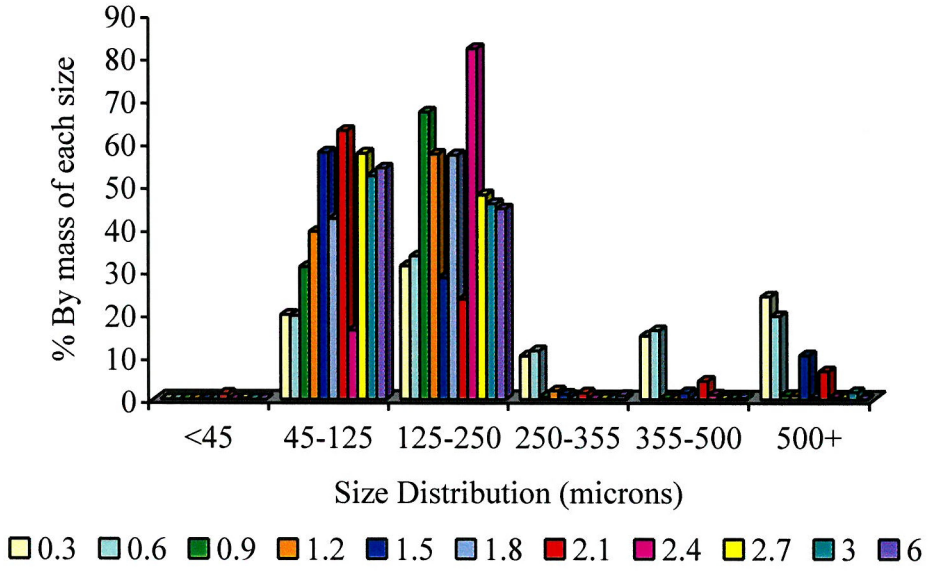

Figure 2.19: Size distribution of the 11 cross-linked resins.

Even though conditions of synthesis had been optimized for maximum yield of beads, the varying cross-linked resins showed varying tendencies with respect to bead size. As indicated above, beads less than 45 μm in diameter were unsuitable for the majority of chemical applications due to the very small size. They caused frits to clog and blocked glass sinters. During optimization the stirrer speed was adjusted to minimize production of these particles. As a result there is no real surprise to see that by mass, the proportion of material isolated in this size range was negligible. The majority of the beads produced by each of the experiments were within the 45 – 250 μm size range. These beads were also easiest to manipulate. The suspension conditions also appeared to favor the synthesis of larger beads in the lowest cross-linking categories (0.3% and the 0.6% beads). It may be the case that for any given PVA suspension polymerization system, the dynamics are such as to afford greater stability to larger, less cross-linked beads, and smaller more highly cross-linked beads.

2.2.2.c *Swelling studies*

Swelling parameters are an essential descriptive physical property for beads, and are especially important in verifying the integrity of a series of resins. 100 mg of each of the resins (45 – 125 μm) was swollen in a range of solvents commonly used in SPOC

and also in typical solution phase reaction solvents. The swelling parameter of each of the resins in different solvents was measured (figure 2.20). The dry volumes were found to correspond to the swelling parameters obtained for the acetonitrile series, as acetonitrile was not effective in swelling the resins.

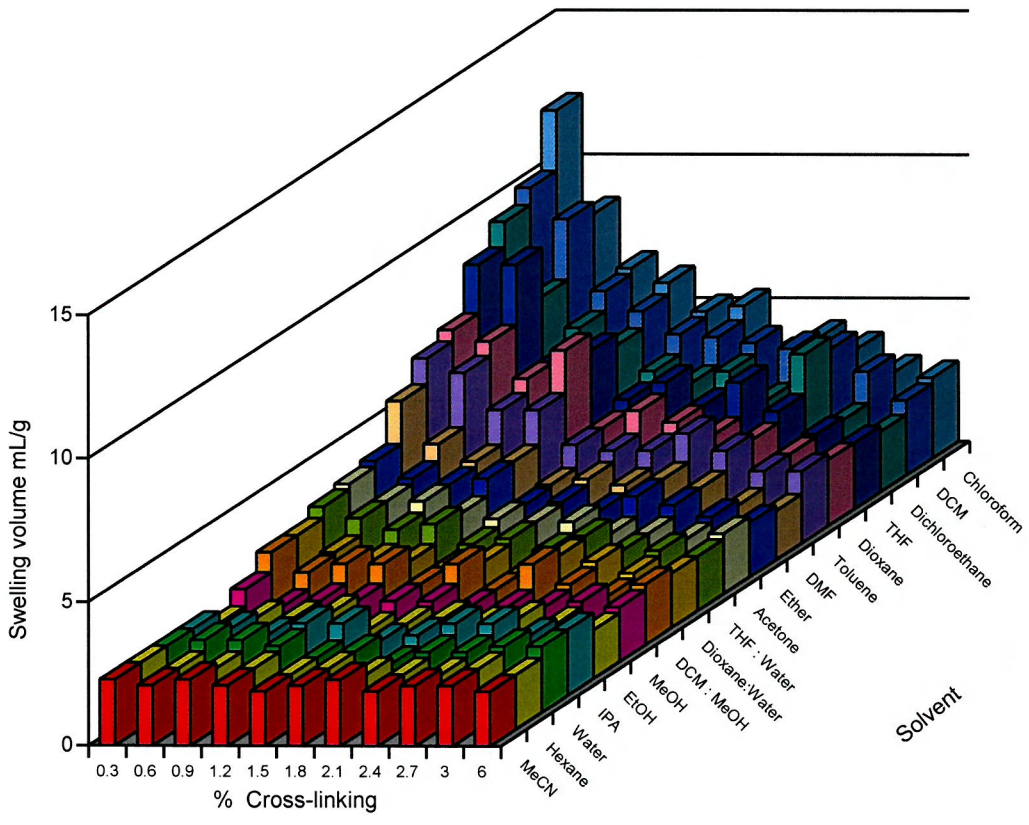

Figure 2.20: Swelling of the resins in a range of common SPOC solvents.

Reactive site accessibility is related to resin swelling, so it is fitting to observe from figure 2.20 that the solvents commonly applied to SPOC today are amongst the solvents which swell the resins most (dichloromethane, THF, dioxane, dimethylformamide, DMF). The data in figure 2.20 also shows that chloroform, DCM and dichloroethane are the best solvents for swelling the entire range of PS-DVB resins, although with increasing cross-linking, the percentage increase in volume on transition from the dry to the swollen state becomes smaller. Tetrahydrofuran (THF), dioxane, toluene and DMF - although excellent solvents for organic compounds, swelled the resins by up to 30-50% of their maximal value. Protic and polar solvents

were not effective in swelling any of the resins, and in the case of acetonitrile (MeCN), there was doubt whether the solvent was able to wet the resin. 'Good' solvents, when mixed with 'bad' solvents, cause massively reduced swelling characteristics, for example in the case of the 0.3% cross-linked resin, notable swelling characteristics were: THF (8.5 mLg^{-1}), water (2.3 mLg^{-1}), THF/ water (3.5 mLg^{-1}), and dioxane (6.8 mLg^{-1}), dioxane/ water (3.2 mLg^{-1}) and DCM (10 mLg^{-1}), MeOH (2.5 mLg^{-1}), DCM/MeOH (3.2 mLg^{-1}). From this, it is possible to infer that in order to allow a solid phase reaction to occur in a solvent that does not swell the resin well or even wet it, the addition of a solvent that does swell the resin more effectively, is paramount.

2.3 CONCLUSION

Having synthesized a range of differently cross-linked resins by suspension polymerization and investigated the relationship between crude yield of beads and size of beads produced with cross-linking, samples of beads with diameters of 45 - 125 μm micrometers were selected and then their integrity as a series of resins investigated by swelling. It was now possible to investigate the behavior of the series in chemical reactions.

CHAPTER 3 - CYCLIC PEPTIDES

3.1 INTRODUCTION

Because of the long history of peptide synthesis and a huge choice in building blocks, SPPS methods have allowed peptides to become ideal synthetic targets. For example, Bayer, Hagenmaier, Jung, and König[157] have synthesized many linear peptides including oxytocin and the 55 amino acid residue peptide ferredoxin **(31)** by these methods. The sequence of ferredoxin (figure 3.1) contains the electron transfer activity from *clostridium pasteurianum* and was determined by Tanaka[158] as long ago as in 1966.

^{1}Ala-Tyr-Lys-Ileu-^{5}Ala-Asp-Ser-Cys-Val-^{10}Ser-Cys-Gly-Ala-Cys-^{15}Ala-┐
└Ser-Glu-Cys-Pro-^{20}Val-Asp(NH_2)-Ala-Ileu-Ser-^{25}Glu(NH_2)-Gly-Asp-┐
└Ser-Ileu-^{30}Phe-Val-Ileu-Asp-Ala-^{35}Asp-Thr-Cys-Ileu-Asp-^{40}Cys-Gly-Asp(NH_2)-┐
└Cys-Ala-^{45}Asp(NH_2)-Val-Cys-Pro-Val-^{50}Gly-Ala-Pro-Val-Glu(NH_2)-^{55}Glu

(31)

Figure 3.1: Amino acid sequence of ferredoxin according to Tanaka.

The structure of the antibiotic gramicidin S was elucidated over 50 years ago and found to be cyclic.[159] Today cyclic peptides offer viable targets for synthesis by solid phase methods, although they are often non-trivial in nature. In their 1997 synthesis of Oscillamide Y, Marsh and Bradley[160] demonstrated the synthesis of a cyclic peptide serine protease inhibitor **(32)**. Similar in structure to other cyclic peptides such as bacitracin A, glidobaktin and konbamide, Oscillamide Y (figure 3.2) is a cyclic hexapeptide produced by the cyanobacterium *Oscillatoria agardhii* and is reported to be a potent inhibitor of chymotrypsin.[161]

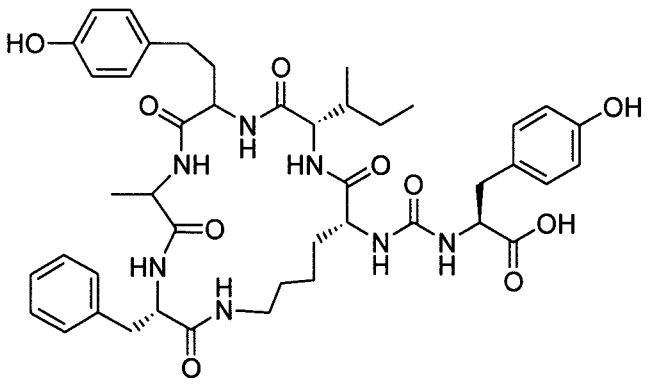

(32)

Figure 3.2: Oscillamide Y.

Cyclic peptides have also gained particular interest as targets for synthesis following the realization that many biologically active peptides are also cyclic compounds. When compared to their free linear forms, these cyclic peptides have constrained flexibility[162] and increased metabolic stability, as many degradative enzymes require free termini in order to perform their hydrolytic cleavages.[163] The size and shape of a substrate also makes enzyme accessibility, i.e. metabolic stability an issue.

3.2 SYNTHESIS OF CYCLIC PEPTIDES

Classical methods of preparation of cyclic peptides involve cyclisation of unprotected linear precursors in solution under conditions of high dilution, but these methods suffer the drawbacks of being low yielding due to oligomerization and also because the products of reaction are often difficult to separate from the starting materials.[164]

Cyclisation of a linear peptide while attached to the solid support has been reported in the literature and has proved to be a very successful technique for solid phase cyclic peptide synthesis.

3.2.1 *Protecting groups*

Because of its insoluble and non-reactive nature, the solid phase can be regarded as a protecting group in itself. Protecting group strategies have developed resulting in the

creation of well-defined sets of orthogonal protecting groups. The principle of orthogonality is exemplified in the schematic synthesis of a dipeptide and subsequent cleavage from the resin shown in figure 3.3.

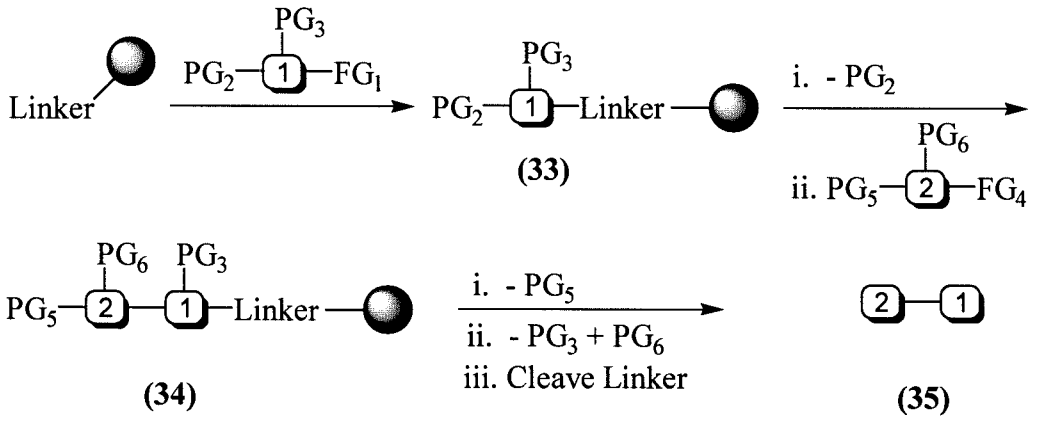

Figure 3.3: The principle of orthogonality as applied to the solid phase synthesis of a dimer. Note PG = protecting group, 1+2 = amino acid residues.

The final steps of the synthesis, i.e. the removal of protecting groups PG_3, PG_6 may be combined with cleavage of the product from the linker. Prior to activation, the resin bound *N*-terminal protecting groups PG_2 in **(33)** and PG_5 in **(34)** are cleaved and the next residue loaded onto the resin. PG_6 and PG_3 are amino acid side chain protecting groups and after synthesis they can be removed to expose the original functional groups. Orthogonality is achieved because PG_2 can be cleaved in the presence of PG_3 in **(35)** or *visa versa* and the next amino acid loaded onto the solid phase.

3.2.2 *Cyclisation*

The methodology outlined in section 3.2.1 can be applied to the synthesis of cyclic peptides **(38)**, for example if a resin bound linear 6-mer consisting of amino acids with side chain protection is generated **(36)** and the orthogonal allyl and Fmoc groups selectively cleaved and appropriately activated, cyclisation will occur (figure 3.4).

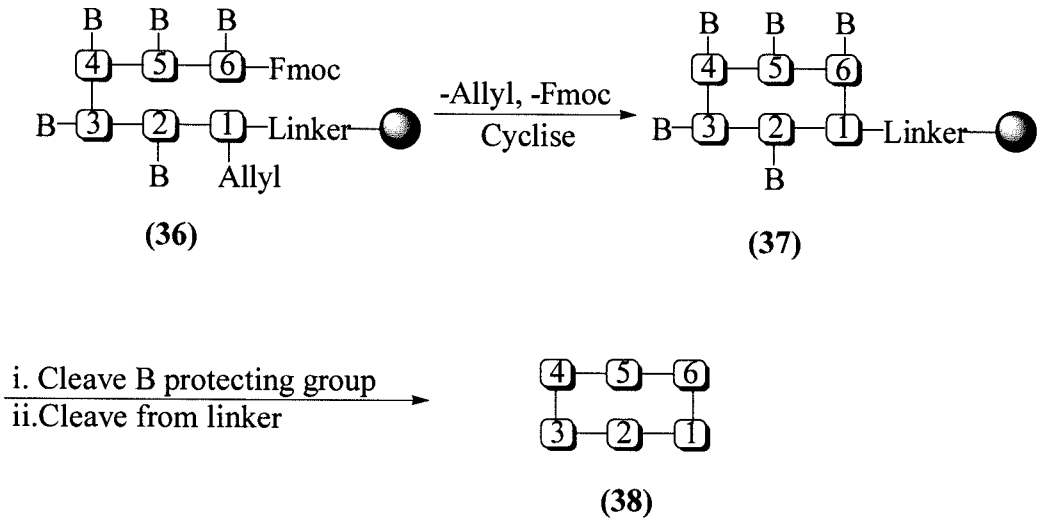

B = ^{t}Butyl ether, ^{t}Butyl ester or Boc amino acid side chain protecting group

Figure 3.4: Adaptation of orthogonal protecting group strategies to synthesize cyclic peptide.

The base cleavable Fmoc group[165] can be used to protect the *N*-terminal of the peptide chain, with orthogonal acid-cleavable protecting groups (*t*-butyl ethers, *t*-butyl esters and Boc groups) used to protect amino acid side chains. The linker chosen for the synthesis is acid labile so that cleavage of peptide **(38)** can occur in one step with deprotection of the side chain protecting groups.

In one of the earliest examples of this, Albericio[166] described 'a novel, convenient three dimensional orthogonal strategy for solid phase synthesis of cyclic peptides. He side-chain anchored a partially protected amino acid residue to a resin (via both the acid cleavable PAC and PAL linkers), and then applied a stepwise solid phase peptide synthesis methodology followed by orthogonal deprotection to yield an α-C carboxyl group. He then activated the free α-C carboxyl group and facilitated cyclisation by condensation with the free *N*- terminal amino group. He synthesized the decapeptide **(39)** by four synthetic strategies, which involved anchorage to the solid support at each of the possible side chain attachment points shown in figure 3.5.

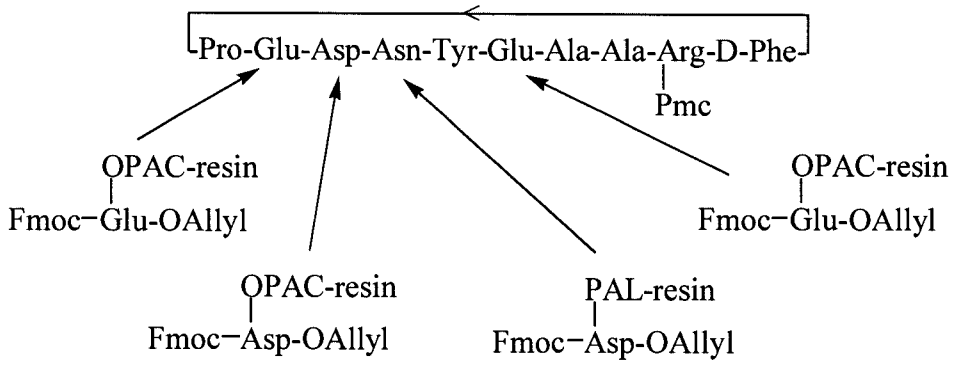

(39)

Figure 3.5: Structure of the target decapeptide and synthesis via four synthetic methodologies.

The amino acids not used for attachment to the solid support were protected by a ^{t}butyl ester group or, in the case of the Asn residue, a trityl protecting group.

Trzeciak and Bannwarth[162] have also reported a head to tail cyclisation to form cyclic peptides **(40 + 41)** by side chain attachment of an Asp residue generating an amide or a carboxylic acid group with the α-carbonyl orthogonally protected as an allyl ester group (figure 3.6).

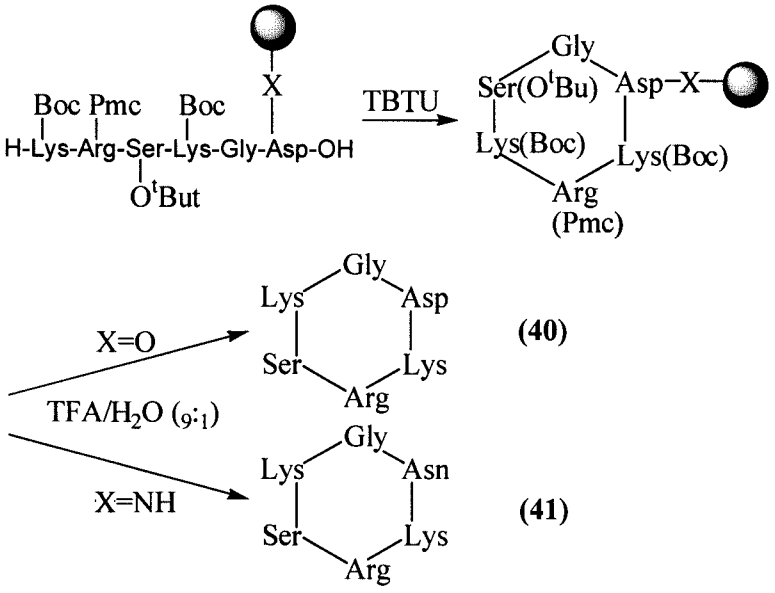

Figure 3.6: Synthesis of cyclic peptides by a head to tail cyclisation method. Note X = variants on the Kaiser oxime linker which allow termination in hydroxyl (X=O) or amid (X=NH) groups on cleavage.

Cyclisation of peptides on the solid support has been achieved using both Boc peptide synthesis strategies[167,168] and in keeping with the popularity of Fmoc chemistry many examples of solid phase cyclisation reactions involving Fmoc chemistry have thus been reported.[169,170] Cyclisation from linear unprotected peptide precursors via thiazolidine formation has also been reported.[171]

These examples have illustrated a fundamental mode of cyclisation: the head to tail (-NH_2 terminal to -CO_2H terminal) cyclisation. Side chain to side chain cyclisations have also been reported.[172] Typically the acidic side chain (e.g. from an aspartic acid residue) of a resin bound peptide is activated to allow cyclisation by an amino terminal (e.g. from a lysine residue) of an amino acid in the chain in a manner analogous to that described in figures 3.5 and 3.6.

3.3 SITE- SITE INTERACTIONS

In an attempt to investigate site-site interactions on resins Mazur and Jayalekshmy[173] conducted studies on the frequency of 'encounters' between substituents on various polystyrene supports. They demonstrated that benzyne derivatives undergo rapid dimerization in solution to form **(42)**, but dimerize significantly slowly when supported on a polymer. In fact, when they analyzed the products of their solid phase reactions, they discovered that the reactive benzyne intermediates formed in the solid phase reaction were so long lived that they found other reaction paths forming **(43)** (figure 3.7).

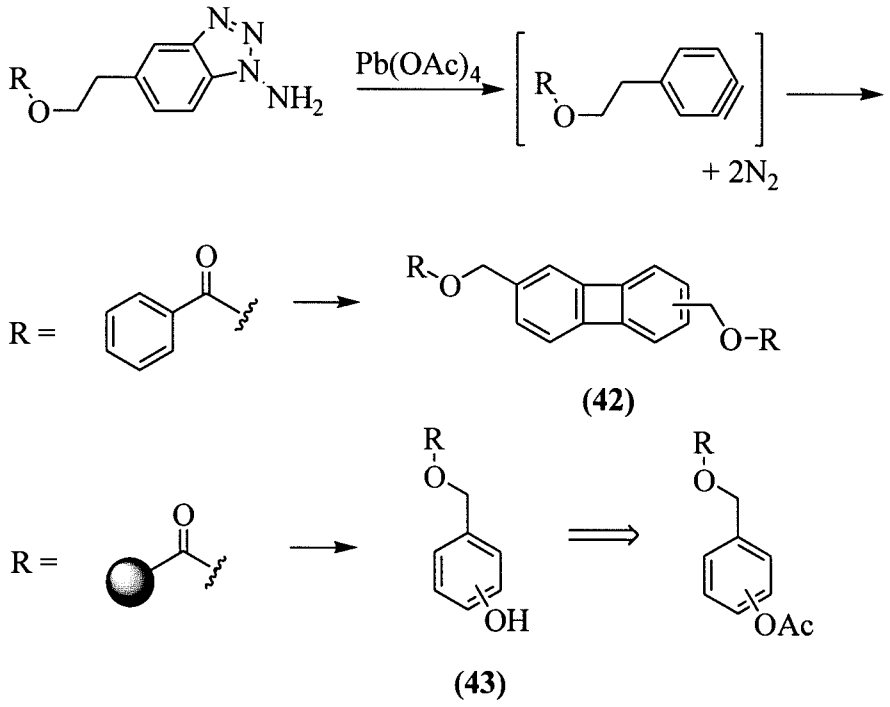

Figure 3.6: Reaction of benzyne and the analogous solid supported benzyne. The resin used was 2% cross-linked PS-DVB.

Although Mazur and Jayalekshmy reported that the reaction was probably not as trivial as summarized above, they were able to conclude from these and other kinetic experiments that the lifetimes of the benzyne derivatives lied in-between the upper and lower limits of the encounter frequency, between 2.6×10^{-2} and $1.1 \times 10^{-3} s^{-1}$. This was consistent with encounter limited bimolecular reactions carried out in non-viscous solvents at concentrations of approximately 1×10^{-11} mol dm^{-3}. As they used approximately 0.1 mmol of reagent in only a few mL of solvent (approx 0.1 mmol dm^{-3}), they concluded that anchorage to the solid support provided the dilutional characteristics observed in the reaction (the so-called 'pseudo-dilution' phenomenon).

The issue of site-site interactions in SPOC has been described in the literature by other groups with varying results. Some have found that standard 2% PS-DVB polymer provides adequate reactive site isolation,[174,175] whilst many other groups[176,177] have reported that this is not the case. Scott and Rebek[178] showed that by reacting a series of PS bound carboxylic acids **(44)** with DCC in DCM and monitoring anhydride **(45)** formation, site-site interactions on a series of cross-linked resins (1%, 2% ,4% PS-

DVB) did exist and were present, although to a lesser extent on the lower cross-linked resins (figure 3.7).

(44) **(45)**

IR: 1685 $cm^{-1}_{(acid)}$, 1715 $cm^{-1}_{(acid)}$

IR: 1785 $cm^{-1}_{(anhydride)}$, 1720 $cm^{-1}_{(acid)}$

Figure 3.7: Investigation of site-site interactions by monitoring the solid phase synthesis of carboxylic anhydrides using DCC.

The resins that they used were typical PS resins of the day, used in synthesis and loaded at 1 mmol of functionality per gram. Their study raised the issue of whether it was the resin cross-linking, or the physical density of functional sites that was more significant in contributing to anhydride formation.

3.4 DILUTIONAL EFFECTS AND FUNCTIONAL GROUP MOBILITY

Using a 2% cross-linked resin with a very low loading[i], Kraus and Patchornik[179] showed that polymer bound molecules can behave as an infinitely dilute solution, even though the actual physical concentration of sites in the beads may be relatively high. They also demonstrated that at sufficiently high concentrations (the concept is similar in principle to that of the [EM] (described below)) resin bound substrates can interact.[180] They treated a highly cross-linked 2% PS-DVB Merrifield resin with a limited amount of enolizable acid forming **(46)**, and then an excess of non-enolizable

[i] 0.1 mmol - 0.3 mmol of functional sites per gram of polymer (10% -30% of loading capacity of the resin used by Scott and Rebek).

acid to generate **(47)**, which contained a relatively high concentration of esters (figure 3.8).

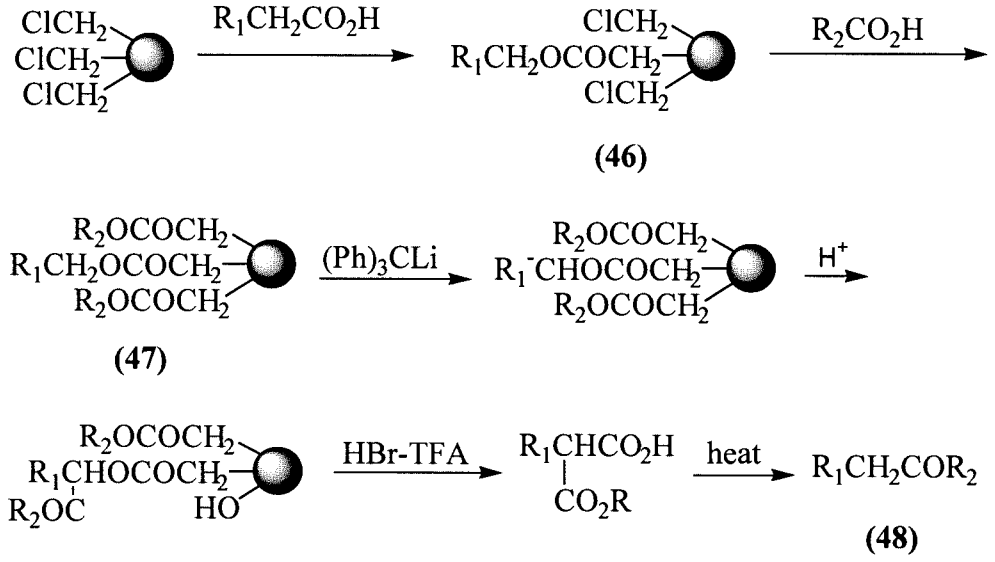

Figure 3.8: Kraus and Patchornik's mixed ester condensation of two acids bound to a polymeric backbone.

Using various R groups, the yields of product **(48)** were observed to be consistently greater than the analogous solution phase reactions. In the case of R_1 = $C_6H_5(CH_2)_2CO_2H$ and R_2 = *p*$ClC_6H_4CO_2H$ the yield of ketone *p*$ClC_6H_4CO(CH_2)_2C_6H_5$ was 85% compared to only 20% for the solution phase reaction. In the case of R_1 = $C_6H_5(CH_2)_2CO_2H$ and R_2 = $C_6H_4CO_2H$ the solid phase reaction yield was 85% compared to 42% in the analogous solution phase reaction. The higher reaction yields represent enhanced steric crowding afforded by the resin (approx 1.5- 2.0 mmol/ g) during the proton abstraction step by trityl lithium.

Grubbs[181] chelated a chlorobis(cyclooctadiene)rhodium(1) dimer with a three-fold excess of polystyryl-diphenyl phosphine. A 20% cross-linked PS-DVB resin released 1.4 mol of bound cyclooctadiene ligand per mole of rhodium complex absorbed by the resin, whilst a 2% cross-linked PS-DVB resin released 2.0 mol per mole of metal complex absorbed. Thus the higher cross-linked resin afforded a lower degree of mobility upon bound functional groups and this was reflected in their ability to bind

the rhodium catalyst. They reported that the 2% cross-linked resin gave the same result as the treatment of 1 mol of the cyclooctadiene dimer with three equivalents of triphenyl phosphine in solution.

Regen[182] covalently attached a nitroxide to a polymer **(49)** (figure 3.9) and, by measuring the rotational correlation times from electron paramagnetic resonance (EPR) spectra, established that as the degree of swelling[ii] in a polymer increases, the rotational correlation time decreases (indicating an increase in mobility).

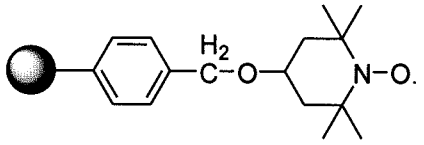

(49)

Figure 3.9: The nitroxide ESR label used by Regen.

3.5 CYCLISATION VS OLIGOMERIZATION

SPPS chemists were really thrust into a field more akin to macrocycle chemistry when it came to the synthesis of cyclic peptides. It had long been known that a side reaction of macrocyclisation in solution phase chemistry is oligomerization and on the solid phase the formation of linear di-, tri- or oligomers instead of cyclic monomers can be a real risk.[183] In a related study, Hodge[184] has described the concept of effective molarity (EM), which is the concentration at which the rate of inter- and intra-molecular reactions become equal. In his study, in a supported ω-bromoalkanoic acid system, lactonization was observed to be more rapid below the [EM], and intermolecular reactions forming oligomers were more rapid above the [EM].

The concept can be applied to solid supported peptides. The [EM] for specific peptides could be investigated by determination of the cyclic/ oligomeric product ratio after cleavage of a solid supported cyclisation reaction. The carbon nitrogen bond of the amide bond has partial double bond character due to resonance, so rotation about a

[ii] Defined as swelled polymer volume/ dry polymer volume.

peptide bond is difficult. Rotation is however possible about the two bonds from the α-carbon atom of the amino acid residue, thus a peptide molecule as a whole is very flexible. Certain peptides may contain residues which give its overall structure a propensity to form either cyclic monomers or polymers.

In peptide synthesis the presence of a glycine or proline residue in a linear peptide sequence is known to induce turns, specifically type II β turns in peptide chains.[185] Proline residues induce a conformational change in a peptide chain due to the rigid N-C-C bond angle and restriction of rotational freedom **(50),** in fact proline is considered to be 'locked' into a single conformation (figure 3.10). Glycine on the other hand, not possessing a side chain, has many more degrees of freedom, which allow many more structures to be explored **(51)** i.e. glycine is a much more 'flexible' residue.

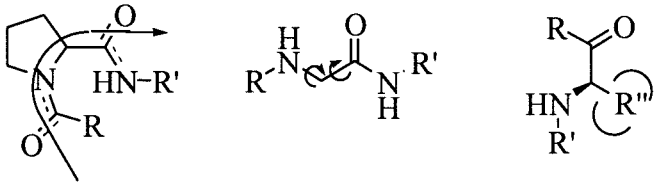

(50) **(51)** **(52)**

Figure 3.10: Certain amino acids impose a conformational restraint upon the molecule that they reside in, a) proline – 'locked', b) glycine – many more degrees of freedom and not constrained by the sterics of the side-chain, c) residues with steric bulk.

Other amino acids such as alanine, leucine and valine experience greater restriction in terms of degrees of rotational freedom **(52)** due to their sterically bulky side chain groups, which overall makes them much 'stiffer' amino acid residues in a linear peptide sequence.[186]

3.6 DISTRIBUTION OF ACTIVE SITES IN A RESIN

It could be assumed that by using post polymerization functionalisation methods[iii] to generate high loading resins, a high level of surface functionalised sites would result, due to the exposed surface; especially if diffusion of the reagents into the matrix is rate-limiting. There is a danger that certain resin bound cyclisation reactions such as those performed on long peptides may become affected by steric overcrowding. Merrifield[187] showed by synthesizing peptides containing tritium, that the distribution of active sites on a resin bead was uniform throughout the polymeric support. He stated that using beads of 20 μm in diameter and considering only surface bound functionality, the resin could contain only 2 μmol of functional sites per gram of resin.[iv] The distribution of functional sites throughout the bead is also uniform in beads synthesized via co-polymerization methods.

3.7 SUMMARY

The literature precedents described above show that factors such as site-site isolation and relative loading in cross-linked PS-DVB beads can all have a marked effect upon the chemistry occurring on the solid phase. The magnitude of the cross-linking has also been shown to affect the mobility of bound ligands and this may be expected to exert an influence on the cyclisation of a linear peptide.

3.8 RESULTS AND DISCUSSION

Using the range of differently cross-linked resins (0.3%, 0.6%, 0.9%, 1.2%, 1.5%, 1.8%, 2.1%, 2.4%, 2.7%, 3.0% and 6.0%), the effect of increasing resin cross-linking upon the efficiency of synthesis of a cyclic peptide was investigated.

[iii] See chapters 1 and 2 for examples.
[iv] This represents 0.1% - 0.2% of the maximal theoretical loading of the beads.

3.8.1 *Solid phase cyclic peptide synthesis*

Peptide synthesis still remains a major driving force in SPOC and this study was intended to perform two main functions. Firstly, to evaluate the range of resins synthesized in the laboratory by using well-defined chemistries as a tool and secondly, to investigate whether pseudo-dilutional effects in SPPS could manifested themselves in the reaction of each of the cross-linked resins.

3.8.2 *Kawaguchipeptin B*

The peptide Kawaguchipeptin B **(53)** was chosen as an interesting target for the multiple parallel solid phase synthesis study (figure 3.11).

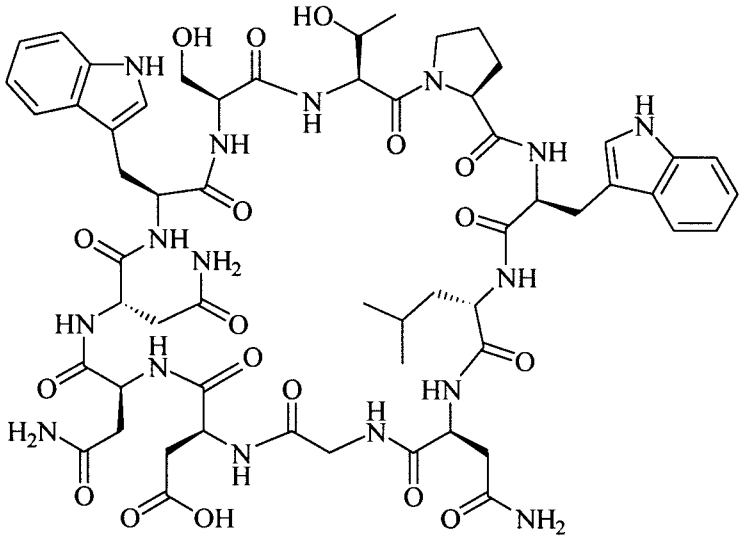

(53)

Figure 3.11: Kawaguchipeptin B.

Kawaguchipeptin B was isolated in 1997 by Murakami[188] and co-workers from the cultured cyanobacterium *Microcystis Aeruginosa* and was found to have antibacterial activity. Kawaguchipeptin B inhibited the growth of the Gram-positive bacterium

Staphylococcus aureus at a concentration of 1μg/ mL (from minimum inhibitory concentration (MIC) studies).

Although isolated and fully characterized, Kawaguchipeptin B had not been chemically synthesized in a laboratory by either solution phase or solid phase techniques. Its structure consisted purely of the L-amino acids: tryptophan (Trp), leucine (Leu), asparagine (Asn), glycine (Gly), aspartic acid (Asp), serine (Ser), threonine (Thr) and proline (Pro). Using a three dimensional orthogonal strategy,[189] a route to the natural product was developed.

3.8.3 *First synthesis of Kawaguchipeptin B*

The chloromethyl resins **(54)** were converted by nucleophillic displacement with phthalimide anion and subsequent hydrazinolysis to the amino methyl resins **(55)**. The resins were then coupled to α-[1-(9*H*-fluoren-9-yl)-methoxyformido]-2,4-dimethoxybenzyl]-phenoxy acetic acid (Fmoc-Rink linker) using DIC, then Fmoc deprotected to give **(56)** (figure 3.12).

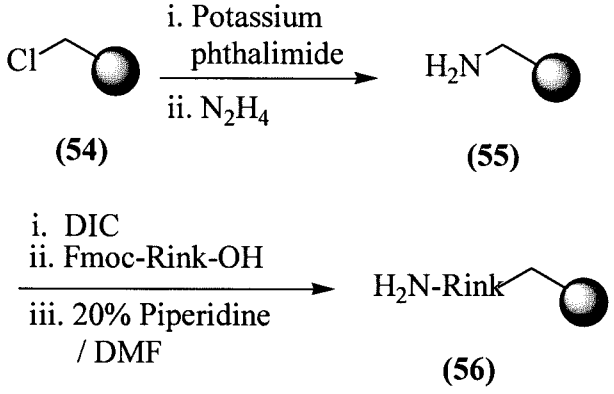

Figure 3.12: Synthesis of aminomethyl resin and subsequent loading with α-[1-(9H-fluoren-9-yl)-methoxyformido]-2,4-dimethoxybenzyl]-phenoxy acetic acid.

Allyl esters have established themselves as viable orthogonal protecting groups in SPPS due to their resistance to acidic and basic conditions[190, 191, 192] used in Fmoc and Boc strategies. Glycine allyl ester **(57)** was prepared in 99% yield by refluxing glycine in benzene with an excess (50 eq.) of allyl alcohol under Dean-Stark conditions[193] and

coupled to Fmoc-Asp(O^{t}Bu)-OH by activation of the *C*-terminal carboxylic acid of the Asp residue, using isobutyl chloroformate to give the dipeptide **(58)** (figure 3.13).

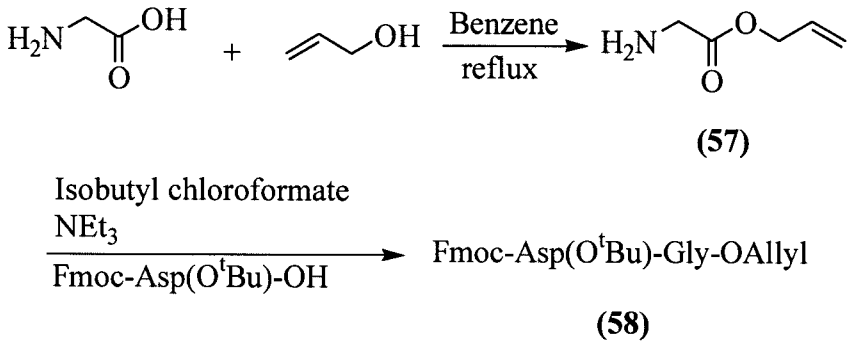

Figure 3.13: Solution phase synthesis of dipeptide (22) for SPPS.

The tertiary butyl ester was cleaved from the dipeptide **(58)** in 99% yield using 50% trifluoroacetic acid (TFA) in DCM for 4 hours. The pendant acid was activated using DIC and loaded on each of the amino methyl resins to give **(59)**.

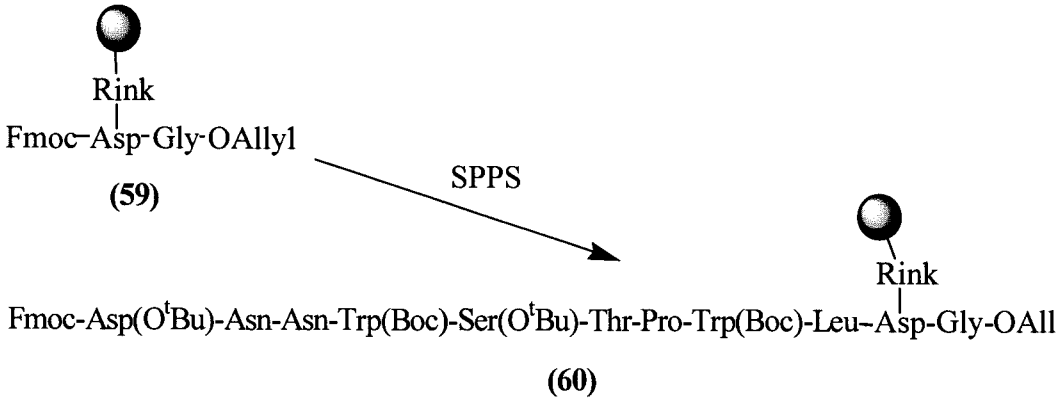

Figure 3.14: SPPS of the linear precursor of Kawaguchipeptin B.

The linear peptide was synthesized on the resin **(60)** using the Fmoc protected amino acids; Fmoc-Leu-OH, Fmoc-Trp(Boc)-OH, Fmoc-Pro-OH, Fmoc-Thr(O^{t}Bu)-OH, Fmoc-Ser(O^{t}Bu)-OH, Fmoc-Trp(Boc)-OH, Fmoc-Asn-OH, Fmoc-Asn-OH, Fmoc-Asp(O^{t}Bu)-OH by a DIC/HOBt coupling method. Two equivalents of the amino acid and DIC were used in each 3 hour coupling with the exception of the first tryptophan residue, which after coupling for 3 hours gave a positive ninhydrin test result. The

coupling protocol was repeated in this case for 3 hours and the reaction completed (figure 3.13).

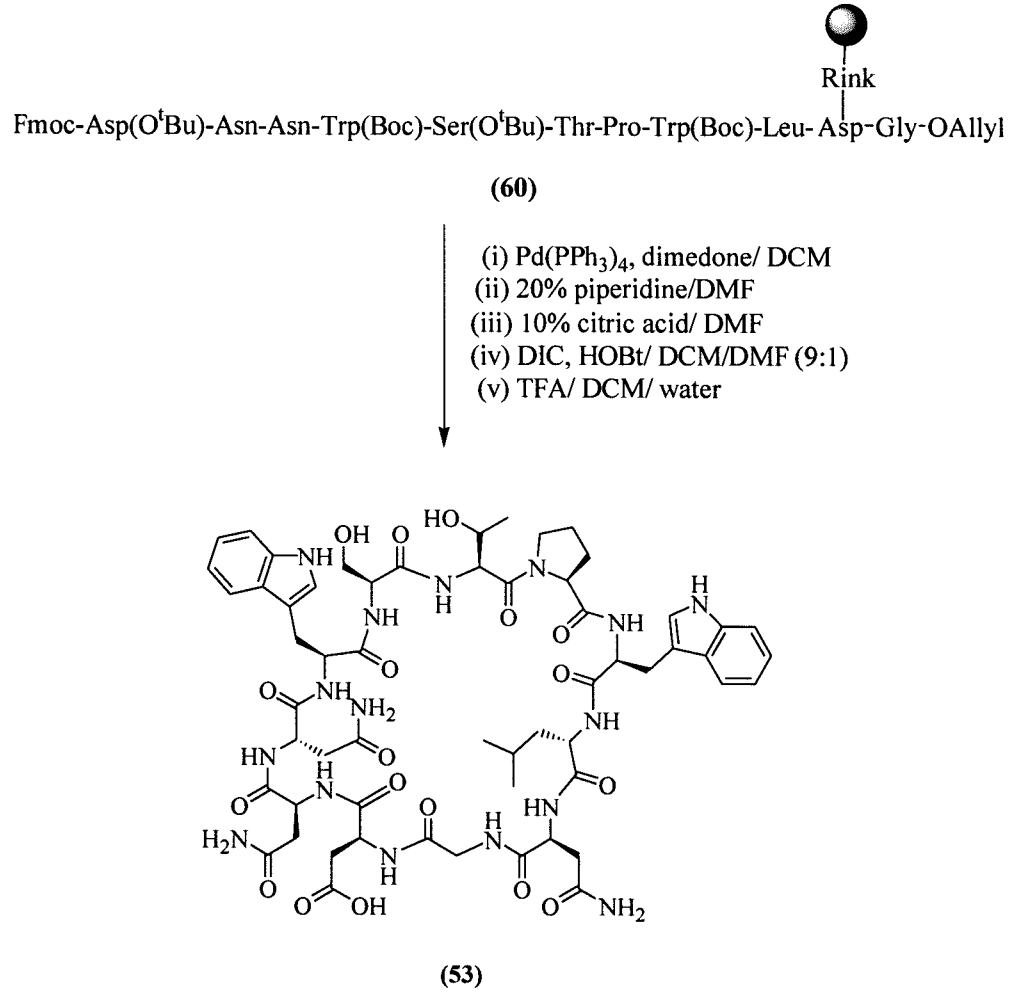

Figure 3.15: Deprotection, cyclisation and cleavage of the cyclic peptide from each of the cross-linked resins

The interaction of allyl groups with Pd has been reported by Trost[194] and more specifically, cleavage of allyl esters by Pd has been reported by Guibe,[192] Kunz[195] and successfully used by many groups.[v] The catalytic palladium mediated deprotection of the allyl group was chosen as it could be undertaken under chemically neutral conditions without affecting other protecting groups.[196] After cleavage of the allyl ester, the *N*-terminal Fmoc protecting group of the linear peptide sequence was

[v] In references 164,165,170 and 189 contained herein.

removed quantitatively using a 20% piperidine/ DMF solution and the resin washed with 10% citric acid to generate the free *C*-terminal acid.[161]

Due to the side chain attachment of the peptide onto the Rink amide linker, the final cleavage step effected full deprotection and also generated the required primary carboxamide functionalility at the terminus of the Asp side chain (thus generating the Asn residue) (figure 3.15).

3.8.4 *Cleavage of linear form of Kawaguchipeptin B from the resins*

A sample of each resin was cleaved, and the HPLC purities of the cleaved compounds monitored. ES-MS spectra were obtained for each of the peaks in the HPLC spectra. Two peaks with a mass of 1302.7 Da eluted from the column suggesting that racemization had occurred during the synthesis (figure 3.16).

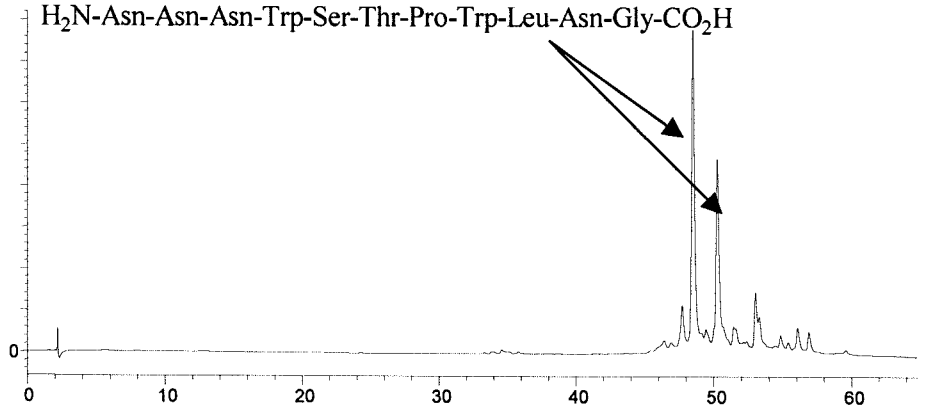

Figure 3.16: Cleaved linear Kawaguchipeptin B

The purity of the linear peptide increased with increasing resin cross-linking from 34% to 67% and 64% in the 2.7% and 6.0% cross-linked resins respectively (figure 3.17).

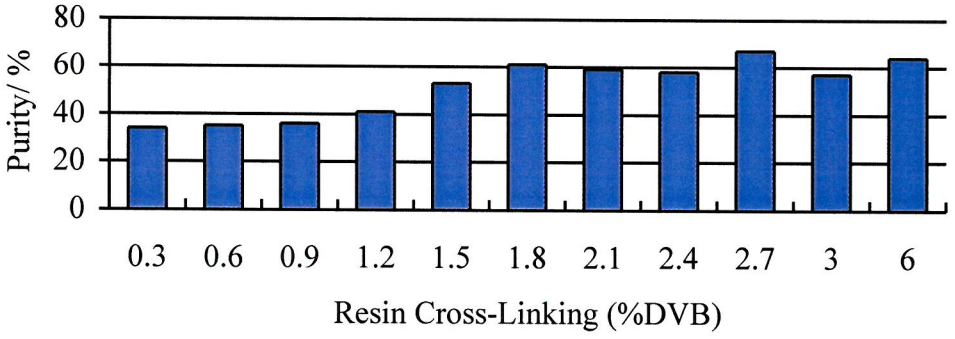

Figure 3.17: Purity of the linear form of Kawaguchipeptin B with increasing resin cross-linking.

3.8.5 *Cyclisation of the linear peptide and cleavage*

The deprotected *N*- and *C*- termini of the linear peptide were cyclised by activation using standard DIC/ HOBt coupling for 16 hours and the resin bound cyclic peptide cleaved using a solution of TFA/ H_2O/ DCM (95:2.5:2.5). The purities were analyzed by RP-HPLC and monitored by ES-MS and the full length pure cyclic peptide fully characterized by NMR techniques. Two peaks in the HPLC (figure 3.18) were identified with the expected mass of 1285.8 AMU for the cyclic peptide, each was concordant (^{1}H NMR spectra) with the expected product, indicating that two distinct Kawaguchipeptin B diastereoisomers had formed.

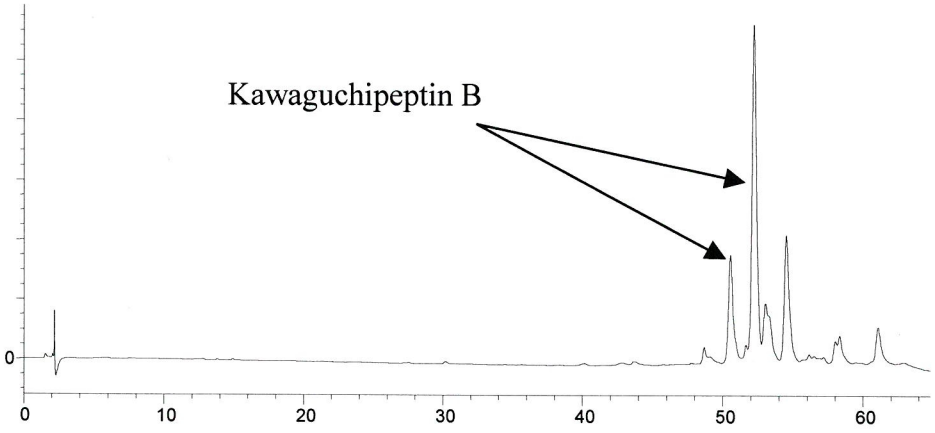

Figure 3.18: Representative HPLC spectrum of the crude cyclised Kawaguchipeptin B synthesis.

The purity of the cyclic peptide increased with increasing resin cross-linking, rising from 28% in the case of the 0.3% resin to over 50% in the case of the 6.0% resin (figure 3.19). The isolated yield of reaction for the peptide was 33% from the 6.0% resin.

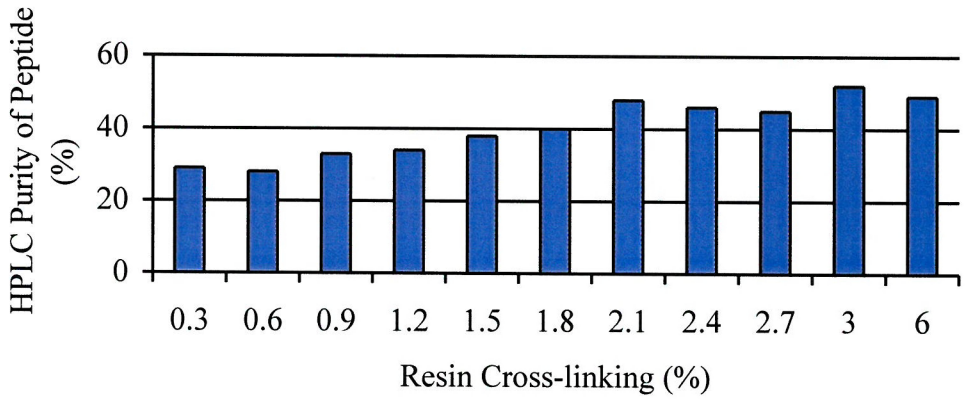

Figure 3.19: Purity of cyclic Kawaguchipeptin B with increasing resin cross-linking.

The number and intensity of bi-products compared to Kawaguchipeptin B generated during the synthesis was seen to increase with decreasing resin cross-linking. Given the data in section 3.1b, it may be expected that the presence of dimers or trimers could explain some of the extra peaks in the HPLC spectra, *i.e.* increased side reactions with increasing flexibility, but the masses of these compounds were of the same order as the cyclised product. The occurrence of dimerization or oligomerization was not observed by mass spectroscopic analysis. The residues proline and glycine are present in the Kawaguchipeptin B peptide sequence (albeit not linked together). The molecule may therefore have been predisposed for bias towards head to tail cyclisation. Computer aided modelling[vi] generated an energy minimized structure for the peptide from the NOE (Nuclear Overhausser Effect) data (figure 3.20).

The location of the deprotected hydrophilic side chains of the Ser, Thr, Asn and Asp residues are visible in the energy minimized structures shown in figure 3.20. There is a predominance of hydrophilic groups positioned away from the central cavity formed

[vi] The program 'Diana' was used to convert the NOE data into a list of atom co-ordinates which were loaded into the modeling program RasMol, which generated 3D images of the peptide.

by the structure. The cavity (inner face) therefore is more hydrophobic than the outer 'face' of the molecule.

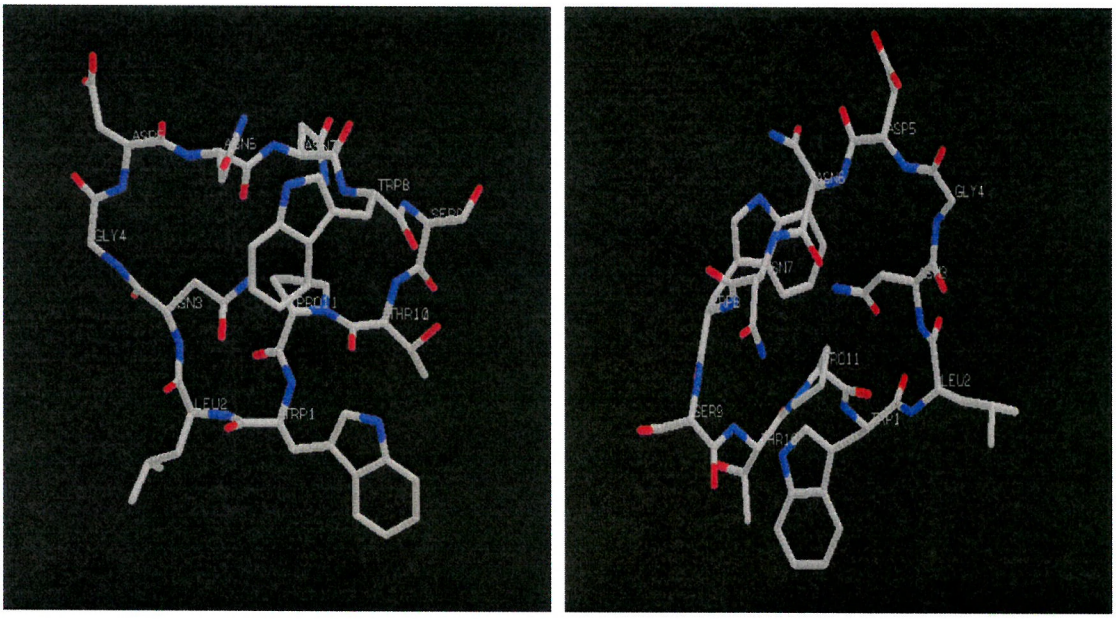

Figure 3.20: Energy minimized Kawaguchipeptin B from the ^{1}H NOE NMR data.

The NOE data (2D-NOESY spectrum) which formed the basis for the images shown in figure 3.20 are shown in figure 3.21. The spectrum was greatly expanded before accurate ^{1}H NMR determinations could be made. The peptide was determined to be cyclic due to the cross-peaks between the Gly Cα proton and the Asp amide proton in the ROESY NMR spectrum[vii], which would not have been present has the molecule not cyclized by condensation of the Asp *N*- termainal and the Gly *C*- terminal.

A growing peptide chain with a high proportion of hydrophilic residues being synthesized on a very hydrophobic resin, would not be expected to explore all of its entropically possible conformations, even in the presence of a good solvent, given the potential for contact with the matrix in some of the possible conformations. It is intuitive and probably more likely that the growing hydrophilic peptide, in the hydrophobic surrounding medium (PS-DVB beads) would have spontaneously cyclised or folded/ collapsed back onto itself. This would also help explain the absence of oligomers in the mass spectra.

[vii] Rotating frame nuclear overhauser spectroscopy. See appendix for annotated ROESY spectrum.

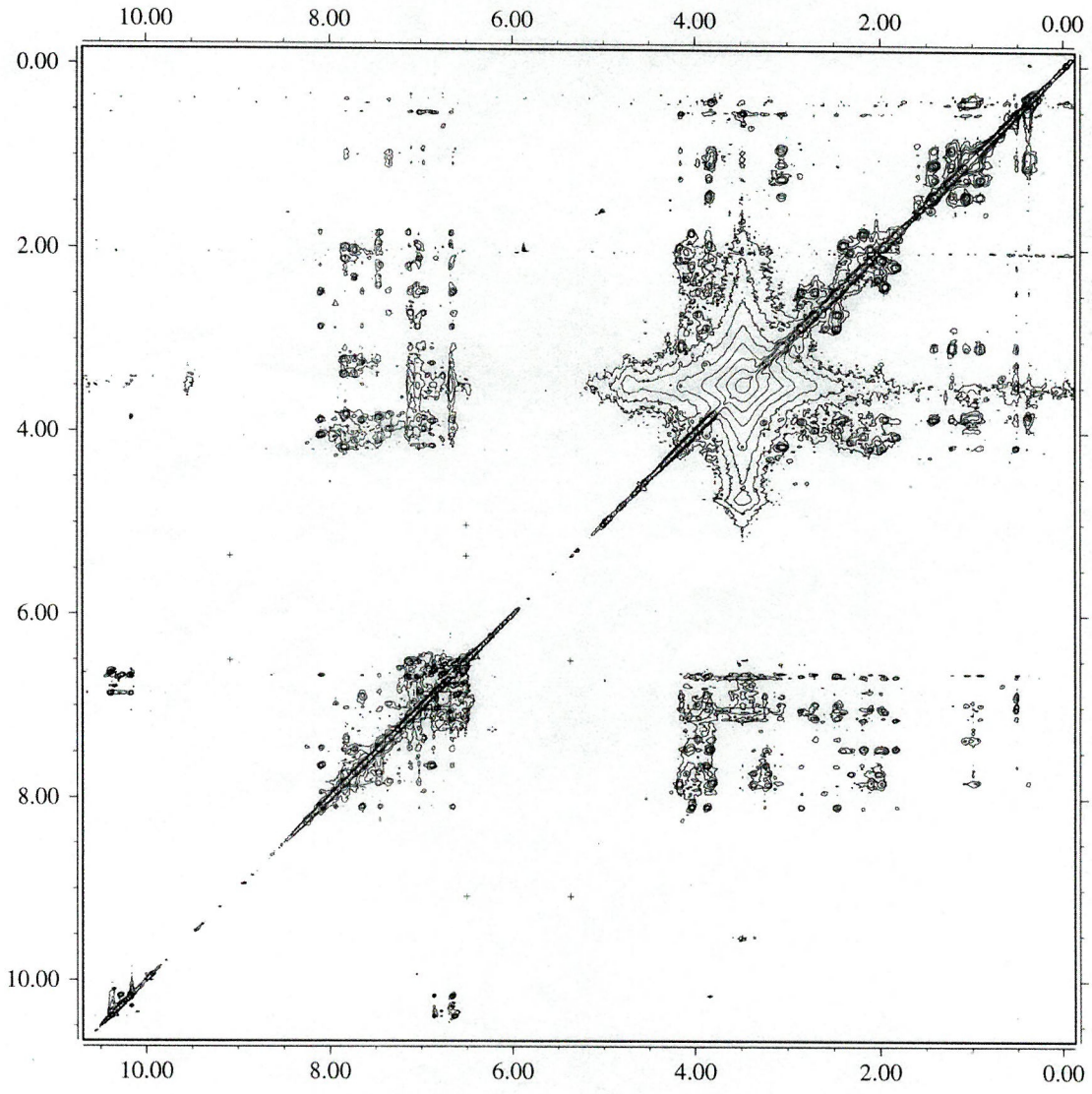

Figure 3.21: NOESY spectrum of Kawaguchipeptin B.

3.9 CONCLUSION

In conclusion, it has been possible to establish that the efficiency of the synthesis of the Kawaguchipeptin B was seen to increase with increasing resin cross-linking (determined by HPLC analysis). Some evidence for the formation of diastereoisomers was evident in the final crude mixture, but because evidence of racemization in the

crude linear HPLC traces was also present, racemization during the solid phase synthesis of the linear resin bound peptide was implied.

CHAPTER 4 – MAGNETIC RESIN

4.1 INTRODUCTION

There has been continued interest in the development of new supports for SPPS.[i] Magnetic supports are a sub-class of these and have found uses in diverse fields, ranging from immunochemistry to molecular cell biology.

4.2 SYNTHESIS AND APPLICATION OF MAGNETIC PARTICLES

Magnetic particles synthesized by emulsion and suspension polymerization methods have been used in the biochemical fields. Using emulsion polymerization methods, Khng, Cunliffe, Davies, Turner and Vulfson[197] synthesized sub-micron magnetic particles for use in the preparative purification of proteins. Particles in the order of 30 nm in diameter were prepared and were surface functionalised with carboxyl groups for the attachment of affinity ligands.

Shiho, Manabe and Kawahashi[198] produced micron sized magnetic composite particles by the controlled hydrolysis of iron (III) chloride in the presence of polymer colloids, urea, poly(vinylpyrrolidone) and hydrochloric acid, followed by calcination of the composite in a stream of hydrogen gas. The hydrogen was found to convert the haematite and iron peroxide to magnetite and Fe. They found that the thickness of the coating could be altered by alteration of the amount of $FeCl_3$ in the system.

Promega have developed magnetic particles, which have been used in a number of DNA purification applications. Their MagneSil™ Paramagnetic Particles consist of a 1:1 ratio of silicon dioxide (SiO_2):magnetite which have an average diameter of 5.0 - 8.5 μm and a pore size greater than 500 Å (figure 4.1).

[i] See also chapter 2 for examples.

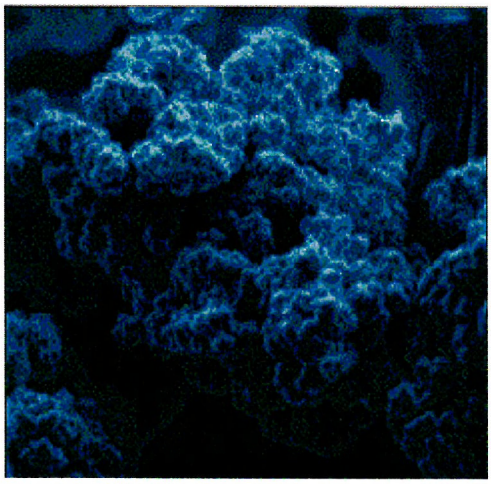

Figure 4.1: Scanning electron micrograph of MagneSil™ Paramagnetic Particles.

The magnetite is completely encapsulated by SiO_2, which eliminates the possibility of leaching and non-specific binding to the iron of magnetite. This technology allows rapid removal of compounds from solution by first binding to the magnetic particles and then by removal from solution. By activation of a suitable magnet and using concentrations of MagneSil™ as low as 0.01 mg/ ml, 90% of the particles can be removed from solution in less than 45 seconds.

Paramagnetic particles are especially useful as supports because when placed in a magnetic field, a few particles will tend to magnetize and self-attract to form a critical particle mass which then starts to move towards the magnet. As paramagnetic particles have no 'memory' of previous magnetic fields, uncontrollable aggregation of the particles can be avoided by simple removal, or pulsing on an off, of the magnetic field.

Other magnetic particles have been synthesized. The DuPont[199] material Magtrieve™ was based on magnetic chromium dioxide particles employed in the magnetic tape industry. Reduction of the reagent is confined only to the surface of the CrO_2 crystal, so the crystal is still ferromagnetic and can be readily removed by simple magnetic separation.

4.3 SYNTHESIS AND APPLICATION OF MAGNETIC BEADS FOR SPOC

Magnetic particles that have been encapsulated within highly cross-linked PS matrixes to form functionalised beads have allowed simplified bead handling protocols, which have facilitated SPOC.

Magnetic supports have been produced by Szymonifka[200] who derivatized standard 1% PS-DVB resin beads **(61)** by nitration followed by reduction to yield a mixture of ferrous and ferric ions. These were converted to ferrosoferric hydroxide by the addition of concentrated ammonium hydroxide, and to magnetite by subsequent heating (figure 4.2).

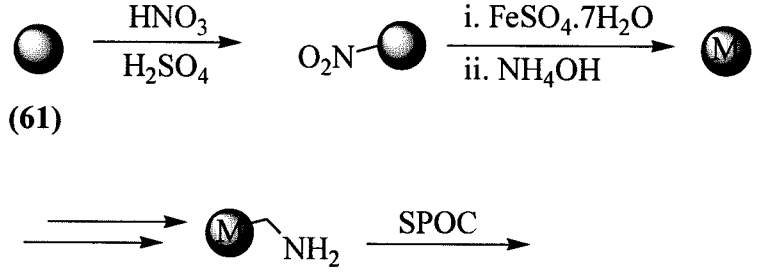

Figure 4.2: Szymonifka synthesis of magnetic beads.

The beads were used as a support for the synthesis of the dipeptide Fmoc-Phe-Ala-OH, but magnetic beads have also been used by Maeda and Sasaki[201] during the synthesis of a library of pentapeptides. The library was applied in the search for a recognition peptide for the nonapeptide target sequence: H-Ser-Try-Tyr-Asp-Asp-Asp-Leu-Glu-Arg-OH, which is characteristic of the CNS dopamine D2 receptor subtype.

Sucholeiki[202] recently described the use of a paramagnetic support, which exhibited relatively high loading capacities (up to 1 mmol/ g). He created a novel paramagnetic bead composite by first creating primary beads composed of magnetite crystals encased in very highly cross-linked polystyrene, and then enmeshing them in larger beads composed of 1-2% cross-linked polystyrene via a suspension polymerization reaction (figure 4.3).

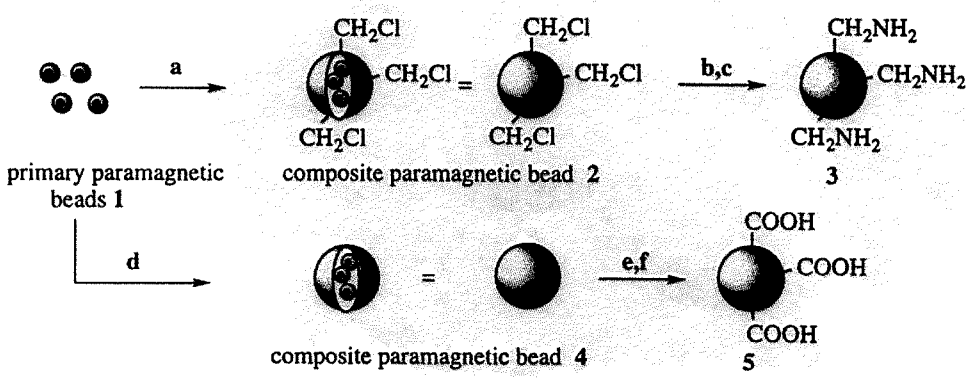

Figure 4.3: Synthesis of a novel paramagnetic composite bead. a) CMS; b) potassium phthalimide; c) N_2H_4; d) styrene; e) butyllithium, CO_2; f) H^+.

These beads were used in a variety of solid phase organic chemistry applications. The support was converted into an efficient scavenger for thiols by functionalizing the beads with an iodoacetamide group. The beads were also used as a solid support in the SPPS of the tetrapeptide sequence; H_2N-Gly-Ala-Ile-Ala-NH_2.

Dynabeads[203] are popular choices for a range of molecular cell biology applications. Although details of their synthesis and derivatisation are not well reported in the literature, they consist of uniformly sized (approximately 4.5 μm) paramagnetic polystyrene beads that have been coated with a layer of polyurethane. The polyurethane surface is activated by *p*-toluene sulfonyl chloride to provide reactive groups for covalent binding of proteins.[204] Over 2500 publications reporting the use of Dynabeads have been published within the last 10 years, and these beads have become common tools for many molecular biologists.

Hewett and Murray[205] conjugated anti-PECAM-1 monoclonal antibodies to the Dynabeads to facilitate the immunomagnetic purification of human microvessel endothelial cells. PECAM-1 is a 130 KDa glycoprotein, which is expressed on the surface of all endothelial cells, not present anywhere else except for white blood cells. The PECAN-1 glycoprotein represented a highly specific marker for endothelia, which

facilitated purification by the beads. Dynabeads[ii] coated with antibodies have also allowed the facile immunomagnetic purification of cells in similar applications by many other research groups.[206, 207, 208, 209]

Miltenyi Biotec's MicroBeads (the MACS system) is composed of iron oxide and a polysaccharide and forms a stable colloidal suspension, which does not precipitate or aggregate in magnetic fields. These super-paramagnetic beads are approximately 50 nm in diameter and also biodegradable. Cells labeled with the beads (figure 4.4) retain their physiological function and can be separated using a high gradient magnetic separation column placed in a strong magnetic field.

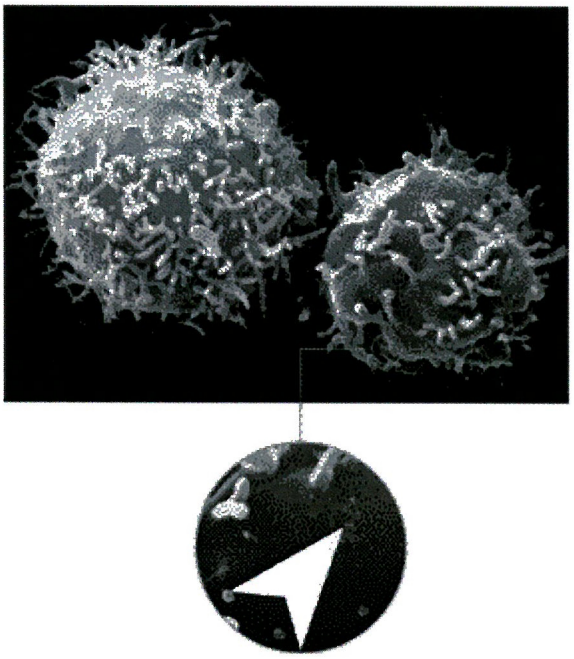

Figure 4.4: SEM of CD8 positive T cells isolated by MACS. The MACS MicroBeads (arrow) are barely visible compared to the T cells (shown as the lighter area at the head of the arrow).

The magnetically labeled cells are retained in the column while non-labeled cells pass through. When the column is removed from the magnetic field, the magnetically

[ii] Information herein obtained from published sources and also the Dynal Company official web site http://www.dynal.net on 13th September 2000.

retained cells may be eluted. Both labeled and non-labeled fractions can be completely recovered.

Recently Anderson, Partington and Jenkinson[210] pioneered a novel method of cell separation based on a dual parameter immunogenic cell selection process. A number of biological cell types were isolated by first positively selecting biological cells using the Miltenyi MiniMacs system, (50 nm Microbeads) and then subjecting those cells to positive or negative selection using streptavidin M280 or anti-rat M450 Dynabeads with a Dynal magnetic separator (figure 4.5). The cells selected with the Dynal magnetic separator were positive for Dynabead bound cells only; and the fact that all of these cells were selected by the smaller MiniMacs magnetic beads system using an alternate selection process meant that two selections processes could be applied to the cell sorting protocol. The magnetic beads with their specificities, were in effect orthogonal and allowed specific cell sorting.

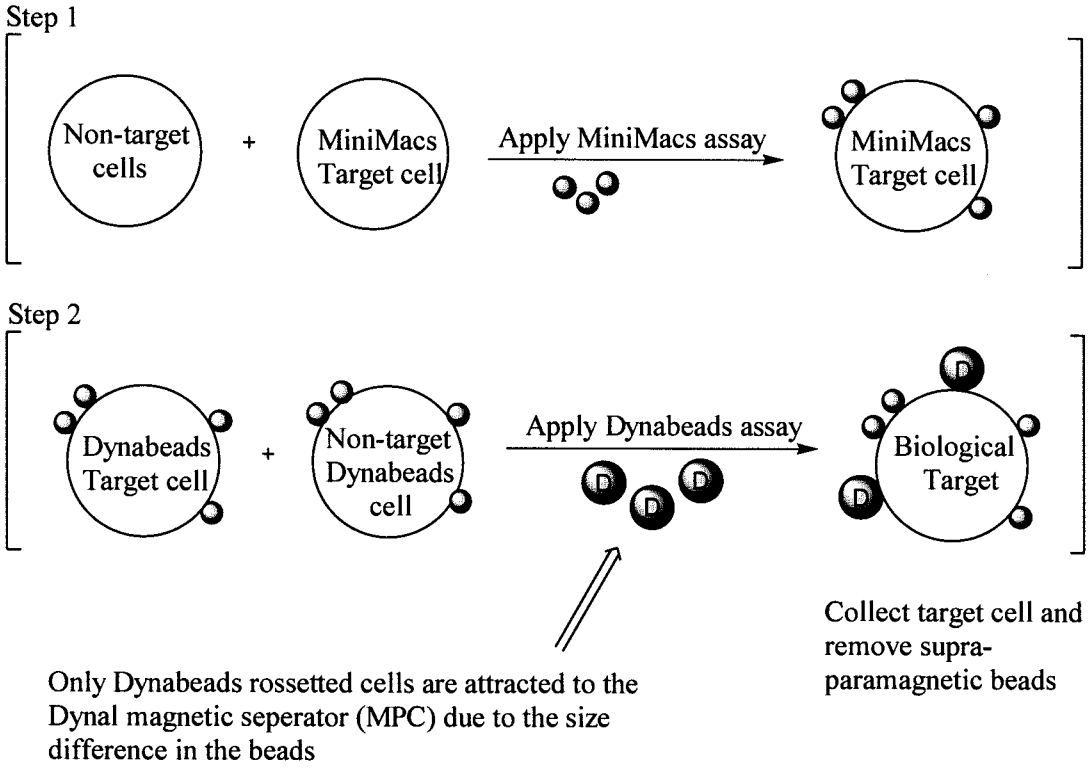

Figure 4.5: Dual parameter biological cell selection base of magnetic beads.

Coated ultramicroscopic (~100 Å) magnetic particles,[iii] (typically coated with a 25 Å layer of inert material to stop uncontrolled attraction in magnetic fields), have been used by Mosbach in affinity chromatography.[211] He immobilized a ligand on the surface of magnetic beads and then separated successfully bound bead conjugates from a pool of mixed ligands. Magnetic beads have also been derivatized with a range of oligonucleotides and used in a number of DNA related applications, including sequencing,[212] purification[213] and the polymerase chain reaction (PCR).[214] The beads used in these applications have ranged from agarose-based materials to polyurethane coated polystyrenes and have been typically in the order of only a few microns in diameter.

4.4 RESULTS AND DISCUSSION

4.4.1 *Synthesis of magnetic beads for SPOC by suspension polymerization*

Beads randomly incorporated with magnetite particles were synthesized by a suspension polymerization reaction with direct incorporation of the magnetite into the polystyrene matrix by its inclusion in the polymerization mixture. This method had not previously been applied to suspension polymerization for the synthesis of magnetic beads.

The beads were prepared by suspension polymerization as previously described. The divinyl benzene content was 2 mol %, whilst chloromethyl styrene was added to give a theoretical loading of 1 mmol per gram.[iv] An aqueous phase consisting of a PVA solution of 2.5 g in 1000 mL water was used in the polymerization, thus providing an organic/ aqueous phase volume ratio of 1.75 %. The magnetite was added once homogeneity in the droplet sizes (attained after approximately 20 minutes of stirring) had been achieved. Prior degassing of the organic phase and the aqueous phase was

[iii] Commercially called Ferrofluids. Trademark A05 from the Ferrofluidics Corporation, Burlington, Mass., USA.

[iv] Due to the reactivity ratio of the chloromethyl styrene and hydrophobicity of both of the parent monomers and the hydrolyzed product, the experimental loading of a polymer synthesized by suspension polymerization is often only 50% of the theoretical loading, based on the initial incorporation of the monomers.

necessary for efficient magnetite incorporation. In cases where prior N_2 degassing had not been applied, the beads were light grey in colour and similar to the traditional Merrifield bead product. Polymerization experiments produced beads, which varied in color from grey to black depending on the amount of magnetite incorporated (figure 4.6).

Figure 4.6: Picture of the beads, en masse, showing traditional (left) and the magnetic beads (right).

The darker the beads, the greater was their attraction to magnetic fields.

4.4.2 *Separation of viable beads*

It was possible to qualitatively determine which beads from successful polymerization experiments had taken up the magnetite crystals due to their attraction to a magnet. Separation of the beads incorporated with magnetite from the un-incorporated beads was carried out on the basis of attraction to an electromagnet suspended above the beads. Separation of magnetite particles from beads incorporated with magnetite was possible by suspending the mixture in a column of dichloromethane. The magnetite that had little or no polymer associated with it dropped to the bottom of the column, while the magnetite that had been incorporated into beads remained buoyant and floated in the column of DCM. The limitation of this method of separation was that beads which had formed, with a very high level of magnetite incorporation would also sink to the bottom of the column with the magnetite particles.

4.4.3 *Nature of incorporation*

Initially, it was not understood how the magnetite was incorporated into the beads. It may have been possible that the magnetite was physically trapped within the polystyrene matrix, but in the absence of further tests this could not be verified.

Most of the magnetite added during the polymerization reactions did not become incorporated into the beads. It was more difficult to remove magnetite from the smaller magnetic beads than from the larger ones, therefore accurate determinations of incorporated magnetite derived from the mass recovered magnetite were not possible. In a trial experiment, of the 1 g of magnetite included in the polymerization mixture, 0.7 g was recovered, but microscopic magnetite particles were observed to have passed through the filtration bags used in the washing process. The magnetite used in the polymerizations was supplied as a powder containing particles of less than 5 microns in diameter.

Directly after polymerization, an initial loss[v] of excess magnetite from the beads was observed. Subsequently, prolonged mechanical shaking, and sonication[vi] whilst suspended in a column of DCM released no further magnetite from the beads. The magnetite was shown to be physically and stably incorporated in the beads, when swollen or shrunk in organic solvents such as DCM and MeOH the beads maintained the same level of magnetite.

By performing suspension polymerizations with two different levels of divinyl benzene cross-linker (1% and 6%), it was discovered that the lower cross-linked beads retained less magnetite once washed and processed than the higher cross-linked beads. *En masse* the higher cross-linked magnetic beads were a darker grey colour and also were more strongly attracted to magnetic fields.[vii] A powerful electromagnet was

---

[v] Demonstrated during processing each batch of magnetic resin synthesized (ranging from 1 % to 6.0 % cross-linking).

[vi] The beads were mechanically shaken whilst suspended in DCM and MeOH, and mixtures thereof, for 48 hours. Sonication was carried out for 10 hours whilst the beads were suspended in DCM and MeOH.

[vii] Measured by speed of attraction of identical sieved batches towards a magnetic field, in a mixture of DCM/ DMF.

placed under a vial of magnetic resin in DCM and energized, the resin was observed to move downwards towards the magnet. This was facilitated by the addition of DMF to the DCM, which made the solution more isocratic.

In order to examine the nature of the incorporation, the beads were viewed under the optical light microscope. Once swollen, the beads appeared to be physically similar to traditional chloromethyl beads (figure 4.7a), except that it was possible to observe a slight grainy/ rough texture on the surface of some beads due to 'flecks' of magnetite (figure 4.7b).

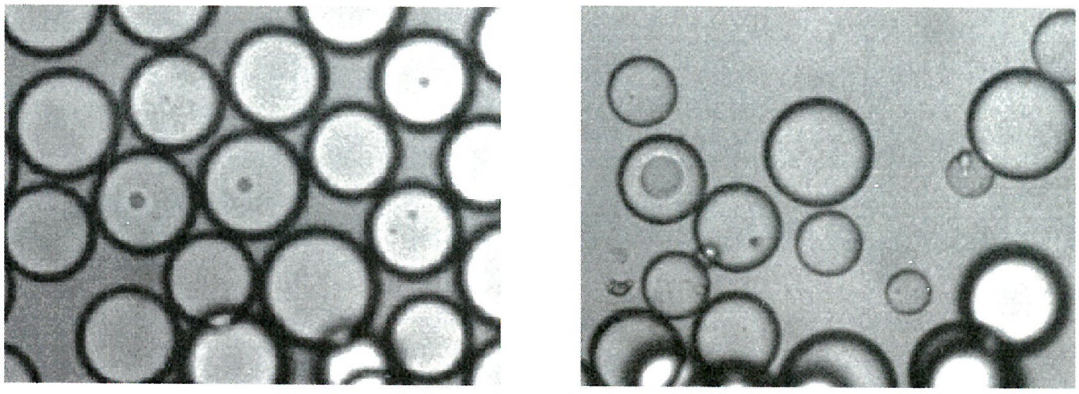

a) b)

Figure 4.7: The magnetic beads appeared similar in physical appearance to traditional non-magnetic beads. a) Sieved magnetic beads b) un-sieved magnetic beads.

It was not possible, using magnifications gained through optical microscopy and resolutions, to identify whether the black magnetite spots/ graininess was located on the surface of the beads or whether it extended into the sub-structure of the beads. Topological studies using an SEM on magnetic beads were undertaken, thus providing greater information regarding the nature of the incorporation. The incorporation of the magnetite into beads appeared to be random and located on the surface of the beads (shown in figures 4.8).

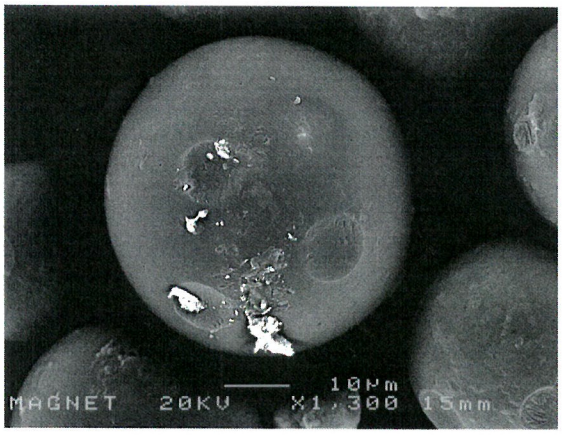

Figure 4.8: SEM images of the magnetic bead synthesized via optimized polymerization methods.[viii]

By using accelerating voltages of 3 kV and keeping the distance from the sample to the probe low (10 mm) it was possible to obtain a clearer image with greater depth of field; of the interaction between the magnetite with the rest of the bead (figure 4.9).

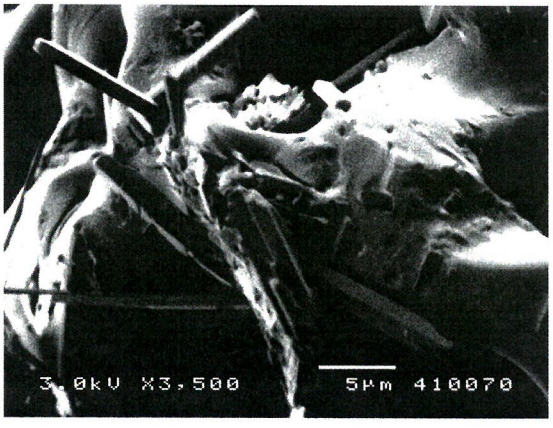

Figure 4.9: SEM image of the interaction of magnetite crystals in a magnetic bead (x3500 magnification image of the bead surface).

In some of the magnetic beads it was possible to observe clearly that the magnetite crystals were embedded at random angles in the polystyrene beads. The image is consistent with the observation that lower cross-linked beads retain less magnetite

[viii] See chapter 2 for details.

within their structures, while the more highly cross-linked resins retain a greater amount of magnetite.

Although the magnetite crystals appear to penetrate the surface of the bead (figure 4.9), the SEM cannot easily indicate the presence of magnetite far beneath the surface of the bead as the technique is not confocal in nature. An X-ray analysis of a region of the surface of a magnetic bead not visibly containing magnetite was carried out (figure 4.10b) and indicated the presence of iron under the surface[ix]. The secondary electrons generated by the surface were indicative of the presence of Fe and Au.

[ix] To a depth of 5 micrometers.

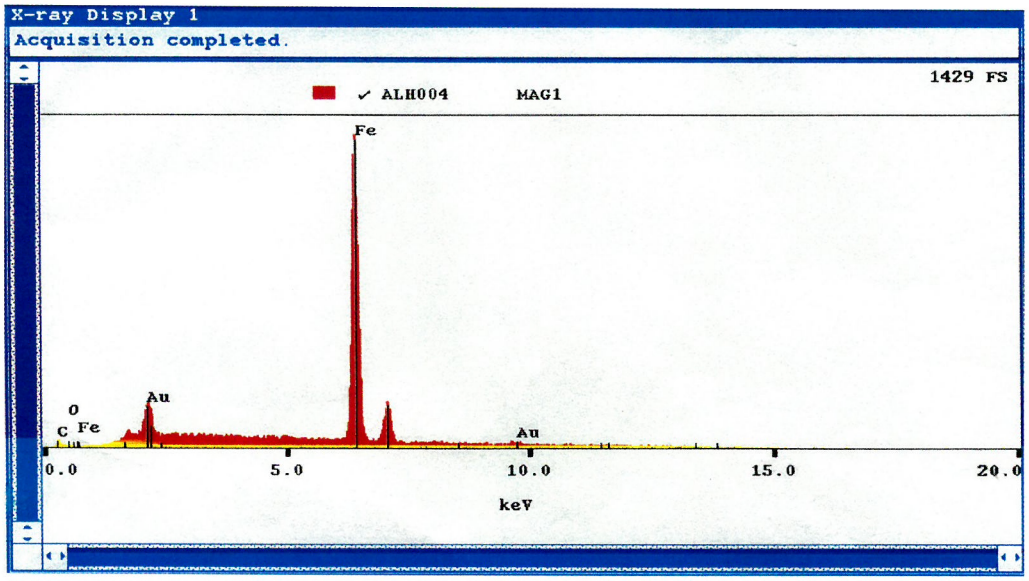

a)

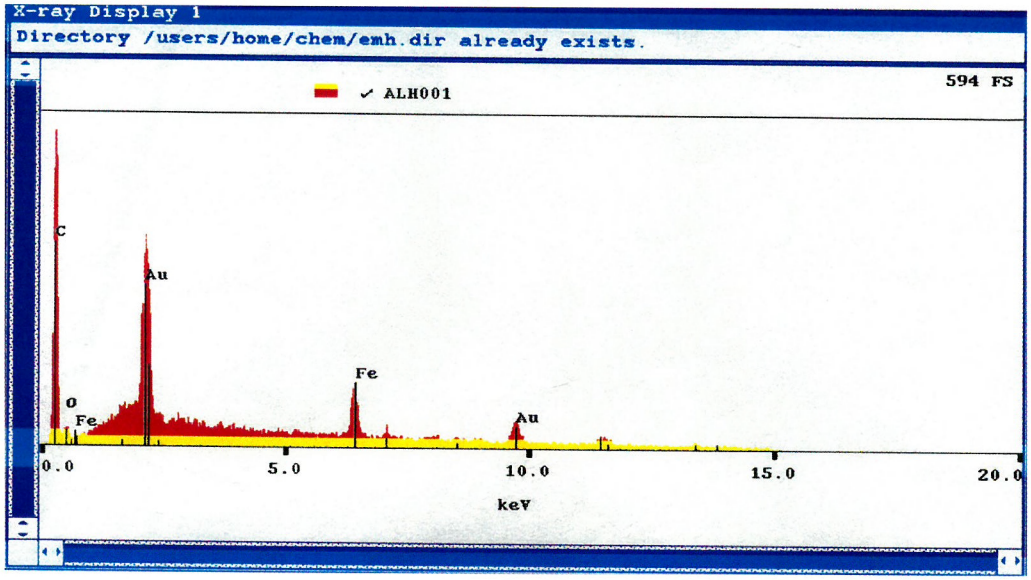

b)

Figure 4.10: X-Ray analyses of the bead shown in figure 4.8: a) Magnetite crystals on the surface, b) Surface of magnetic bead not housing magnetite particles.

4.4.4 *Quantification of iron in a magnetic bead*

To quantify the iron incorporated into the magnetic beads, a colourimetric test for the presence of iron (Fe(III)) in solution was modified. In 1937 Melon and Swank[215] published a paper entitled 'Determination of Iron'. They quantified work previously

carried out by Yoe and Hall[216] in 1932, who described the use of the 7-iodo-8-hydroxy-quinoline-5-sulfonic acid reagent (ferron) (figure 4.11) for use in the colourimetric determination of iron.

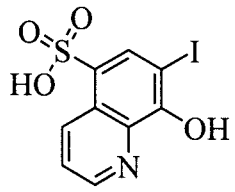

Figure 4.11: 7-iodo-8-hydroxy-quinoline-5-sulfonic acid (the ferron reagent).

They reported that the presence of other metals, such as copper, nickel, chromium, cobalt and aluminium could interfere with the results of the ferron reagent. At constant pH, Beers Law is valid for the ferron-iron (III) complex. The absorbance of the complex is measured at 360 nm at pH 5, using a sodium acetate buffer. A calibration was produced using standard solutions consisting of 0.2% buffered ferron solution with Fe(III).

In order to determine the quantity of iron incorporated into the magnetic beads, a sample of the beads was stirred in HCl for 2 hours, which transformed the Fe(II) in the mixed oxide Fe_3O_4 into Fe(III), forming $FeCl_3$, the beads then lost their paramagnetic properties. The amount of iron chloride was determined from the absorbance and thus the total amount of iron calculated. The iron content was 4 mg per gram of polymer, which equated to 0.7 μmol per gram. This incorporation was sufficient to attract the smaller beads in the batch (<250 μm) towards a magnetic field in the absence of solvent, and the larger beads (250 -500 μm) towards a magnetic field when swollen in an isotactic solution of DCM/ DMF. 30 g of magnetite was added to the original suspension, which resulted in an overall uptake into the beads of 1.07 g (3.5% incorporation).

4.4.5 *Stability*

Even though the magnetic beads were unstable to concentrated HCl, they showed a resistance to other strong acids (100% TFA). Prolonged (16 hours) treatment of the

beads at room temperature with 12 M sodium hydroxide did not cause discernable alteration of their attraction to a magnetic field.

4.4.6 *Swelling properties*

The beads were sieved and the fraction sized from 45 - 125 μm collected (13 % by total mass of beads). The swelling properties this fraction were investigated and compared against a batch of standard 2% PS-DVB resin.[x] The swelling properties were found to be almost identical for all of the major classes of solvent used (figure 4.12).

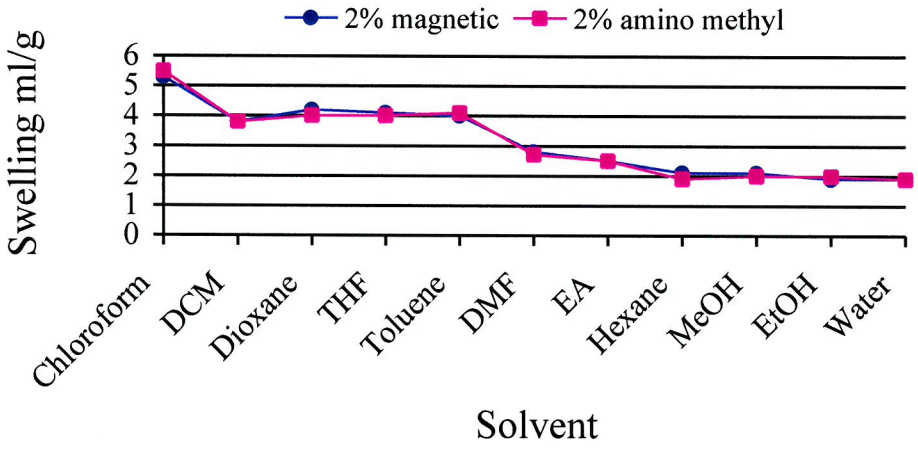

Figure 4.12: Swelling properties of the magnetic resin compared to commercial 2% resin.

The beads were as mechanically sound as non-magnetic commercial resin (determined by comparisons of rapid stirring of the magnetic resin compared to commercial resin, with a magnetic flea in a round bottomed flask). It was then necessary to establish the resin's chemical behavior.

[x] 100-200 mesh.

4.4.7 *Magnetic SPPS*

Following conversion to aminomethyl resin **(30)**, the Fmoc-Rink linker was loaded onto resin and the synthesis of the tripeptide Phe-Ser-Ala-NH_2 **(62)** performed using Fmoc/ ^{t}Bu methods (figure 4.13).

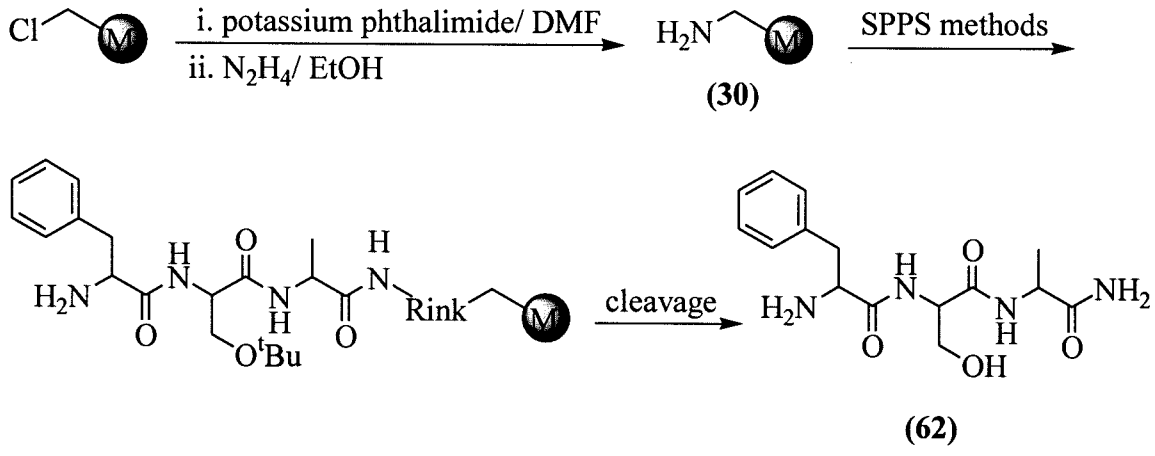

Figure 4.13: Synthesis and cleavage of Phe-Ser-Ala-NH_2 magnetic resin.

The peptide was isolated from the resin in 90% yield, following cleavage with TFA/ DCM/ water (95%, 2.5%, 2.5%). The magnetite in the resin sample had not leached during the synthesis or the cleavage step as determined by ferron analysis, demonstrating the stability of the resin under conditions of synthesis.

4.4.8 *Magnetic scavenger resins*

The magnetic resin was applied to the field of scavenger reagents and resin quenchers. A 2 x 2 array of sulfonamides was synthesized by the reaction of amines (heptylamine **(63)** and cyclohexylamine **(64)**) with an excess of sulfonyl chlorides (2,4-dinitro-benzenesulfonyl chloride **(65)** and dabsyl chloride **(66)**) (figure 4.14).

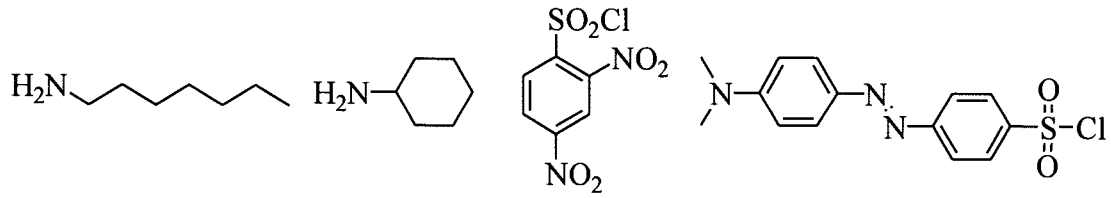

(63) **(64)** **(65)** **(66)**

Figure 4.14: Reagents used in the 2x2 array of synthesis of sulphonamides.

The excess sulfonyl chloride and hydrolyzed sulfonic acid were quenched using magnetic aminomethyl resin (figure 4.15).[217]

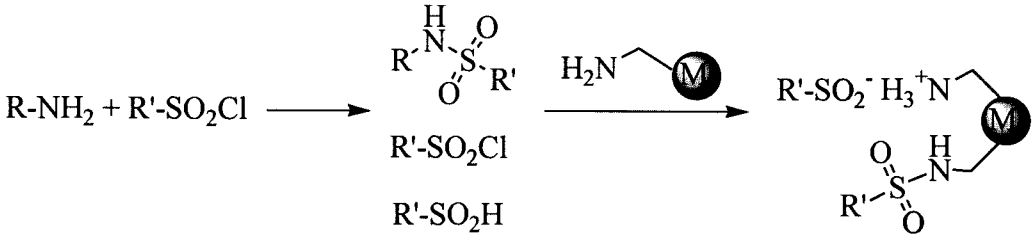

Figure 4.15: The use of magnetic aminomethyl scavenger resin in the array synthesis of sulfonamides.

The reactions between the sulfonic acids and the amines were rapid, requiring 3 hours at room temperature in DCM. In each case, the magnetic amino methyl resin was added to the reaction vials and the vials shaken. The magnetic resin was removed from the reaction vial by simple insertion and removal of a magnet. The reactions and the resin scavenging were monitored by HPLC and represented in figure 4.16.

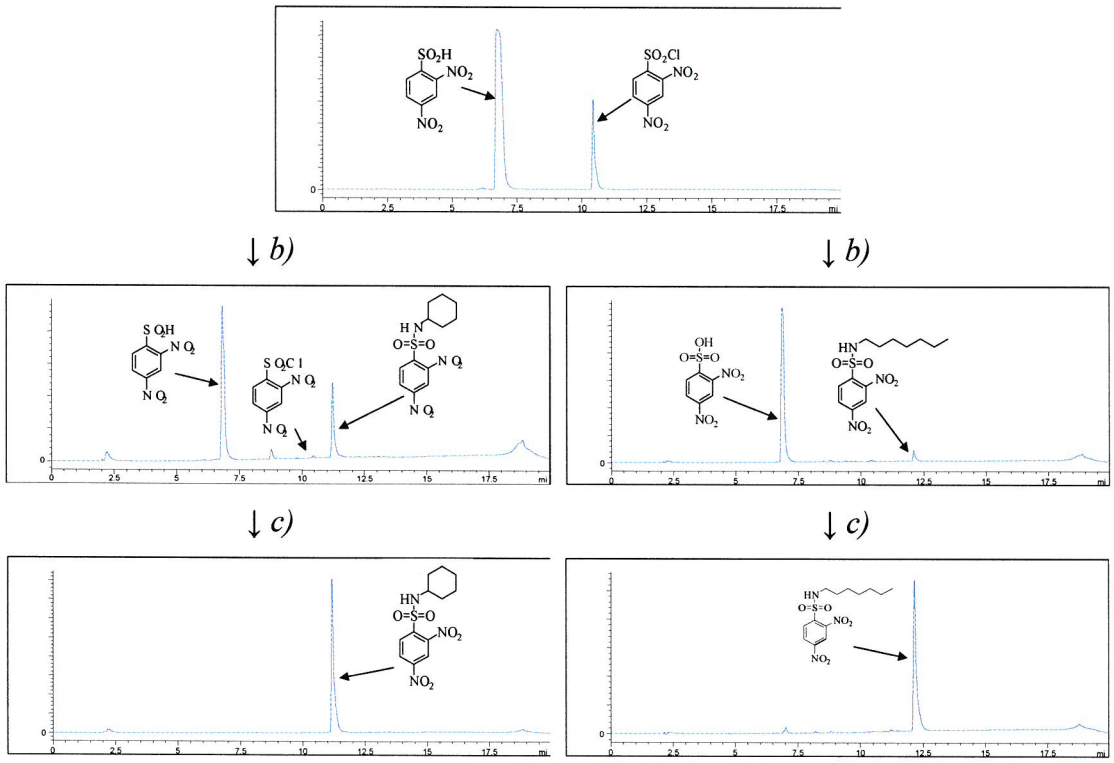

Figure 4.16: The synthesis and quenching of the sulfonamide library: a) Neat 2,4-dintro-benzenesulfonyl chloride, b) addition of amine forming the sulfonamide, sulfonyl chloride and sulfonic acid, c) magnetic aminomethyl resin removes by-products leaving pure sulfonamide in solution.

The purities of the sulfonamides following scavenging are shown in table 4.1.

Sulfonamide	Purity/ %
N-Cyclohexyl-2,4-dinitro-benzenesulfonamide **(67a)**	100
N-Heptyl-2,4-dinitro-benzenesulfonamide **(67b)**	97
N-Cyclohexyl-4-(4-dimethylamino-phenylazo)-benzenesulfonamide **(67c)**	96
4-(4-Dimethylamino-phenylazo)-*N*-heptyl-benzenesulfonamide **(67d)**	89

Table 4.1: Purities of array of sulfonamides following scavenging.

4.5 CONCLUSION

In conclusion, a magnetic resin was synthesized by a novel method involving traditional suspension polymerization. The nature of the incorporation of the magnetite was akin to physical embedding throughout the polystyrene matrix. The amount of magnetite incorporated was quantified by a modified colorimetric test for iron involving the sulfonic acid compound 'ferron'. The resin was demonstrated to be useful for SPPS applications, but could also be manipulated in an additional way to conventional resin, by a bar magnet. This proved to be a convenient facet, which was successfully exploited and demonstrated in the solution phase array synthesis of sulfonamides from corresponding sulfonyl chlorides and amines.

CHAPTER 5 – INVESTIGATION OF KINETICS WITH SOLID SUPPORTS

5.1 MACROPOROUS ION AND GEL TYPE EXCHANGE RESIN - PREVIOUS WORK

Macroporous ion exchange resins were applied to SPOC much earlier than the traditional conventional gel type resins. Examples of the application of ion exchange resins in catalysis were described by Bell[218] as early as 1952 but this was by no means the first. The effects of different parameters on ion exchange resin mediated reactions have been investigated and the results are summarized below.

5.1.1 *Cross-linking and the macroporous resin*

Rodriguez and Setínek[219] investigated the dependence of trans-esterification rates on the cross-linking of ion exchange resins used as solid phase catalysts in solution phase reactions (figure 5.1).

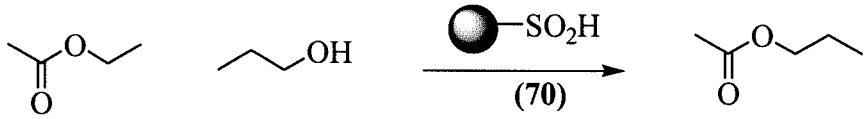

(68) **(69)**

Figure 5.1: Rodriguez and Setínek's 're-esterification' of ethyl acetate with 1-propanol.

They noted, as other researchers have, that the catalytic activity of macroporous ion exchange resins increased with increasing cross-linking due to the increase in surface area of the resins.[220] They used macroporous resins that had comparable ion exchange capacities but differed in surface area, density and porosity as a function of increasing cross-linking (table 5.1).

Resin MS - (% cross-linking)	Exchange capacity (mmol/ g)	Surface area (m^2/ g)	Porosity (%)	Median pore radius (Å)
MS-10	4.00	16	13	225
MS-15	3.81	35	45	445
MS-25	3.80	44	58	445
MS-40	3.20	120	59	320
MS-60	3.02	227	63	225

Table 5.1: Macroporous resin data for the resins used by Rodrigueuz and Setínek.

In the reaction of ethyl acetate **(68)** and propanol **(69)** using macroporous resin bound sulfonic acids **(70),** they observed that the reaction rate decreased by only a small degree in trans-esterification reactions with increasing cross-linking (figure 5.2, line 3).

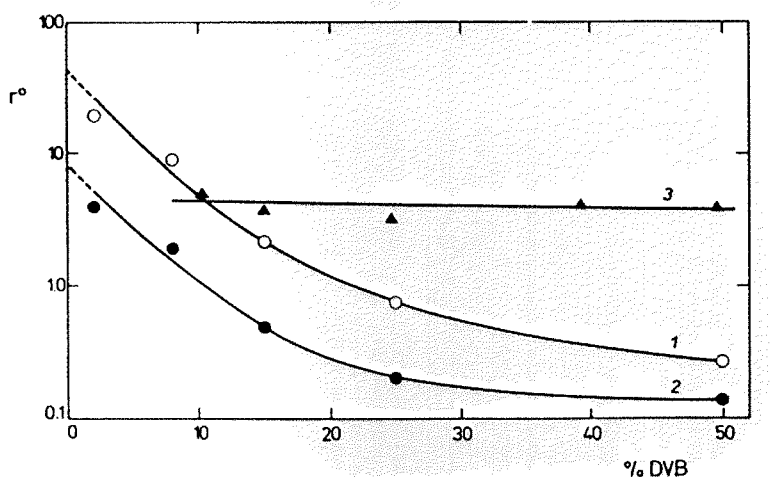

Figure 5.2: Initial rate of trans-esterification reaction with ion exchangers in dioxane. Curves 1 + 2 are two experiments, which show the initial rate (mole/hr $kg_{catalyst}$) using gel type ion exchangers. Line 3 shows the initial rate (mole/hr $kg_{catalyst}$) using macroporous ion exchange resin.

In the gas phase, the increase in initial reaction rate as a function of increasing resin cross-linking was more pronounced (table 5.2).

Resin Cross-linking/ %	Initial rate of reaction/ mole/ hr $kg_{catalyst}$
10	6
15	10
25	13
40	17
60	16

Table 5.2: Initial rate of reaction as a function of macroporous resin cross-linking.

This trend represented a 280% increase in the reaction rate in the gas phase within a series of cross-linked resins from 10 - 60% resin. Many other researchers[221,222,223] have also reported that the rate of gas phase reactions increases with increasing cross-linking with macroporous resins. This increased rate is due to the increased surface area of the catalyst.

The effect of substrate structure on the rate of reactions catalyzed by ion exchange resins has also been studied by Beránek, Setínek and Kraus.[224] They investigated the reactivity and adsorptivity of reaction components and correlated them with polar and steric constants in the re-esterification reaction of esters with alcohols in the gaseous phase.

In the reaction of ethyl acetate **(68)** with alcohols, it was observed that the rate constant (*k*) decreased with increasing steric bulk in the alcohols used (figure 5.3).

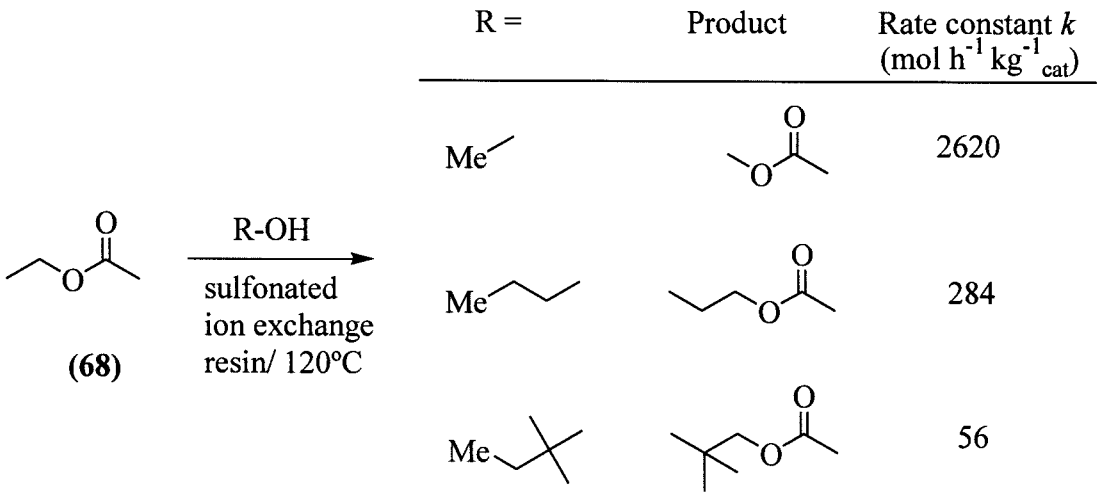

Figure 5.3: Rate constants using different alcohols in a trans-esterification reaction with ion exchange resins.

They found that their reaction was best described by the equation:

$$r^{o} = \frac{k K_A K_B P_A^{o} P_B^{o}}{[1+K_A P_A^{o}+(K_B P_B^{o})^{1/2}]^3}$$

where:

	r^{o}	=	initial reaction [mol h^{-1} $kg^{-1}_{catalyst}$]
	k	=	rate constant [mol h^{-1} $kg^{-1}_{catalyst}$]
	K_i	=	adsorption co-efficient [atm^{-1}]
	P_i^{o}	=	initial partial pressure [atm]
	A/B	=	indices representing the ester and alcohol respectively

Although they did not mention individual constants for physical parameters such as pore or particle size, these would have been incorporated into the adsorption co-efficient K_i used in the rate equation.

The rate constants for the reactions of ethyl esters (formate **(71)**, acetate **(72)** and isobutyrate **(73)**) with 1-propanol are summarized in figure 5.4. The results show that the steric bulk of reactants again affects the rate of resin-catalyzed reactions.

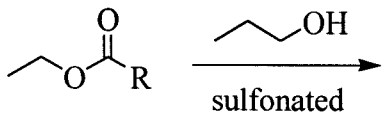

R =	Rate constant k (mol h^{-1} kg^{-1}_{cat})
H **(71)**	37050
CH_3 **(72)**	284
(73)	56

Figure 5.4: Rate constants using different esters in re-esterification with macroporous ion exchange resin.

5.1.2 *Gel resin reactions*

The issues of substrate specificity and site accessibility with respect to cyclisation of a linear resin bound molecule to produce a resin bound cyclic or oligomerized species were addressed in chapter 3. Given that gel type resins are almost exclusively used in SPOC today, it is important to identify various factors such as reaction kinetics, resin swelling and resin compatibility of reactants, which can all influence solid supported reactions.

5.1.3 *'Microenvironment effects' and gel resin reactions*

Sung, Stratford and Hodge,[225] in their study of the reaction of aldehydes with diethylzinc, using various solid supports noted that blank 2% cross-linked resin was also able to catalyze the reaction of benzaldehyde **(74)** with diethylzinc **(75)** to give 1-phenylpropanol **(76)**. Their purpose-built polymer supported ephedrine and camphor derivatives permitted the transformation (figure 5.5) with enantioselectivity and chemical yield (typically 80% compared to 14% by the blank resin). It was also observed that the % ee tended to be greater in toluene than hexane. For a 1% cross-linked PS-DVB resin,[i] the % ee in toluene was between 74-80%, for a 2% cross-linked

[i] Loaded at ca. 1 mmol/ g.

resin the % ee was 72%. There was not a significant difference in the % ee of the product on comparison of a 1% or 2% cross-linked resin loaded at either 1 or 2 mmol/ g.

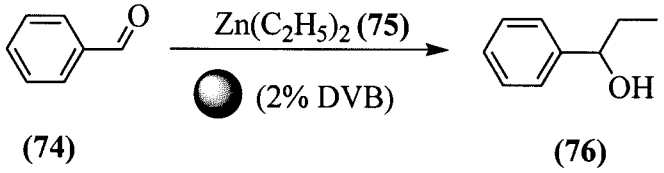

(74) (76)

Figure 5.5: Reaction of diethyl zinc with benzaldehyde.

They reasoned that the blank effect was due to the absorption and concentration of the reactants into the beads. This explanation does appear to be valid, since Gut and Merrifield[226] in a study entitled 'Rate Measurement in Solid Phase Peptide Synthesis' published in 1968 had also noticed this effect. They reported that when they added an *O*-nitrophenylsulfenyl derivative in DMF to dry resin, a rapid decrease in transmittance was observed, corresponding to an increase in effective concentration outside of the beads. They believed that there was selective uptake of DMF by the resin, with exclusion of the solute molecules. A 100 mM solution of the *O*-nitrophenylsulfenyl derivative was estimated to be approximately 45 mM in the resin phase in their case due to the uptake of extra solvent from the medium.

5.1.4 *Cross-linking and swelling in gel resin reactions*

Cross-linking is intimately connected to resin swelling, so attempts to describe one of these must include rationale in terms of the other. The effect of resin cross-linking on reaction rate has been investigated, albeit not extensively. The earliest of such reports described reactions on gel type resins, which were carried out in order to compliment the main subject of the studies using macroporous resins.[227] In such a study, Kurusu reported that cross-linking in gel PS-DVB type resin generates 'micropores', and that a resin with a higher DVB content contains smaller micropores. Thus, in the Prins reaction of styrene with methanal to generate 1,3-dioxanes, Kurusu noted that the yield

of 4-phenyl-1,3-dioxane was the highest in resins with the largest micropores (lowest cross-linking).

Ševčíj, Štamberg and Procházka[222] reported in their esterification of diethylene glycol with pivalic acid, that a higher rate of esterification was observed with microporous gel SX-1 beads (cross-linked at 8%) than with the macroporous styrene-divinyl benzene sulfonated resins (KP-1, cross-linked at 10%) (figure 5.6). The curves 1 - 4 were supported by entries in the following legend.

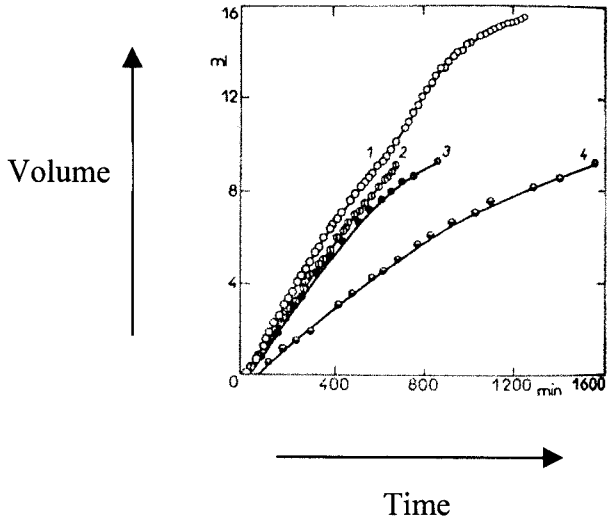

Curve	Pivalic acid	Glycol*	Catalyst	$CHCl_3$	mmeq. catalyst
1	0.5	0.5[a]	Gel	50	10
2	0.5	0.5[a]	Macro	50	10
3	0.5	0.5[b]	Gel	50	10
4	0.5	0.5[b]	Macro	50	10

Figure 5.6: Volume of water distilled from the esterification as a function of time.[228]
Note: a = ethylene glycol, b = diethylene glycol.

The reduction in rate of reaction shown between curves 1 to 2 in figure 5.6 was due to the change from gel type resin to a macroporous one. The effect was slight, but more

pronounced when the effect of steric bulk of reactants was considered, as demonstrated in curves 3 and 4.

5.1.5 *Swelling and gel reactions*

Collman[228] investigated the properties of resin bound transition metal complexes and noted that on binding rhodium (I) **(77)** or iridium (I) complexes to a resin bound ligand **(78)**[ii] two triphenyl phosphine molecules were released per metal atom introduced into the polymer **(79)** (figure 5.7).

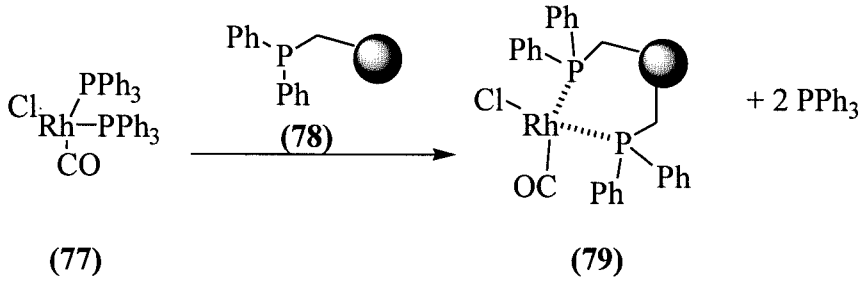

(77) **(79)**

Figure 5.7: Attachment of a rhodium(I) transition metal complex (77) to polystyrene resin.

Having discounted 'non-statistical' functionalisation, which could have caused pockets of highly substituted resin and which would explain this observation, Collman reported that the most plausible explanation for the finding was that once swollen, the polymer chains were sufficiently mobile to bring non-adjacent sites together, which would have allowed displacement of an extra phosphine ligand per metal atom introduced.

Studies specifically aimed at exploring the effect of resin swelling in solid phase organic chemistry have been reported. Stille,[229] using a PS bound rhodium (I) complex to reduce 2-(acetylamino)prop-2-enoic acid **(80)** to **(81)** in ethanol observed no reduction; but on anchoring the catalyst to a poly(2-hydroxyethyl methacrylate) resin also using ethanol as the solvent, observed complete hydrogenation of the double

[ii] Resin was a 2% DVB cross-linked polystyrene resin, loaded at 1.2 mmol/ g.

bond in the substrate, thus demonstrating that adequate swelling of the supporting resin was absolutely critical for the reaction to occur (figure 5.8).

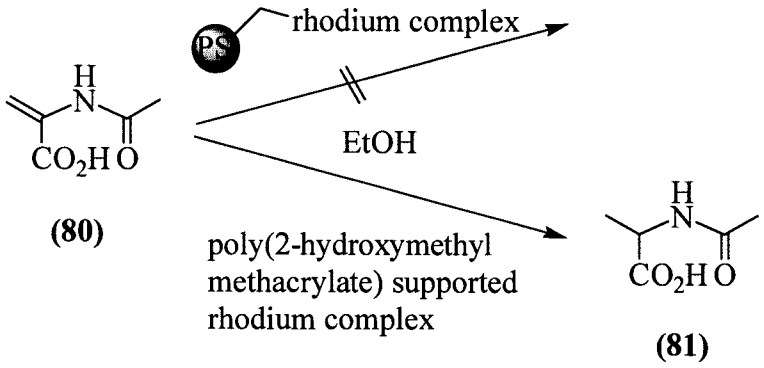

Figure 5.8: Reduction of 2-(acetylamino)prop-2-enoic acid by a rhodium (I) complex supported on polystyrene and poly(2-hydroxymethyl methacrylate).

That swelling is closely related to resin mobility was also demonstrated by Kagan[230] in 1973, who showed that a polymer bound Rh(I)diop complex[iii] would catalyze the asymmetric hydrogenation of α-ethylstyrene and methyl atropate in benzene, but not in ethanol.

5.1.6 *Kinetics of gel resin reactions*

The kinetics of reactions supported on a range of differently cross-linked PS-DVB resins have not been well reported in the literature, but examples demonstrating the kinetics of reactions using single batches of resin beads on single step reactions are more common. Often the restraint lies in the optimization of reliable methods for monitoring the solid phase reactions.[iv] Yan[231, 232] has reported a number of applications of FTIR and single bead FTIR Microspectroscopy which allow monitoring of organic reactions by this non destructive technique. In the acetylation of chloromethyl resin, Yan[233] applied single bead FTIR Microspectroscopy to monitor the progress of the reaction at 1740 cm^{-1}. By removing a drop of resin suspension from the reaction at various times, washing the beads and then transferring the beads to a

[iii] Diop = 2,3-*o*-isopropylidene-2,3-dihydroxy-1,4-bis(diphenylphosphino)butane.
[iv] See chapter 1 for earlier examples.

NaCl plate under the microscope, the IR spectrum of a single flattened bead was taken (figure 5.9).

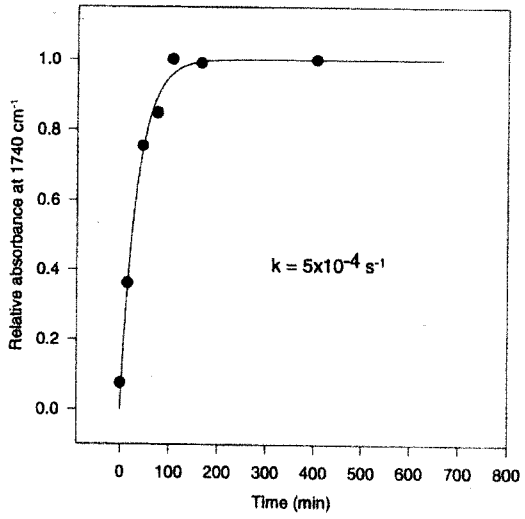

Figure 5.9: Time course of acetylation reaction of chloromethyl resin. The progression of the reaction, measured at 1740 cm^{-1} is plotted against time.

Fitting the data to the first order rate equation: $[B] = 1-e^{-kt}$

where [B] represented the concentration of acetylated product, the rate constant for the reaction was calculated to be $5x10^{-4}$ s^{-1}. Yan concluded from this that the solid phase reaction proceeded 'faster than has been generally been speculated', presumably by his peers at the time. In his paper he proceeded to report that the reaction on Tentagel beads did not occur faster than on the Wang resin, suggesting that diffusion of substrate into a bead co-polymerized with 1% DVB was not rate-limiting in the reaction.

5.2 RESULTS AND DISCUSSION

5.2.1 *Kinetics of cleavage of Methyl Red from the series of Rink loaded aminomethyl resins*

5.2.1.a *Loading of Methyl Red onto the Rink loaded aminomethyl resins*

The chloromethyl PS-DVB resins were all converted to the aminomethyl resins **(30)** by reaction with potassium phthalimide in DMF under conditions of reflux, followed by hydrazinolysis in ethanol for 16 hours. The acid labile Fmoc Rink linker was loaded onto each of the resins by DIC activation to give **(82)**. The Fmoc group was cleaved using a solution of 20% piperidine in DMF and the commercially available azo-dye Methyl Red loaded onto the Rink linker, via DIC activation of the pendant acid of the dye group to give **(83)** (figure 5.10).

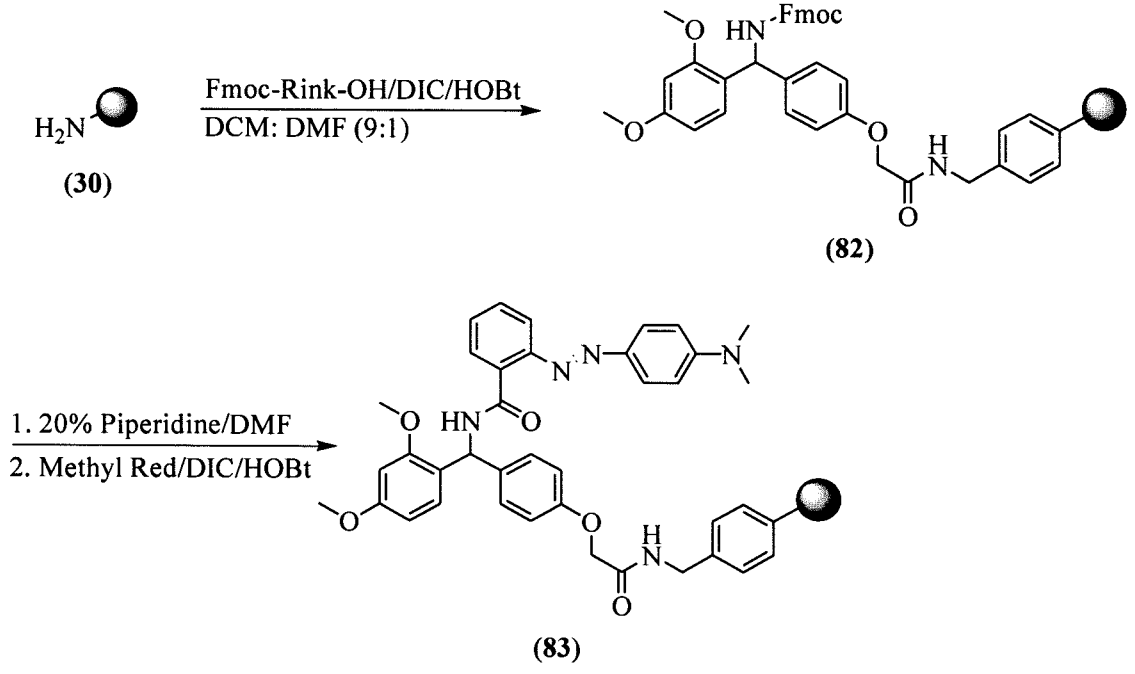

Figure 5.10: Loading of Rink Linker and Methyl Red onto each PS-DVB Resin.

5.2.1.b *Cleavage of the Methyl Red from the resins*

The rate of release of the dye from **(83)** was measured by UV-VIS spectroscopy following cleavage using a solution of TFA:H_2O:DCM (95:2.5:2.5) to generate **(84)** (figure 5.11).

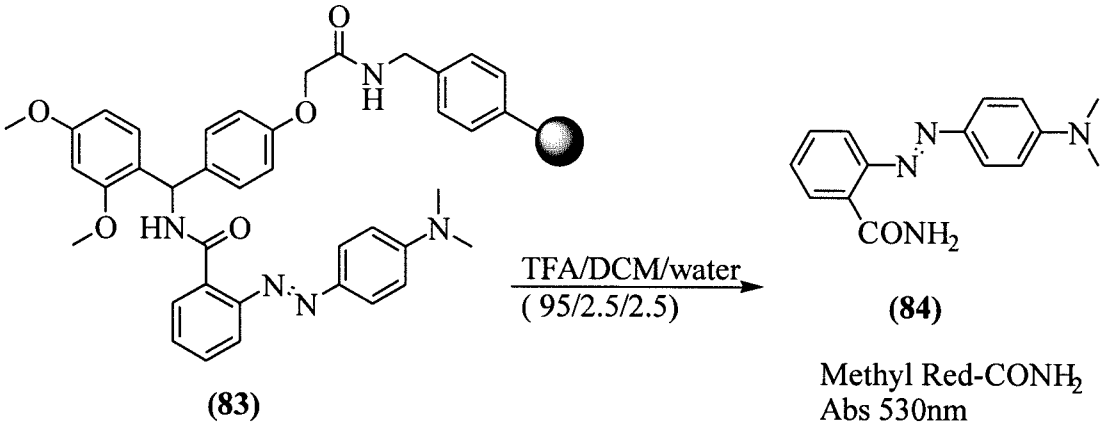

Figure 5.11: The cleavage of Methyl Red from the Rink loaded PS-DVB resins.

Upon addition of the cleavage solution to the 0.3% cross-linked resin, the solution turned almost immediately pink, which darkened rapidly to a deep red colour. In contrast addition of the cleavage solution to the 6.0% cross-linked resin, caused the colour of the solution to increase in intensity to a strong red (λ_{max} = 530 nm) but over a much larger time scale (figure 5.12).

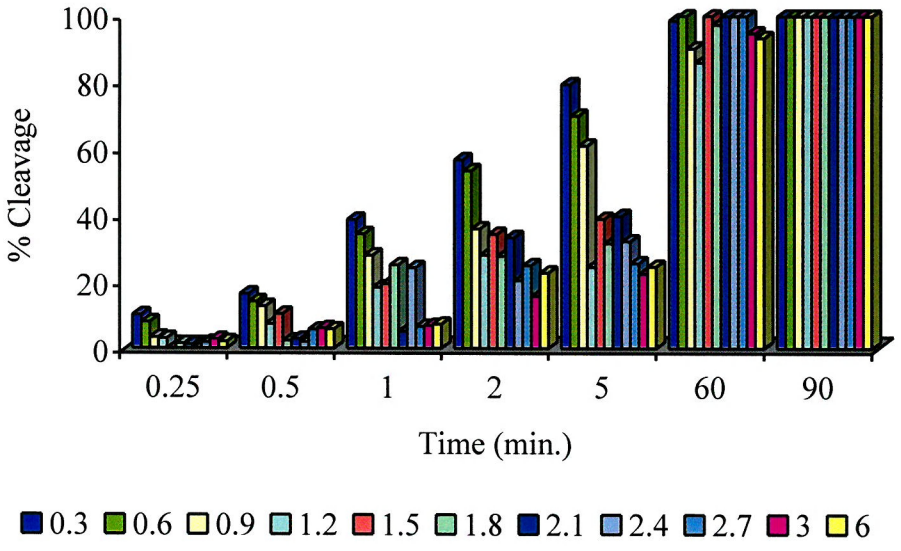

Figure 5.12: Cleavage of Methyl Red from the range of Rink loaded PS-DVB resins.

The initial rate of release of the dye **(84)** from the 0.3% cross-linked resin was over 5 times that of the 6.0% cross-linked resin, indicating the ease of diffusion of the cleavage solution, in and the products of the cleavage reaction, out of the beads. The initial rates of reaction were calculated by differentiation of the initial increase in absorbance of the solution for each resin with time (figure 5.13). The dramatic differences in reaction rates were attributed to differences in resin cross-linking.

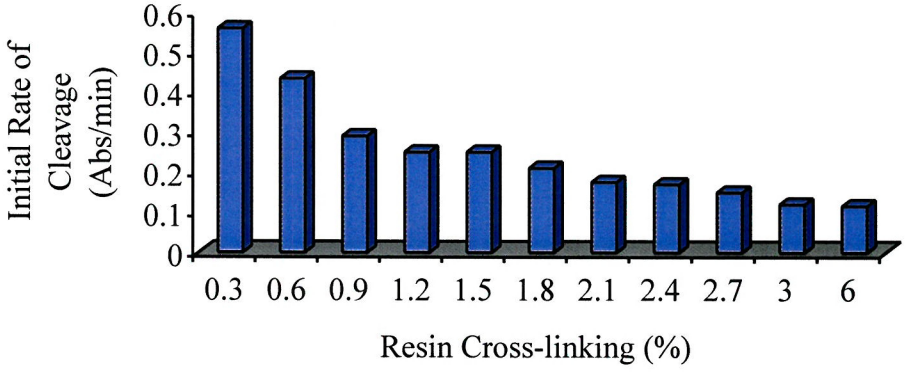

Figure 5.13: The initial rate of cleavage reaction with increasing resin cross-linking.

The initial rates of reaction fell with increasing resin cross-linking. The maximum theoretical reaction rate corresponds to reaction in the solution phase, which was best achieved in the case of the 0.3% resin. The minimum rate of reaction would implicate

a resin, which was so highly cross-linked that the reagents could not penetrate the matrix in order to react. Such an example may result in chemical reaction solely at the solvent/ resin interface.

5.2.2 *Suzuki reaction*

To investigate the effect of resin cross-linking on the rate of an organic reaction, the Suzuki reaction was chosen and carried out on the each of the resins. The palladium catalyzed carbon-carbon bond forming Suzuki reaction,[234,235,236] has gained increasing popularity[237] in recent years and closely resembles the mechanism of the Stille[238,239] coupling reaction. Little is known about the exact nature of the structures in the transition state catalytic cycle of the reaction[240] on the solid phase but in solution, the reaction can be represented as shown in figure 5.14 – presumably the two are related.

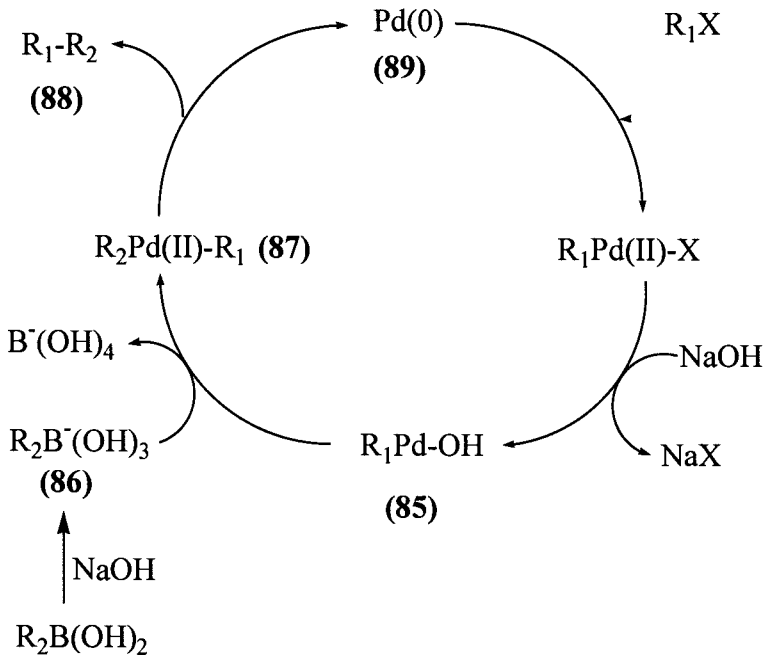

Figure 5.14: Mechanism of the Suzuki reaction, classic solution phase version.

On the solid phase the mode of catalysis is heterogeneous since the resin is not fully soluble. A base is required for successful completion of the Suzuki reaction, and in practice sodium or potassium carbonate is used in the reaction, but these bases are only

sparingly soluble in the popular solvent of choice – DMF. Oxidative addition of the halide component with the palladium (0) species occurs initially to generate Pd(II). The relative rate of reactivity decreases in the order of I > OTf > Br > Cl. One equivalent of base is required to form the boronate and the other is required in the displacement, which forms palladium hydroxide **(85)**. This is followed by transmetallation involving the R_2 constituent of the boronate **(86)** to the Pd metal center producing the Pd(II) species **(87)**. The Pd(II) complex now contains both halves of the intended product. Reductive elimination of the product **(88)** then follows with displacement of the product from the metal center, which regenerates the catalytically active Pd(0) complex **(89)**.

5.2.2.a Loading of 4-iodobenzoic acid onto the resins

Each of the differently cross-linked resins was converted to the aminomethyl form **(30)** and loaded with the Rink linker and deprotected as described above. 4-iodobenzoic acid was loaded onto the Rink linker via the amine group by DIC activation to produce the resin bound iodo-compound **(90)**. The resins were then reacted in the presence of phenylboronic acid, palladium tetrakis-triphenylphoshine and potassium carbonate in DMF at 80°C to generate **(91)** (figure 5.15).

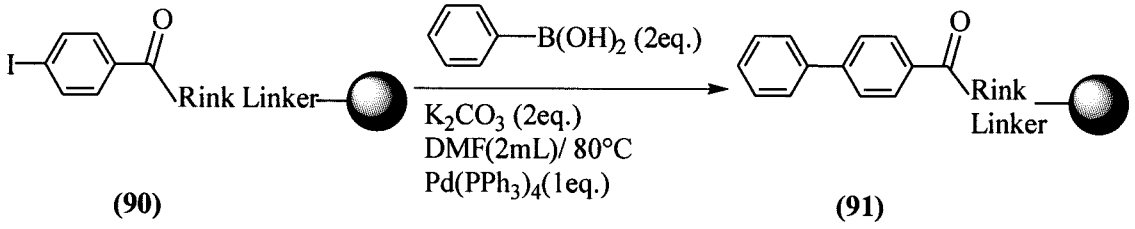

Figure 5.15: Suzuki reaction of Rink loaded PS-DVB resins with 4-iodobenzoic acid.

5.2.2.b *Cleavage from resin*

Aliquots of resin **(92)** were withdrawn with time and the resin bound products cleaved using a solution of TFA:H_2O:DCM (95:2.5:2.5) to give a mixture of **(93)** and **(94)** (figure 5.16).

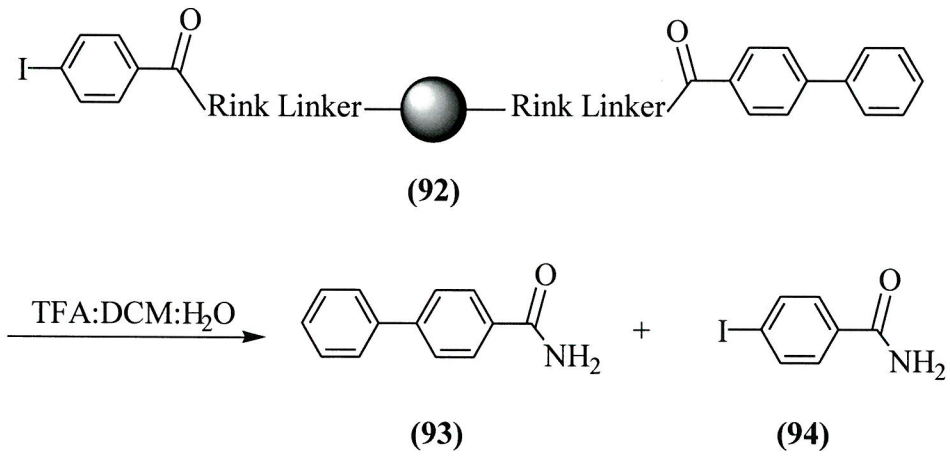

Figure 5.16: Cleavage of Suzuki product from each of the PS-DVB resins.

The course of the reaction was monitored by RP-HPLC and MS analysis of the crude cleavage product (figure 5.17) from each of the resins.

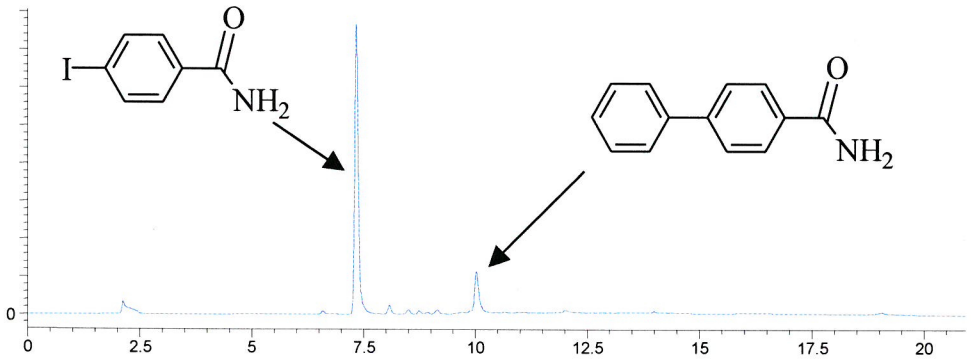

Figure 5.17: Monitoring of the Suzuki reaction by HPLC.

With each resin the Suzuki reaction occurred successfully. The rate of formation of the biaryl product **(93)** with time varied with resin cross-linking. The most rapid reaction was observed in the case of the 0.3% resin, and the rates were observed to decrease with increasing cross-linking across the series (figure 5.18).

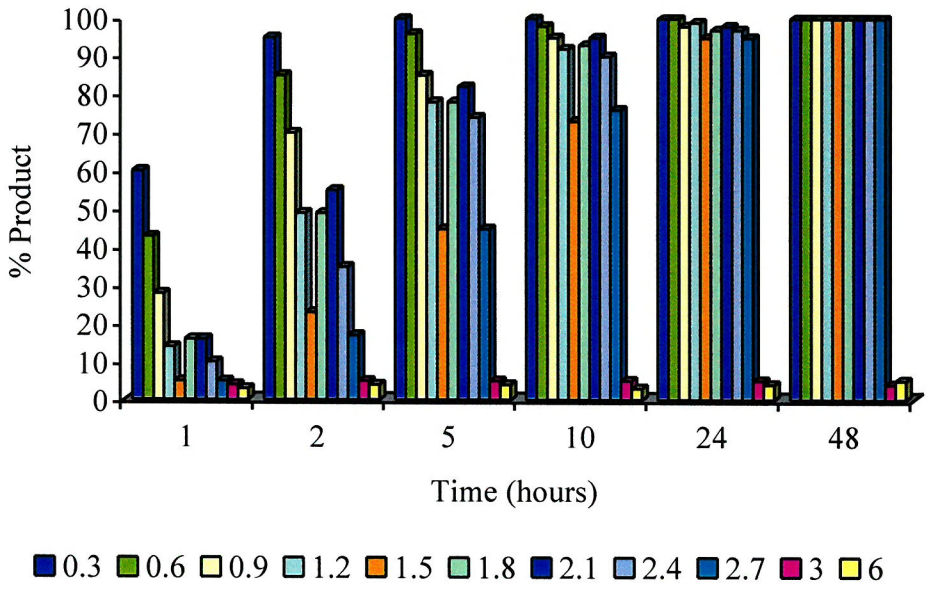

Figure 5.18: Cleavage of product of the Suzuki reaction of phenylboronic acid and 4-iodobenzoic acid loaded via the Rink linker from each of the resins, with time.

The initial rate with the 0.3% cross-linked resin was 47 times that of the 6.0% resin (although the reaction with the 6.0% resin was not observed to proceed to completion). These results gave an insight into the accessibility of the reactants into the polymeric matrix, in a manner, which parallels the Methyl Red cleavage experiments described above.

The half-lives of the Suzuki reactions on the resins were calculated (figure 5.19).

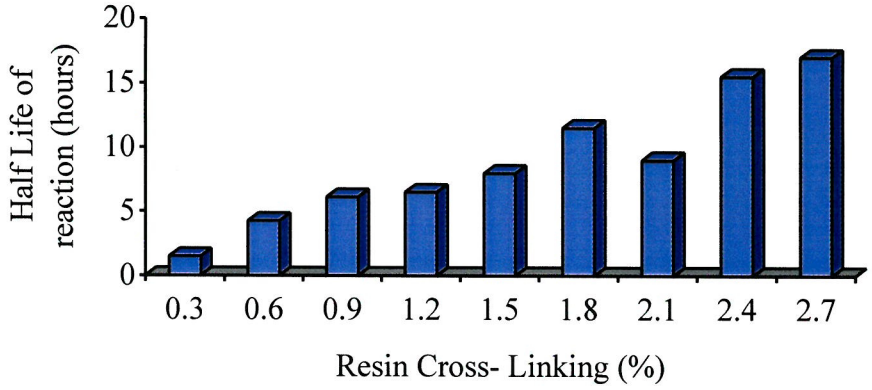

Figure 5.19: Half-life of the Suzuki reaction of phenyl boronic acid and Rink loaded 4-iodobenzoic acid on the 0.3% -2.7% cross-linked resins.

The reaction using the 0.3% PS-DVB resin was 50% complete after the first hour of reaction at 80°C, but in contrast the corresponding reaction with the 2.7% resin showed only a 6% conversion to **(93)** after 1 hour. Complete conversion to **(93)** was demonstrated in all the resins (0.3% to 2.7%) after 48 hours.

The 3.0% and 6.0% resins displayed unusual behavior. The reaction yield for these resins was between 3 - 5% only. No other products were observed and the starting material was present after 48 hours. This effect was initially believed to be due to restricted site accessibility to the palladium tetrakis triphenylphosphine catalyst in these relatively highly cross-linked resins but this hypothesis could not be validated as the same catalyst facilitated the allyl ester hydrolysis in the final stages of the synthesis of Kawaguchipeptin B[v].

The Suzuki reaction was repeated on the 3.0% resin in a range of different solvents, including the same solvent (THF: DCM, 1:1) as was employed for the allyl deprotection reaction during the Kawaguchipeptin B synthesis as well as in methanol, dioxane, THF: DCM and DMF. In methanol the yield was only 1.7% while in the case of dioxane and THF: DCM, the reaction proceeded to completion.

[v] Described in chapter 3.

These results highlight the importance of resin swelling. At 40°C the reaction carried out in DMF gave a final yield of 4.9%, which was similar to that performed in DMF at 80°C. The fact that the reaction occurred to the same extent at 40°C as at 80°C in DMF suggests that the rate of reaction in both cases was sufficient to allow the reaction to progress to the same level of completion (yielding approximately 4.9% in both cases), in respect of other limiting factors *i.e.* resin swelling. Methanol is a very poor solvent for swelling polystyrene resins, and even though it was able to dissolve the substrates effectively, the yield of **(93)** was only 1.6%, indicating an even greater degree of inaccessibility of the matrix towards the reagents. This is reinforced by the two reactions performed in dioxane and THF: DCM. These solvents (even in the case of the highest cross-linked resins) have been shown to swell the resins to a greater extent than in the case of methanol and DMF,[vi] and not surprisingly reactions performed using these solvents were observed to proceed to completion.

5.3 CONCLUSION

These studies have shown that the choice of solvent and the cross-linking of the resin is very important for a resin-supported reaction. Cleavage of the dye Methyl Red from the acid labile Rink linker showed that the lowest cross-linked resins (0.3% - 1%) in the range allowed much more rapid cleavage than higher cross-linked resins in the series. The Suzuki reactions performed on each of the resins demonstrated two essential factors in solid phase organic chemistry. Firstly, the rate of formation of the biphenyl product **(93)** on the resin was observed to decrease with increasing resin cross-linking until the point at which the resin swelling became limiting in the Pd catalyzed reaction. Secondly sufficient resin swelling was not permitted by the DMF for the higher cross-linked materials, which appeared to facilitate chemical reaction on the surface of the beads only. In changing to solvents that allowed a greater level of resin swelling (THF: DCM and dioxane), the Suzuki reaction was observed to proceed to completion.

[vi] See chapter 2 for details.

CHAPTER 6 - POLYMER SUPPORTED IMIDAZOLE - PRECEDENTS

6.1 INTRODUCTION

The acid/ base properties of amino acid side chains are important for the function of proteins. The amino acid histidine is present in many proteins, due to the specific properties of the imidazole side chain group (figure 6.1).

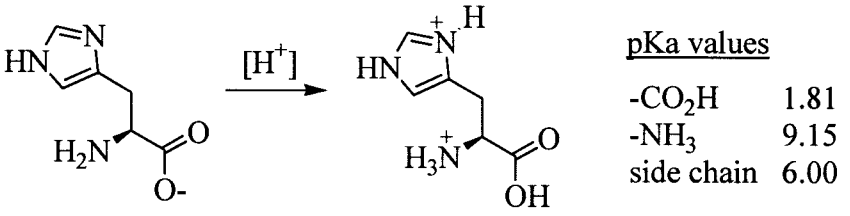

Figure 6.1: Acid-base properties of histidine.

The pKa of the side chain group of histidine is 6; therefore at the physiological pH the ratio of imidazole to imidazolium ion is 10:1. Organisms have successfully exploited this property by incorporation of histidine into the active sites of many enzymes and proteins. In many proteins, histidine is present with other amino acids whose side chains 'communicate' with each other to facilitate the overall desired reaction, for example in papain.[241]

Papain is a proteolytic enzyme produced by the fruit of the papaya tree. It has a broad specificity for peptide bonds and consists of a single polypeptide chain of 212 amino acid residues. The structure is held together by 4 disulphide bonds with the active site of the enzyme consisting of cysteine and histidine residues. The pKa of the imidazole group of the histidine residues is shifted to 8.2 by the microenvironment of the peptide, thereby making the histidine group more basic (figure 6.2).

There are many other examples of histidine playing a paramount role in the function of biological molecules (e.g. in the active sites of aldolase, carboxypeptidase,

chymotrypsin, glyceraldehydes 3-phosphate dehydrogenase, lactate dehydrogenase and RNase A).

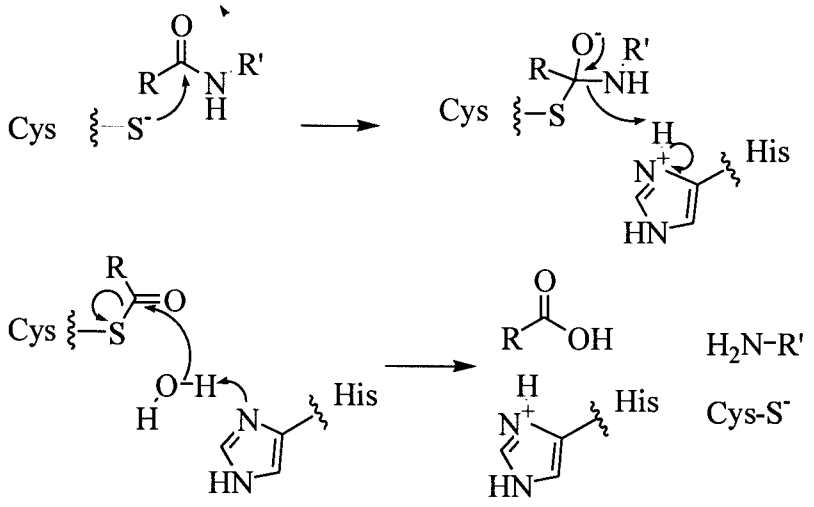

Figure 6.2: Catalytic reaction of papain using the imidazolium ion of His 159 and thiol group of Cys 25.

The imidazole group is also a constituent part of the biologically important porphyrin ring, which is associated with many proteins, especially those which have transition metal prosthetic groups. Collman and Reed[242] described the synthesis of ferrous-porphyrin complexes. They synthesized a model for oxygenated myoglobin by treating a complex of Fe(*meso*-tetraphenylporphyrin) (Fe(TPP)) with a resin bound imidazole (figure 6.3), to yield a six-coordinate Fe(II) species **(95)**.

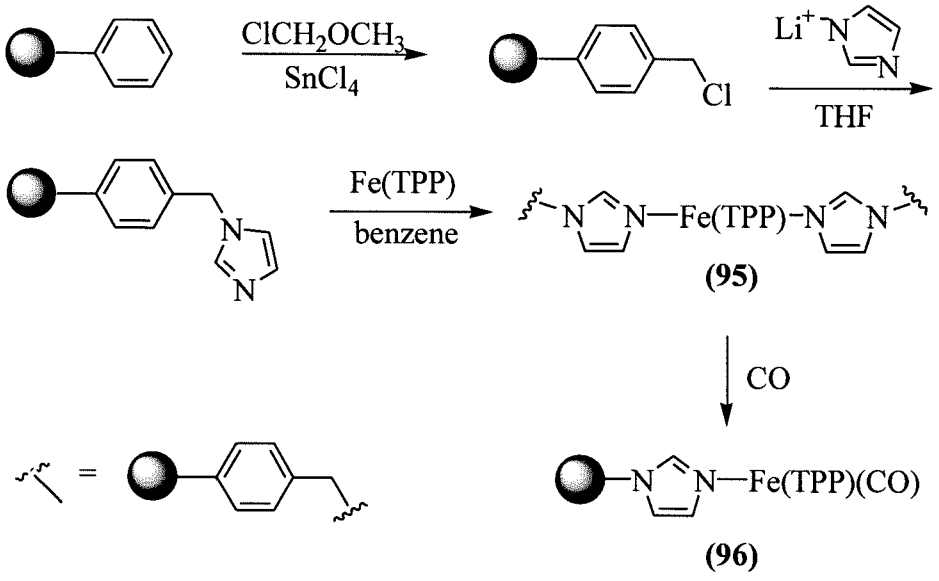

Figure 6.3: Collman and Reeds synthesis of ferrous-porphyrin complexes.

The reversible oxygenation of myoglobin results from a five co-ordinate high spin Fe(II) porphyrin complex placed in a hydrophobic pocket in the molecule. Collman and Reeds oxygenated model of this was six co-ordinate and was also able to bind CO ligands strongly **(96)**. Just as its biological counterpart, the CO ligand remained tightly bound to the complex on heating.

Other applications of the solid supported imidazole groups exist. Reedijk and Sherington[243] demonstrated selective and rapid uptake of copper(II) ions by a resin consisting of 4-[(2-aminoethyl)mercaptomethyl]-5-methylimidazole supported on a poly(glycidyl methacrylate-co-ethylene glycol dimethacrylate polymer. Their resin showed a high affinity for Cu(II) in solution (0.42 mmol Cu/ g), with rapid uptake kinetics ($t_{½}$ = 8-20 minutes for a 16 mM solution) and also a high affinity for Cu(II) in mixed solutions. In such a mixed solution at pH 5 the polymer bound; Cu(II) (0.42 mmol Cu/ g) with the highest affinity and Cd(II) (0.1 mmol Cd(II)/ g), Zn(II) (0.12 mmol Zn(II)/ g) and Ni(II) (0.15 mmol Ni(II)/ g) with approximately the same level of affinity. The insertion of imidazole groups into a polymer was thus demonstrated to be useful in the selective uptake of certain metal ions in solution.

A major industrial application, the decontamination of waste-waters also uses this principle. In this field, Bergbreiter[244] has performed the sequestration of trace metals

using both water-soluble and fluorous phase-soluble polymers based on the polymer poly(N-isopropyl acrylamide)-co-(N-acryloxy succinimide) (PNIPAM-c-NASI). This polymer and also one which had been synthesized by co-polymerization of vinyl imidazole and (PNIPAM-c-NASI) bound Fe(III)[i] also complexed Cu(II).[ii]

These examples demonstrate popular uses of imidazole groups on the solid phase. The imidazole groups proven chemical versatility provides a precedent for the design and construct of a novel imidazole bound PS based resin.

6.2 RESULTS AND DISCUSSION

6.2.1 *Suspension polymerization - the initial attempt*

Using suspension polymerization methods described in chapter 2, it was envisaged that imidazole could be incorporated into a PS-DVB polymer by inclusion of the commercially available *N*-vinyl imidazole monomer into the mixture, however it was discovered that the original polymerization system was not suitable, given the hydrophilicity of the imidazole monomer **(97)** (figure 6.4).

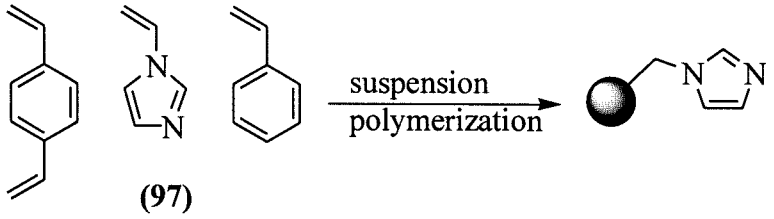

(97)

Figure 6.4: The synthesis of PS-supported imidazole by co-polymerization of N-vinyl imidazole. Note imidazole is directly attached to the polymer backbone.

Microanalysis of the beads synthesized by the suspension polymerization gave an immeasurable nitrogen content, which indicated no incorporation of the imidazole monomer into the beads. The suspension polymerization reaction is only effective for

[i] The polymer bound 99% of a 14.4 ppm solution of Fe(III).

cases when there is a marked difference in solubility of the two phases used. In traditional suspension polymerization reactions, styrene, divinyl benzene and (when used) the chloromethyl styrene are all insoluble in water. In the synthesis shown in figure 6.4, *N*-vinyl imidazole was discovered to be soluble in both the organic and aqueous phase. There was little partitioning of the monomer in the organic droplets, and therefore no incorporation of the *N*-vinyl imidazole monomer.

6.2.2 *Suspension polymerization and the successful attempt - hydrophobicity*

In order to increase the hydrophobicity of the *N*-vinyl imidazole monomer, the molecule was made more hydrophobic by the incorporation of a benzene ring into the structure. There were no literature precedents for this but from the transformation, the monomer was required to retain sufficient imidazole character and also the vinyl group for inclusion into the polymerization mixture. The monomer 1-(4-vinyl-benzyl)-1*H*-imidazole **(98)** appeared to offer the most convenient solution (figure 6.5).

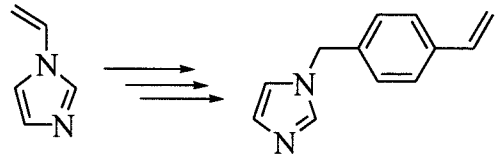

(98)

Water soluble More hydrophobic

Figure 6.5: A hydrophobic imidazole moiety containing a vinyl group.

This was prepared by treating imidazole in THF with one equivalent of sodium hydride, followed by addition of chloromethyl styrene (drop-wise) (figure 6.6). The reaction was facilitated (Finkelstein) using potassium iodide.

[ii] 1.23 g of a 10:1 NIPAM-vinyl imidazole co-polymer bound 98% of a 269.2 ppm solution of Cu(II) ($CuSO_4$) on heating.

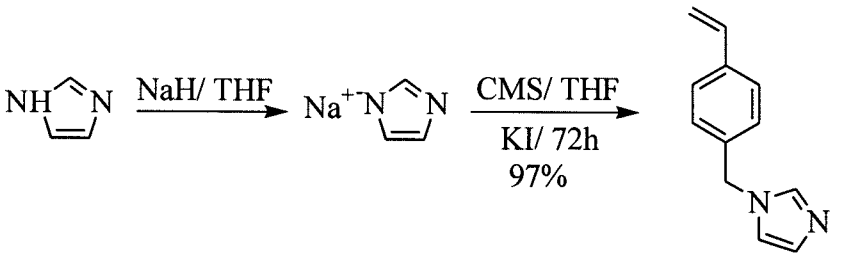

(98)

*Figure 6.6: Synthesis of 1-(4-vinyl-benzyl)-1H-imidazole **(98)**.*

Product **(98)** was obtained in 97% yield after stirring for 72 hours at room temperature and extraction with ethyl acetate. A small-scale co-polymerization of **(98)** with styrene and divinyl benzene (1%) and yielded 1.24 g (2% by mass) of PS-DVB supported poly (styrene-co-DVB-co-1-(4-vinyl-benzyl)-1*H*-imidazole) resin **(99)**, loaded at 0.7 mmol imidazole/ g; (nitrogen content 1.4 mmol/ g) (figure 6.7).

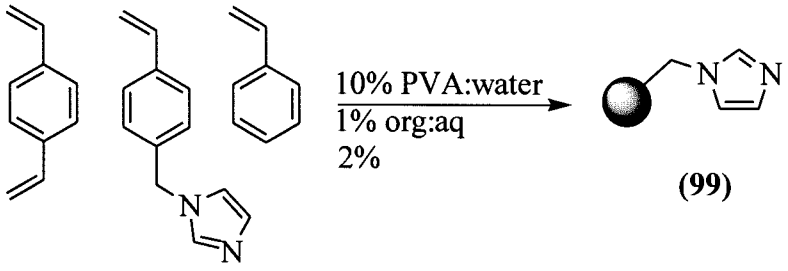

(98) **(99)**

Figure 6.7: Synthesis of poly (styrene-co-DVB-co-1-(4-vinyl-benzyl)-1H-imidazole) resin.

The relatively low yield of reaction was consistent with previous observations that the suspension polymerization reaction cannot be simply scaled down by reduction of the volume of the organic phase. Such a change alters the organic: aqueous phase ratio, which affects the fluid dynamics of the suspension system by making the suspension more characteristic of the aqueous phase, and also alters the size of the droplets formed during the pre-equilibrium phase of the reaction.

6.2.3 *Can poly (styrene-co-DVB-co-1-(4-vinyl-benzyl)-1H-imidazole) resin chelate copper?*

In order to demonstrate whether poly (styryl-co-DVB-co-1-(4-vinyl-benzyl)-1H-imidazole) resin would bind copper(II), a solution of glycine, copper(II) sulphate in THF: water was prepared and added to the beads. The beads were gently shaken for 3 days to allow the solvent to penetrate the beads. A glycine solution was chosen due to its high water solubility and the fact that amino acids are known to bind copper(II) ions in solution, forming a deep purple-coloured complex **(100)** (figure 6.8).

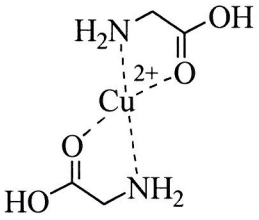

(100)

Figure 6.8: Copper(II)-glycine complex (λ_{706} nm).

As the copper was removed from the copper-glycine complex, reduction in intensity of the deep purple colouration was observed. The beads were also observed to turn from an off-white/ cream colour to an intense blue/green colour (figure 6.9).

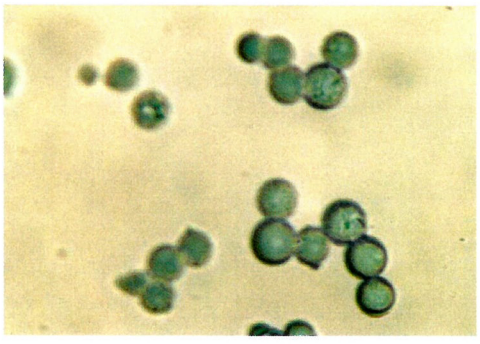

Figure 6.9: Blue/green beads observed after incubation of poly (styrene-co-DVB-co-1-(4-vinyl-benzyl)-1H-imidazole) resin in a solution of glycine, copper sulphate in THF: water for 72 hours.

A second batch of the imidazole resin was synthesized by an identical method to that used in the synthesis of the first analytical batch but on a larger (50 g) scale and cross-linked at 2 mol% with respect to DVB. The yield of reaction was consistent with the yields reported in chapter 2 for a 2% cross-linked resin, indicating that the relationship between the cross-linking of the resin and the overall yield of reaction may hold true for other functional monomer systems as well as chloromethyl styrene. The size distribution of the 2% cross-linked beads is shown in figure 6.10.

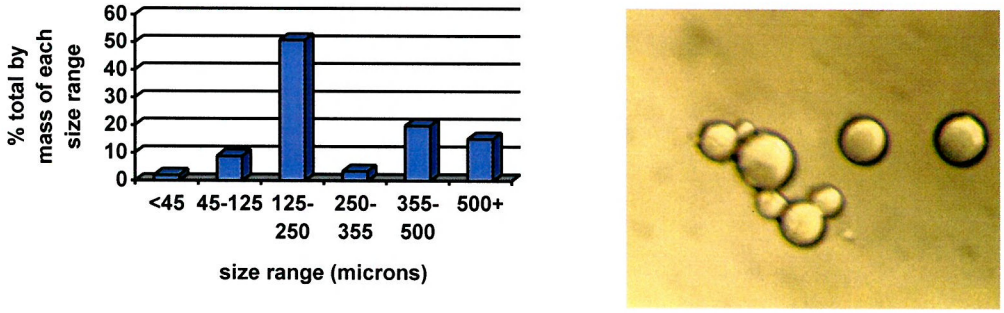

Figure 6.10: Size distribution of the 2% cross-linked PS-DVB imidazole resin. Pictured on right: enlarged photograph of beads in the 45 - 125 micron size range.

Particles with diameters in the range 45 – 355 μm were spherical, but above this diameter there was a tendency for the generation of non-spherical and more irregularly shaped particles. The polymerization system was therefore more efficient at producing smaller beads.

Microanalysis of this gave a content of 87.44% carbon, 7.85% of hydrogen and 3.09% by mass of nitrogen, thus indicating that the average repeating unit for the resin was $C_{33}H_{36}N$. This corresponded to a loading of 1.12 mmol/ g compared to the theoretical loading of 2 mmol imidazole/ g.

The beads were placed in increasing concentrations of $CuSO_4$ (0.05 M, 0.10 M and 2.0 M) in DMF and shaken gently for 36 hours (figure 6.11). The resins were then washed and each filtrate concentrated and made up to 10 mL with DMF. The filtrates were monitored spectroscopically and thus the amount of copper chelated in the resin, calculated.

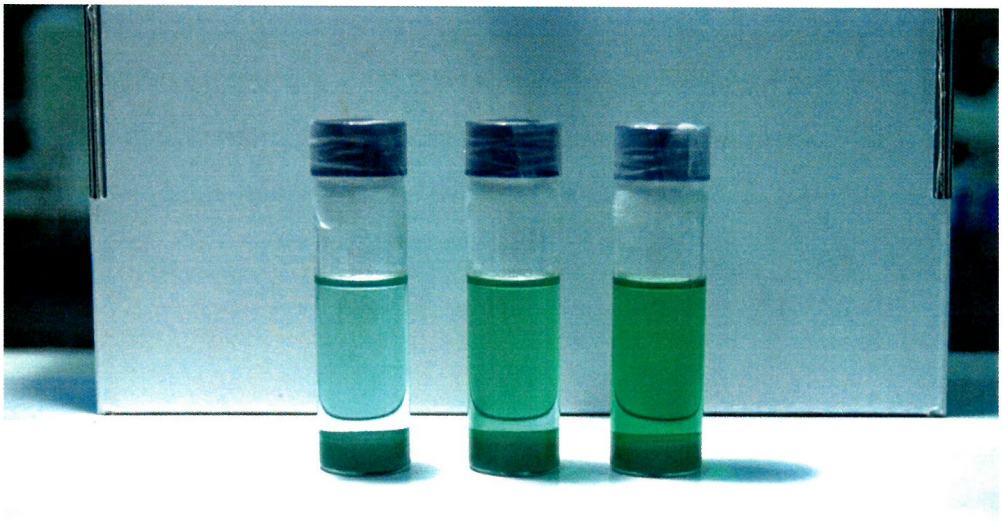

Figure 6.11: PS-DVB imidazole resin beads (1 g) in increasingly concentrated solutions (0.05 M, 0.10 M and 0.20 M) of $CuSO_4$ in DMF.

Calibration was carried out with increasingly concentrated solutions of $CuSO_4$ in DMF by measuring the absorbance at 270 nm.

It was therefore possible to measure the concentrations of Cu(II) in the filtrates shown in figure 6.11 (table 6.1).

Experiment	**Total mass of $CuSO_4$ in DMF/ mg**	**Supernatant concentration/ mol/ dm^3**	**Mass of $CuSO_4$ in supernatant/ mg**
1	**80**	0.003	5
2	**160**	0.043	68
3	**320**	0.140	223

Table 6.1: Calculation of remaining $CuSO_4$ in supernatant. The total mass of $CuSO_4$ in DMF (column 2) represents the solution that the beads were initially suspended in. Supernatant concentration (column 3) refers to the mass in solution after 36 hours.

Excess $CuSO_4$, which could not be bound by the resins due to saturation, remained in solution. Each 1 g sample of resin bound approximately the same amount of $CuSO_4$ (75, 92 and 96 mg) as determined by UV-Vis spectrometry. As the loading of the resin was 1.12mmol /g this suggests that the binding of the Cu(II) to the resin occurred approximately in the ratio 1:2. The average binding ratio was 2.06, which suggests that the 2% cross-linked PS-DVB resin was sufficiently flexible to allow two imidazole groups to manoeuvre sufficiently close together in order to chelate a Cu(II) ion (table 6.2).

Experiment	Mass of $CuSO_4$ bound by beads/ mg	$CuSO_4$ bound in beads/ mmol	Molar ratio of imidazole groups : Cu bound by resin
1	75	0.470	2.38
2	92	0.577	1.94
3	96	0.602	1.86

Table 6.2: Calculation of $CuSO_4$ bound in beads.

6.2.4 *Can poly (styrene-co-DVB-co-1-(4-vinyl-benzyl)-1H-imidazole) resin be acylated?*

A number of small-scale tests were carried out whereby the PS-DVB imidazole resin was added to a solution of sulfonyl chloride in order to demonstrate whether the supported imidazole could be sulfonated to form **(100)**. The imidazole resin was shaken with tosyl chloride in DCM for 16 hours and then washed (figure 6.12).

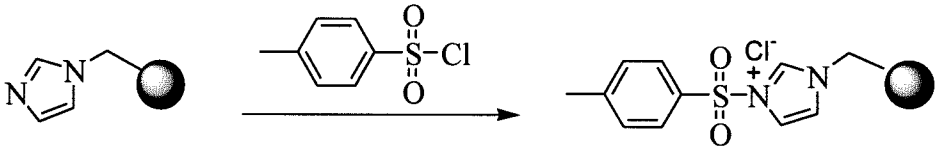

(99) **(100)**

Figure 6.12: Sulfonation of PS-DVB imidazole resin with tosyl chloride.

Once loaded with tosyl chloride, it was envisaged that the sulfonated poly (styrene-co-DVB-co-1-(4-vinyl-benzyl)-1*H*-imidazolium) resin **(100)** could act as an sulfonating

agent for a range of nucleophiles. Thus the resin was shaken in DCM with benzylamine in order to effect sulphonamide formation, but this reaction failed (figure 6.13).

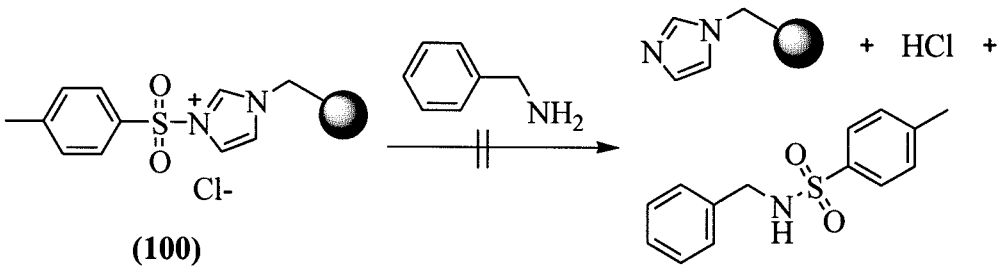

(100) **(101)**

Figure 6.13: Attempts to acylate benzylamine with tosyl loaded imidazole resin.

6.2.5 *The synthesis of ethyl benzoate*

6.2.5.a *Application of poly (styrene-co-DVB-co-1-(4-vinyl-benzyl)-1H-imidazole) resin to the reaction of benzoyl chloride and ethanol*

The poly (styrene-co-DVB-co-1-(4-vinyl-benzyl)-1*H*-imidazole) resin was applied to the synthesis of the ester ethyl benzoate in order to determine whether the resin could act as a base catalyst for the reaction (figure 6.14).

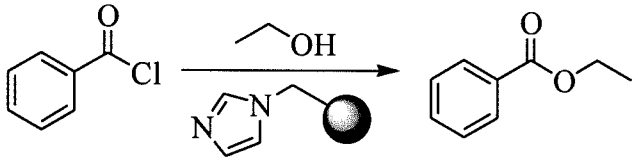

(102)

Figure 6.14: Synthesis of ethyl benzoate catalysed by PS-DVB imidazole resin.

The reaction of benzoyl chloride with ethanol at room temperature occurs relatively slowly compared to the reaction of benzoyl chloride with the more powerful nucleophiles, such as amines. Thus benzoyl chloride and ethanol were dissolved in DCM in the presence and absence of PS-DVB imidazole resin, and aliquots of reaction mixture withdrawn and quenched with time, though by monitoring the formation of

ethyl benzoate[iii] with time, in EtOH and also DCM, a significant increase in formation of the ester was not detected.

6.2.5.b *Reaction scavenging using PS-DVB isocyanate resin*

During the synthesis of **(102),** ethanol was used in a five fold excess with respect to acyl chloride) (figure 6.14), thus it was necessary to remove the alcohol from the reaction in order to isolate pure ethyl benzoate. A generic protocol for removal of the alcohol from the solution phase reagents via a resin bound reagents, specifically a PS-DVB-isocyanate resin, synthesized by a novel solid phase method was developed. The reaction mixture was filtered and the filtrate dissolved in DCM and one equivalent of DIPEA added (with respect to ethanol). PS-DVB-isocyanate resin (4 equivalents) was added and the mixture shaken at room temperature for 16 hours.

6.2.5.c *Synthesis of isocyanate resin*

The isocyanate group is reactive towards nucleophillic attack. The reaction of an isocyanate with an amine to form an urea is rapid and has formed the basis for a number of applications in SPOC.[245] Rebek[246] demonstrated one of the earliest reports of a solid supported isocyanate group in 1975, by preparing the resin by heating a polystyrene bound amine with phosgene in xylene. Given the toxicity of the reagents used in the synthesis, many researchers have preferred to use polymer supported isocyanate from commercial sources.[247, 248, 249]

In 1998, Petillo[250] demonstrated the synthesis of isocyanates by the chlorosilane-induced cleavage of carbamates **(103)** (figure 6.15). They verified the presence of isocyanates in the reaction mixture by IR analysis (λ=2250 cm^{-1}), and noted that cleavage of the alkyl carbamates was strongly influenced by the steric properties of the alkyl substituent R', with Me ≈ Et > *i*-Bu > CH_2CCl_3 > *t*-Bu.

[iii] In the aqueous HPLC solvent system used in the analysis, benzoyl chloride hydrolyses to form benzoic acid, thus formation of benzoyl chloride was monitored (λ_{254} nm).

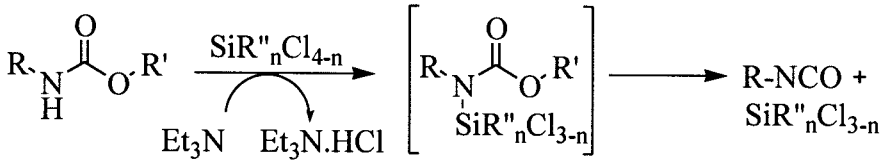

(103)

R = *p*-Me-Ph-
R' = Me, Et, ^{i}Bu, ^{t}Bu, CH_2CCl_3, *p*-OMePh, *p*-NO_2Ph
R" = Me, H

Figure 6.15: Synthesis of isocyanates by the chlorosilane-induced cleavage of carbamates.

Given the strong steric dependency on the properties of the 'R' group, the reaction did not translate well when applied to the resin. Treatment of a PS-DVB resin bound carbamate prepared by the reaction of $(Boc)_2O$ with aminomethyl resin yielded insignificant amounts of isocyanate.

Previously Knolker, Braxmeier and Schlechtingen[251] synthesized phenyl isocyanates from hindered anilines using Boc and dimethylamino pyridine (DMAP) in acetonitrile (figure 6.16).

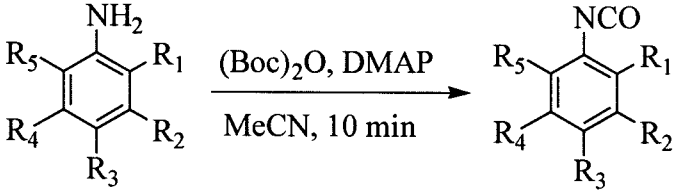

Figure 6.16: Synthesis of isocyanates from hindered anilines using $(Boc)_2O$ and DMAP in MeCN.

As the backbone of PS-DVB resin represents a hindered structure, it was reasoned that this could provide the steric mass afforded by 'R' substituents on the aniline. The reaction was optimised for synthesis of immobilised isocyanates by substitution of the hindered aniline with aminomethyl resin (figure 6.17).

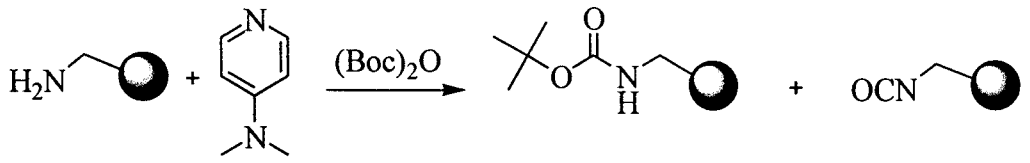

IR C=O str 1710 cm^{-1} N=C=O str 2250 cm^{-1}

C=O str 1160 cm^{-1}

Figure 6.17: Optimisation of the synthesis of isocyanates from anilines, developed by Knolker, Braxmeier and Schlechtingen.

The reaction was monitored by IR spectroscopy and the yield of reaction calculated by comparison of the areas of the N=C=O stretch of the isocyanate group at 2250 cm^{-1} with both the C=O and C-O stretches of the carbamate by-product at 1710 cm^{-1} and 1160 cm^{-1} respectively (figure 6.18).

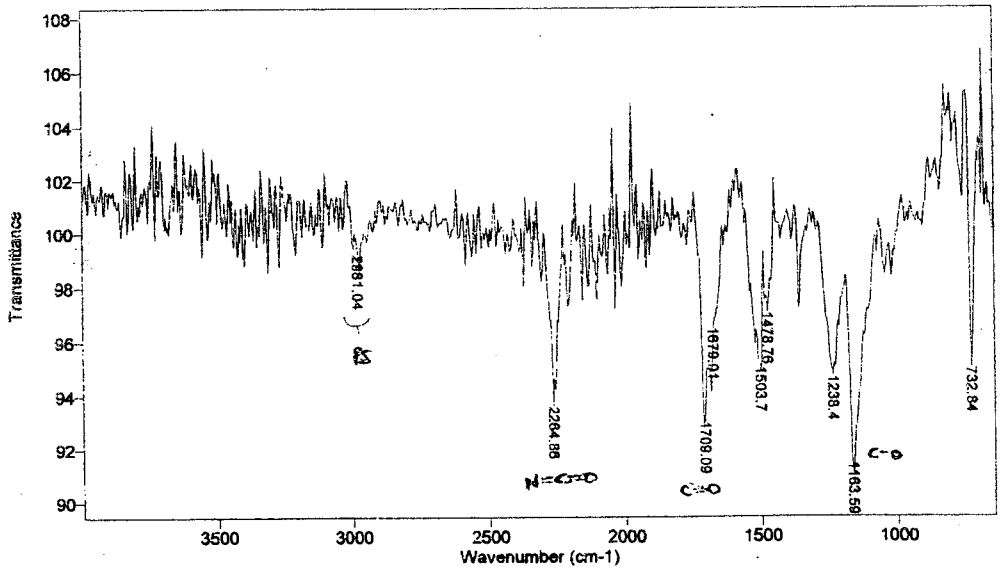

Figure 6.18: IR spectrum of isocyanate and Boc functionalised PS-DVB resin.

The reaction yielded either resin bound isocyanate, Boc protected amine or mixtures of the two, and was more successful when carried out in DCM rather than acetonitrile

(entries H, I, J), and the highest yield of 60% was obtained after one hour of reaction (entry D). Using 1.4 eq. of DMAP, the yield was 50% after 45 minutes (entry C), but on increasing the number of equivalents to 2, an identical yield was obtained in 22.5 minutes (entry K) (table 6.3).

Entry	Temp/ °C	Solvent	Resin	Time/ min	Eq. of Boc_2O	IR yield (%)
A	-78	DCM	PS	45	1.4	0
B	0	DCM	PS	45	1.4	50
C	20	DCM	PS	45	1.4	50
D	-78 → 20	DCM	PS	90	1.4	60
E	-78	DCM	PS	135	1.4	40
F	20	DCM	PS	45	1.4 (-DMAP)	0
G	20	DCM	MPA	45	2	0
H	20	MeCN	PS	22.5	2	0
I	20	MeCN	PS	45	2	0
J	20	MeCN	MPA	22.5	2	0
K	20	DCM	PS	22.5	2	50
L	20	DCM	PS	82.5	2	33
M	20	DCM	MPA	22.5	2	50
N	20	DCM	MPS-80	22.5	2	0

Table 6.3: Optimisation of conditions for the synthesis of supported isocyanate. MPA = macroporous polyamine resin (Amberlite), MPS = macroporous aminomethyl polystyrene resin (20%, loaded at 0.5 mmol/ g).

6.2.5.d *Application of isocyanate resin to the synthesis of ethyl benzoate*

Using the method described above (table 6.3, entry K), 15 g of PS-DVB isocyanate resin was synthesized in 50% yield from aminomethyl resin[iv] and used in the scavenging of the solution phase alcohol.

[iv] Aminomethyl resin synthesized from 1% DVB cross-linked commercial Merrifield resin, loading 1.1 mmol/ g.

The reaction was then filtered, Amberlte® IR-120 added and the mixture shaken at room temperature for a further 6 hours. The ethyl benzoate was isolated by filtration in 82% purity and 78% yield.

6.3 CONCLUSION

Having synthesized a novel catalytic imidazole based PS-DVB resin, which was demonstrated to bind copper in a ratio expected for binding to Cu(II), the resin was then used as a catalyst in the synthesis of ethyl benzoate. Although the catalysis was unsuccessful, a resin bound PS-DVB-isocyanate resin was synthesized and successfully employed for the scavenging of the excess alcohol used in the reaction, thus providing a facile route for the removal of alcohols in solution.

CHAPTER 7 – EXPERIMENTAL

7.1 GENERAL INFORMATION

NMR spectra unless stated otherwise were recorded using a Bruker AC300 spectrometer operating at 300 MHz for ^{1}H and 75 MHz for ^{13}C, a Bruker DPX400 spectrometer operating at 400 MHz for ^{1}H and 100 MHz for ^{13}C (δ scale in parts per million). Coupling constants (*J*) were measured in Hz.

ESI mass spectra were recorded using a VG Platform Quadrupole Electrospray Ionisation mass spectrometer, measuring mono-isotopic masses. FAB mass spectra were recorded on a VG analytical 70-250-SE normal geometry double focusing mass spectrometer using argon as a bombarding gas in a 3-nitrobenzyl alcohol (3-NBA) matrix. High resolution accurate mass measurements were carried out at 10,000 resolution using mixtures of polyethylene glycols and/ or polyethylene glycomethylethers as mass calibrants for FAB.

Infra-red spectra were recorded on a BIORAD Golden Gate FTS 135. All samples were run as either neat solids or oils. In the case of solid phase samples, the solid phase used was dried *in vacuo* from DCM and then Et_2O.

Melting points were determined using a Gallenkamp melting point apparatus and are uncorrected.

Analytical HPLC spectra were obtained using a Hewlett Packard HP1100 Chemstation, using a Phenomenex C_{18} prodigy 5 μm (150 mm x 3 mm) column. The gradients used were based on two solvents: water with 0.1% TFA (solvent 1) and acetonitrile with 0.042% TFA (solvent 2).

Preparative HPLC spectra were obtained using a Hewlett Packard HP1100 Chemstation with an automated fraction collector using a Phenomenex C_{18} prodigy

5μm (250 mm x 10 mm) column. The gradients used were based on two solvents: water with 0.1% TFA (solvent 1) and acetonitrile with 0.042% TFA (solvent 2).

Aluminium backed silica plates (0.25 mm layer of silica gel 60 with the florescent indicator Alugram SIL G/UV_{254}) were used for thin layer chromatography (TLC). UV (254 nm) was used to visualize compounds unless stated otherwise.

All amino acids used were configured L unless stated otherwise.

Electron microscope images were recorded on a JEOL 6400 Scanning Electron Microscope and JEOL 5500 High Pressure Scanning Electron Microscope.

Unless otherwise stated, room temperature = 18°C.

7.2 GENERAL EXPERIMENTAL PROCEDURES

7.2.1 *Quantitative ninhydrin test*[88]

A known mass of resin (<5 mg) was treated in a small test tube with 6 drops of reagent A (described below) and 2 drops of reagent B (described below) and heated in a solid aluminium block at 110°C for 10 mins. The tube was cooled and 60% ethanol solution (2 mL) added to the tube. The contents of the tube were filtered through a pipette charged with a plug of glass wool and the blue filtrate collected in a 25 mL volumetric flask. The resin was washed using a solution of tetraethyl ammonium chloride (Net_4Cl) (0.5 M in DCM, 2 x 0.5 mL) and the sample made up to 25 mL using 60% aqueous ethanol. The absorbance at 570 nm was then measured against a reagent blank. The amount of primary amine present on the resin was then calculated using the equation:

Loading (mmol/ g) = (A x V)/ (ε_{570} = W) x 1000

ε_{570} = Molar extinction co-efficient (15000/ Mcm).

V = diluted volume (25 mL).

W = mass of resin (mg).

A_{570} = absorbance measured at 570 nm.

Reagent A

Solution 1 – Reagent grade phenol (40 g) was dissolved in absolute ethanol (10 mL) with warming and then stirred over Amberlite mixed-bed resin MB-3 (4 g) for 45 mins. The mixture was then filtered.

Solution 2 – Potassium cyanide (65 mg) was dissolved in water (100 mL). A 2 mL aliquot of this solution was diluted with pyridine (freshly distilled from ninhydrin) and stirred over Amberlite mixed-bed resin MB-3 (4 g). The solution was filtered and mixed with solution 1 to form reagent A.

Reagent B:

Ninhydrin (2.5 g) was dissolved in absolute ethanol (50 mL).

7.2.2 *Quantitative Fmoc test*[65]

To a known mass (<5 mg) was resin was added a solution of 20% piperidine/ DMF (1 mL). The resin was allowed to stand for 15 mins and the solution filtered through a glass pipette with a glass wool plug and the filtrate diluted to 25 mL with 20% piperidine/ DMF. The absorbance at 302 nm was recorded, measured against a blank of 20% piperidine/ DMF. The loading was calculated from the following equation:

Loading = (A_{302} x V) / (ε_{302} x W) x 1000

A_{302} absorbance of the piperidyl-fulvene adduct.

V = volume of the volumetric flask (25 mL).

W = mass of the resin sample (mg).

ε_{302} = molar extinction co-efficient of the adduct at 302 nm (7800/ Mcm).

7.2.3 *General procedure for DIC/ HOBt resin coupling*

A known mass of resin (x mg) was swollen in a solution of DCM (4 mL). Protected Fmoc-aa-OH (2 eq.) was dissolved in DCM:DMF (9:1) (5 mL) and HOBt (5 mg, catalytic) and DIC (2 eq.) added. The solution was allowed to stand at RT for 20 mins and then transferred to the swollen resin. The mixture was shaken at RT for 2 h and the resin filtered and washed with DCM (2 x 10 mL), DMF (2 x 10 mL), DCM (2 x 10 mL), MeOH (2 x 10 mL), Et_2O (2 x 10 mL) and dried *in vacuo* to yield the title compound.

7.3 EXPERIMENTAL TO CHAPTER 2

7.3.1 *Synthesis of PS-DVB (2%) resin, loading 1.6 mmol/ g (30a)*

Gelatin (0.67 g) was dissolved in water (225 mL) and transferred to a 5 neck goldfish bowl flask. The flask was purged with nitrogen for 20 mins and to this added a previously stirred mixture of styrene (65.7 g, 0.6 mol), chloromethyl styrene (21.4 g, 140 mmol), divinyl benzene (1.82 g, 14 mmol) and benzoyl peroxide (0.75 g, 3 mmol). The reaction was heated at 80°C for 16 hours whilst stirring with an anchor stirrer at 200 rpm. The suspension was added to crushed ice (500 mL) and water (1500 mL) added. The mixture was stirred at 0°C for 1 hour and the beads filtered and washed with water (2 x 1 L), THF:water (1:1) (2 x 200 mL), THF (2 x 200 mL), DCM:THF (1:1) (2 x 100 mL), DCM (2 x 100 mL), Et_2O (1 x 100 mL) and dried in vacuo for 16 hours to yield 62.2 g (70%) by mass of chloromethyl resin.

Size distribution: <45 microns 0 g; 45-125 microns 0.6 g; 125-250 microns 2.91 g; 250-500 microns 10.88 g; 500+microns 39.62 g.

7.3.2 *Mechanical agitation*

100 mg of chloromethyl resin was suspended in each of DCM (10 mL), MeOH (10 mL), THF (10 mL) and shaken for 4 hours and an aliquot of suspension removed from the vials.

7.3.3 *Microscopic manipulation*

A sample (5 mg) of chloromethyl resin was swollen in THF (0.5 mL) and viewed using an optical microscope and tweezers used to remove the satellite beads.

7.3.4 *Coulombic forces*

10 mg of chloromethyl resin was suspended in aqueous 1 M, 2 M and 3 M sodium chloride solutions and THF (5 mL) added the mixture shaken for 4 hours and an aliquot of each suspension removed from the vials. The aliquots were examined by optical microscopy.

7.3.5 *Sonication*

100 mg of chloromethyl resin was suspended in each of DCM (10 mL), MeOH (10 mL), THF (10 mL) placed in an ultrasonic bath for 1, 5, 10, 30, 60, 180 mins. Aliquots of each were removed from the 15 suspensions. This method provided the most effective means of separating satellites from parent beads but the effect was not quantitative and subsequent applications of ultrasound energy to the beads in their suspensions appeared to release varying amounts of satellites.

7.3.6 *Cross-sectional analysis*

A sample (5 mg) of polystyrene beads (which had pits and craters visible on the surface) was set in the commercially available TAAB-thermoset resin and heated at 60°C for 16 hours. The block of resin containing the beads was removed and sections taken using a glass knife, mounted on a Cambridge Monotome Rocker. The sections were prepared for SEM analysis by vacuum sputtering with Au (10-5 Torr, with a 5 KV potential difference).

7.3.7 *Fragment analysis*

A sample of beads (100 mg) was cooled to –196°C with liquid nitrogen and ground to a coarse powder using a pestle and mortar. Fragment analysis by SEM was then effected by application of the vacuum sputtering process described above.

7.3.8 *pH studies of suspension*

1% PVA solution was made up as follows: PVA (1 g, Mw 85-150 KDa, degree of hydrolysis 89%) was dissolved in water (100 mL) at 30°C solution stirred for 5 hours.

Solutions of PVA (5 mL, 1%), PVA (5 mL, 1%) and benzoyl peroxide (30 mg, 0.1 mmol), PVA (5 ml, 1%) and chloromethyl styrene (5 g, 3.25 mmol), PVA (5 mL, 1%) and benzoyl peroxide (30 mg, 0.1 mmol) and chloromethyl styrene (5 g, 3.25 mmol) were heated in a water bath at a rate of 1°C/ minute. Aliquots of the suspension (2 μL) were withdrawn at defined temperatures and the pH values recorded (table 7.1).

	Temperature/ °C										
	20	**55**	**56**	**57**	**58**	**59**	**60**	**61**	**62**	**63**	**64**
PVA	5	5	5	5	5	5	5	5	5	5	5
PVA + benzoyl peroxide	5	5	5	5	5	5	5	5	5	5	5
PVA + chloromethyl styrene	5	5	5	5	5	5	5	4.5	4.5	4.5	4.5
PVA + benzoyl peroxide + chloromethyl styrene	5	4	4	4	4	3	3	3	3	3	2

	Temperature/ °C										
	65	**66**	**67**	**68**	**69**	**70**	**71**	**72**	**73**	**74**	**75**
PVA (cont)	5	5	5	5	5	5	5	5	5	5	5
PVA + benzoyl peroxide (cont)	5	5	5	5	5	5	5	5	5	5	5
PVA + chloromethyl styrene (cont)	4.5	4.5	4.5	4	3.5	3	2.5	2.5	2.5	2	2
PVA + benzoyl peroxide + chloromethyl styrene (cont)	1	1	1	1	1	1	1	1	1	1	1

Table 7.1: Monitoring the effect of heating a number of suspension components on the resulting pH of the suspension.

7.3.9 *Synthesis of chloromethyl resin by pH monitored suspensions (30c)*

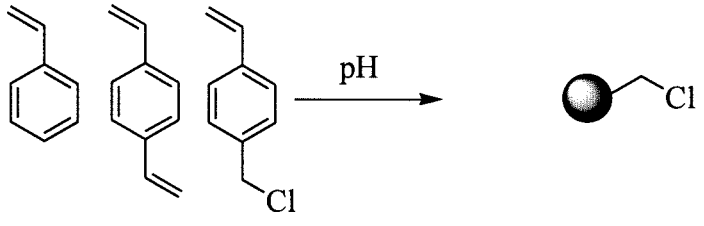

Three suspension polymerization reactions were carried out as shown in the general procedure below, which specific changes to the reaction protocols described below.

General procedure for suspension polymerization

Organic phase made up as follows. Styrene (73.3 g, 0.705 mol), chloromethyl styrene (15 g, 0.098 mol), divinyl benzene (1.2 g, 0.008 mol), toluene (30 mL) and benzoyl peroxide (0.7 g, 0.003 mol) stirred together at room temperature and nitrogen bubbled through the solution for 3 hours.

Organic phase (100 mL) was added to an aqueous phase consisting of PVA (100 mL of a 10% solution, 85-150 KDa, 87-89% hydrolysed), H_2O (900 mL) in a 1 L capacity Goldfish bowl[i] and heated at 60°C, stirred and bubbled with nitrogen for 30 mins. The suspension was allowed to equilibrate for 25 mins and nitrogen passed over the suspension and the suspension heated to 85°C for 6 hours. The heat was removed and the suspension poured into ice and stirred slowly in an open atmosphere for 16 hours. The beaded resin product was filtered using polypropylene filter sheeting and washed with H_2O (10 L), THF:H_2O (3 L), THF (1 L), Et_2O (0.5 L), MeOH (0.5 L), Et_2O (0.5 L) and dried *in vacuo*.

pH monitored suspension 1: pH prior to heating at 85°C = 5, pH following reaction = 0

pH monitored suspension 2: Droplet equilibrium was carried out for 1 hour prior to heating to 85°C and the pH of suspension then monitored during the reaction and sufficient sodium phosphate added to the suspension to maintain pH 7 (table 7.2).

pH monitored suspension 3: Droplet equilibrium was carried out for 1 hour prior to heating to 85°C and the pH of suspension was monitored during the reaction and sufficient sodium phosphate added to the suspension to maintain pH 7 (table 7.2).

[i] See Appendix for details of reactor geometry.

Time /mins	pH (expt 2)	Notes	pH (expt 3)	Notes
0	7	Suspension at 60°C	3/ 4	+2 g Na_2HPO_4 pH → 7, suspension at 65°C
15	6	Suspension at 85°C	6/7	
30	4	+2 g Na_2HPO_4 pH → 7/8	6	+2 g Na_2HPO_4 pH → 7
45	7		7	
60	5	+2 g Na_2HPO_4 pH → 7/8	6/7	
75	7		6	+2 g Na_2HPO_4 pH → 7
90	7		6/7	
105	5/6	+2 g Na_2HPO_4 pH → 7/8	6/7	
120	7		6	+2 g Na_2HPO_4 pH → 7
135	5/6	+2 g Na_2HPO_4 pH → 7/8	6/7	
150	7		6	+2 g Na_2HPO_4 pH → 7
165	7		7	
180	6/7		6/7	
195	6	+2 g Na_2HPO_4 pH → 7	6	+2 g Na_2HPO_4 pH → 7
210	-		6/7	
225	7		6/7	
240	6/7		6	+2 g Na_2HPO_4 pH → 7
255	6	+2 g Na_2HPO_4 pH → 7/8	7	
270	7		7	
285	7		7	
300	7		7	
315	6	+2 g Na_2HPO_4 pH → 7	6/7	
330	7		6/7	
345	6/7	+4 g Na_2HPO_4 pH → 7	6	+4 g Na_2HPO_4 pH → 7

Table 7.2: pH during two suspension polymerization reactions and the effect on suspension pH of adding sodium phosphate.

7.3.10 *Synthesis of chloromethyl resin by suspension polymerization (30d)*

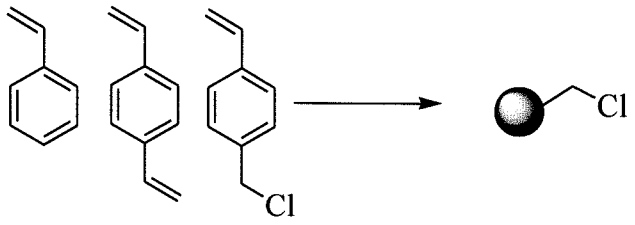

General procedure for suspension polymerization reactions

Pre-mixed organic phase (figure 3) was added to the aqueous phase (2.5 g PVA, (87-89% hydrolysed, Mr 85-150 kDa), H_2O (1000 mL) at 60°C and degassed with nitrogen for 30 mins) whilst stirring (in a 2.5 L 'Goldfish Bowl'). The suspension was allowed to stir for 25 mins and the suspension heated at 90°C for 6 hours. The heat was removed and the suspension poured into ice and stirred slowly in an open atmosphere for 16 hours. The beaded resin product was filtered using polypropylene filter sheeting, washed with H_2O (10 L), THF:H_2O (3 L), THF (1 L), Et_2O (0.5 L), MeOH 0.5 L, Et_2O (0.5 L) and dried *in vacuo*.

IR (υ_{max}/ cm^{-1}): 696 C-Cl (s)

7.3.11 *Synthesis of the range of cross-linked PS-DVB resins*

The organic phase was made up as shown in table 7.3.

Resin Cross-Linking/ %	Styrene		Divinyl Benzene		Vinyl Benzyl Chloride	
	mmol	mL	mmol	mL	mmol	mL
0.3	128.6	14.71	0.4	0.053	17.1	2.41
0.6	128.1	14.65	0.9	0.118	17.1	2.41
0.9	127.7	14.61	1.3	0.17	17.1	2.41
1.2	127.3	14.56	1.8	0.24	17.1	2.41
1.5	126.8	14.51	2.2	0.29	17.1	2.41
1.8	126.4	14.46	2.6	0.34	17.1	2.41
2.1	126.0	14.41	3.1	0.41	17.1	2.41
2.4	125.5	14.36	3.5	0.46	17.1	2.41
2.7	125.0	14.30	4.0	0.53	17.1	2.41
3.0	124.6	14.26	4.8	0.63	17.1	2.41
6.0	120.3	13.76	8.8	1.16	17.1	2.41

Table 7.3: Amount of styrene, divinyl benzene and chloromethyl styrene added to the organic phase.

To the organic phase was added benzoyl peroxide (1.25 g, 5 mmol).

The isolated yield of chloromethyl resin shown in table 7.4.

Cross-linking/ % DVB	0.3	0.6	0.9	1.2	1.5	1.8	2.1	2.5	2.7	3.0	6.0
Yield/ %	44	44	53	57	60	60	65	82	79	74	75

Table 7.4: Purified yields of PS-DVB resins.

	Cross-linking/ % DVB										
Size/ μm	**0.3**	**0.6**	**0.9**	**1.2**	**1.5**	**1.8**	**2.1**	**2.4**	**2.7**	**3.0**	**6.0**
500+	24	19.4	1	1	10.3	0.5	6.6	0.5	0.3	1.7	0.1
355-500	14.8	16.1	0.2	0	1.6	0	4.3	1.1	0.1	0.2	0.4
250-355	10.2	11.4	0.6	2	1.2	0	1.5	0.1	0.1	0	0.9
125-250	31.2	33.5	67.2	57.4	28.5	57.2	23.4	82.1	47.8	45.8	44.6
45-125	19.8	19.6	31	39.3	57.8	42.3	62.9	16.2	57.2	52.3	54.1
<45	0	0	0	0	0.1	0	1.3	0	0.2	0	0

Table 7.5: Size distribution of range of cross-linked PS-DVB resins.

7.3.12 *Resin swelling experiments*

Swelling experiments were conducted by the addition of solvent to 100 mg resin in 12 mL polypropylene tubes followed by mechanical agitation[ii] to remove trapped bubbles, solvent removal *in vacuo* and re-equilibration for 15 mins with mechanical agitation. Readings were recorded when consistency between the following two sampling methods was achieved. The solvent was removed by gravity with agitation of the tubes and also by compression of a syringe barrel until the resin posed a resistance to the compression. The resin was then washed with DCM (3 x bed volumes), an the solvent removed *in vacuo* and Et_2O (2 x bed volumes) an then removed *in vacuo*, followed by the addition of the new solvent.

Table of results for the swelling parameters for each of the different cross-linked PS-DVB resins in each solvent used are shown in table 7.6.

[ii] By application of a sharp tapping motion to the side of the tubes.

	Resin cross-linking										
	0.3	**0.6**	**0.9**	**1.2**	**1.5**	**1.8**	**2.1**	**2.4**	**2.7**	**3.0**	**6.0**
Chloroform	12.1	8.5	6.6	6.1	5.1	5.3	3.6	4.2	3.8	3.0	2.8
DCM	10.0	8.9	6.4	5.7	4.9	4.8	4.6	4.4	4.4	3.6	2.6
Dichloroethane	9.4	6.8	5.7	5.1	4.2	3.8	4.2	3.2	4.8	2.5	2.1
THF	8.5	8.5	5.1	5.5	3.8	4.4	3.6	4.4	3.4	2.6	2.3
Dioxane	6.8	6.4	5.1	6.1	3.4	4.0	3.6	3.2	3.0	2.5	2.3
Toluene	6.4	5.9	4.6	4.6	3.4	3.2	3.2	3.8	3.2	2.5	2.5
DMF	5.5	4.0	3.4	3.4	2.6	2.8	2.6	2.8	2.5	1.9	1.7
Ether	4.0	3.4	3.2	3.4	2.5	2.6	2.3	2.8	2.5	2.1	1.9
Acetone	3.8	3.2	3.2	2.8	2.6	2.5	2.5	2.1	2.1	1.9	2.1
THF:water	3.6	3.2	2.8	3	2.3	2.5	2.1	2.6	2.1	2.1	1.9
Dioxane:water	3.2	2.6	2.3	2.3	2.1	2.3	1.9	2.5	2.3	1.9	1.9
DCM:MeOH	3.2	2.5	2.8	2.8	2.1	2.8	1.9	2.8	2.1	1.7	2.1
MeOH	2.5	1.9	2.1	2.1	2.1	2.1	1.9	1.9	1.9	2.1	1.9
EtOH	1.9	2.1	2.1	2.3	1.7	1.9	2.1	1.9	2.1	1.9	1.7
IPA	2.3	2.3	2.1	2.5	2.5	1.9	2.1	2.5	2.5	2.1	2.3
Water	2.3	2.5	2.5	2.3	1.9	2.1	1.7	2.1	2.1	2.3	2.3
Hexane	2.3	2.1	2.1	2.1	1.9	2.2	1.9	1.9	1.9	2.1	1.9
MeCN	2.3	2.1	2.3	2.1	1.9	2.1	2.3	1.9	2.1	2.1	1.9

Table 7.6: Resin swelling experiments in a range of different solvents. (Data quoted in the table are quoted in units of mL per gram of resin (45 -125 microns)).

7.4 EXPERIMENTAL TO CHAPTER 3

7.4.1 *Synthesis of aminomethyl resin (30b)*[57]

General procedure for the synthesis of aminomethyl resin.

Chloromethyl resin (**48**) (45 - 125 μm, 1 g, 0.5 mmol) was swollen in DMF (10 mL) and dioxane (4 mL) for 20 mins and potassium phthalimide (1 g, 5 mmol) added and the mixture heated at 100°C for 8 h. The resin was cooled, filtered and washed with hot DMF (2 x 50 mL), DMF/ water (1:1) (2 x 50 mL), water (2 x 50 mL), dioxane/ water (1:1) (2 x 50 mL), dioxane (2 x 50 mL), EtOH (2 x 50 mL), MeOH (2 x 50 mL), DCM (2 x 50 mL), Et_2O (50 mL) and dried *in vacuo* to give phthalimidomethyl resin.

IR (υ_{max}/ cm^{-1}): 1714 C=O (s)

The phthalimidomethyl resin (1 g) was suspended in EtOH (10 mL) and hydrazine hydrate (1 mL) added. The mixture was heated at 76°C for 8 hours, cooled, filtered and washed with hot DMF (2 x 50 mL), DMF/ water (1:1) (2 x 50 mL), water (2 x 50 mL), dioxane (2 x 50 mL), MeOH (2 x 50 mL), DCM (2 x 50 mL), Et_2O (50 mL) and dried *in vacuo* to yield the title compound.

Quantitative ninhydrin tests were carried out on each of the aminomethyl resins after coupling with Fmoc-Gly-OH (0.297 g, 1 mmol) using DIC (0.132 g, 1 mmol) and HOBt (5 mg, 0.04 mmol) (table 6.7).

Cross-linking/ %	Loading mmol/ g
0.3	0.47
0.6	0.50
0.9	0.52
1.2	0.51
1.5	0.47
1.8	0.46
2.1	0.52
2.4	0.51
2.7	0.47
3.0	0.48
6.0	0.52

Table 6.7: Loading of aminomethyl resins.

7.4.2 *Synthesis of glycine allyl ester tosyl salt (57)*[193]

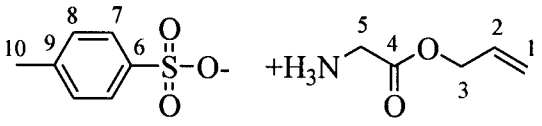

Glycine (10 g, 133 mmol) and *p*-toluene sulfonic acid (*p*TsOH) (30 g, 157 mmol) were added to allyl alcohol (80 mL) and benzene (200 mL). The mixture was heated at reflux under Dean-Stark conditions for 16 hours. The solvent was then azeotropically removed *in vacuo* by the addition on two portions of methanol (50 mL each). The dark brown crude mixture was extracted with Et_2O (50 mL) and the solution decanted. The compound was dried *in vacuo* to yield 35.2 g (92%) of a brown oil.

IR (υ_{max}/ cm^{-1}): 1010, 1035 S=O (s), 1178 O=S=O (s), 1755 C=O (s).
M/z (ES$^+$): 157 (100%, $[M+H+MeCN]^+$).

δ_H (300MHz, $CDCl_3$): 2.33 (3H, s, $^6CH_3$); 3.70 (2H, d, *J*11, $^5CH_2$); 4.48 (2H, d, *J*6, $^3CH_2$); 5.35 (1H, dd, *J*16, 2; 1H, dd, *J*10, 2, $^1CH_2$); 5.75 (m, ^2CH); 7.10 (2H, d, *J*8, ^8CH); 7.70 (2H, d, *J*8, $^9CH_2$).

δ_C (75MHz, $CDCl_3$): 40.6 (^1C); 167.3 (^2C); 66.8 (^3C); 131.2 (^4C); 119.2 (^5C); 140.7 (^6C); 126.1 (^7C); 129.1 (^8C); 141.2 (^9C); 21.5 (^{10}C).

7.4.3 *Synthesis of Fmoc-Asp-Gly-OAllyl (58b)*

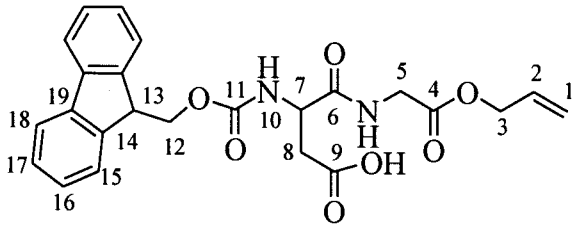

Fmoc-Asp(O^{t}Bu)-OH (11 g, 28.2 mmol) was dissolved in dry THF (50 mL) at -78°C (acetone/ CO_2 bath). To this was added dropwise isobutyl chloroformate (4.56 g, 33.4 mmol) and triethylamine (NEt_3) (2.8 g, 29.4 mmol). The solution was vigorously stirred under nitrogen for 20 mins and **(57)** (10 g, 34.8 mmol) in DCM (30 mL) added dropwise. NEt_3 (2.8 g, 29.4 mmol) was added addition of **(57)**. The mixture was allowed to warm to room temperature and stirring applied for 16 hours. The mixture was extracted with EtOAc (2 x 100 mL). The organic layer was retained and washed with 10% sodium hydrogen carbonate ($NaHCO_3$) (50 mL), citric acid (50 mL), brine (50 mL) and water (50 mL) and dried over magnesium sulfate (5 g). The organic fraction was filtered and concentrated *in vacuo* to yield 6.12 g (43 %) of Fmoc-Asp(O^{t}Bu)-Gly-OAllyl **(58)**.

Fmoc-Asp(O^{t}Bu)-Gly-OAllyl **(58)** (6.12 g, 12 mmol) was dissolved in TFA:DCM (1:1) (30 mL) for 4 hours and the solvent removed *in vacuo* to yield 6.1 g of the title compound in 99 % yield.

IR (υ_{max}/ cm^{-1}): 3429 C=C (s), 1660 C=O (m).
M/z (ES$^+$): 565.4 (100%, $[M+H+TFA]^+$).

M.p.: decomposes >160°C.

HRMS (FAB) $C_{24}H_{24}N_2O_7$ Calc. 453.1662, Found 453.1664.

δ_H (300MHz, $CDCl_3$): 2.7x – 2.9x (2H, 8 line ABX system, J_{AX}5.5, J_{BX}5.9, J_{AB}16, $^{8}CH_2$); 4.07 (2H, d, *J*11, $^{5}CH_2$); 4.22 (1H, t, *J*7, ^{13}CH); 4.43 (2H, d, *J*6, $^{3}CH_2$); 4.62 (1H, d, *J*5, ^{7}CH); 5.29 (1H, dd, *J*18, 6; 1H, dd, 10, 6; $^{1}CH_2$); 5.89 (m, ^{2}CH); 7.13 (1H, d, *J*7, ^{10}NH); 7.31 (2H, t, *J*7, ^{17}CH); 7.40 (2H, t, *J*7, ^{16}CH); 7.60 (2H, d, *J*7, ^{18}CH); 7.78 (2H, d, *J*7, ^{15}CH).

δ_C (75MHz, $CDCl_3$): 119.1 (^{1}C); 131.6 (^{2}C); 66.2 (^{3}C); 171.1 (^{4}C); 41.6 (^{5}C); 169.2 (^{6}C); 51.2 (^{7}C); 37.6 (^{8}C); 171.1 (^{9}C); 156.3 (^{10}C); 67.4 (^{11}C); 47.3 (^{12}C); 120.2, 125.2, 127.6, 127.9 ($^{13\text{-}17}C$).

7.4.4 *Synthesis of Fmoc-Asp(Rink-PS-DVB)-Gly-OAllyl resin (59)*

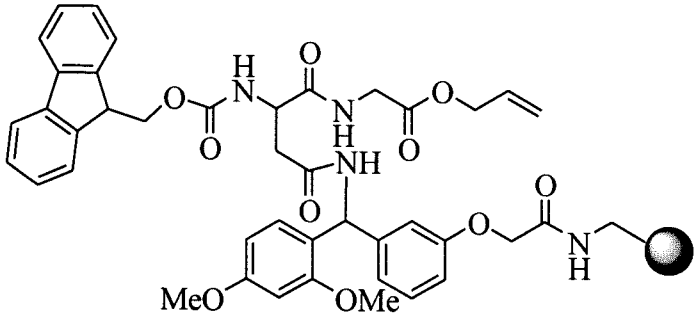

To 1 g (0.5 mmol) of each cross-linked aminomethyl resin was added a pre mixed suspension of DCM:DMF (9:1) (10 mL) and Fmoc-Rink linker (4-[(R,S)-α-[1-(9H-fluoren-9-yl)-methoxyformido]-2,4-dimethoxybenzyl]-phenoxyacetic acid (540 mg, 1 mmol), DIC (1,3-di-isopropylcarbodiimide) (126 mg, 1 mmol) and HOBt (1-hydroxybenzotriazole) (20 mg). The resulting resin suspension was shaken for 3 h and coupling completion monitored by the standard ninhydrin test. The resins were each treated with 20% piperidine/DMF (5 mL) for 3 mins and then again for 1 min and washed with DCM (10 x bed volumes), DMF (3 x bed volumes), DCM (10 x bed volumes) and dried *in vacuo*.

Fmoc Asp(O^{t}Bu)-Gly-OAllyl (509 mg, 1 mmol) was dissolved in DCM:DMF (9:1) (10 mL) and DIC (126 mg, 1 mmol) and HOBt (20 mg, 0.1 mmol) were added and allowed to stand for 20 mins. The resulting suspension was added to each resin and shaken for 3 hours until the resin tested negative by the ninhydrin test.

A sample of resin (5 mg) was shaken in TFA:DCM:H_2O (95:2.5:2.45) (1 mL) for 2 hours and filtered. The solvent was removed *in vac*uo and the sample analyzed by MS and RP HPLC.

M/z (ES$^+$): 452.4 (35%, $[M+H]^+$); 474.4 (48%, $[M+Na]^+$)
RP HPLC (λ = 254 nm) Gradient 0 – 100% MeCN (20 min): 14.6 min.

The Fmoc groups were removed by treating the resin with 20% piperidine/ DMF (2 x 3 mins), and the deprotected resin was washed with DMF, DCM, Et_2O (50 mL each), and dried *in vacuo*.

7.4.5 *Solid phase synthesis of Fmoc-Asp(O^{t}Bu)-Asn-Asn-Trp(BOC)-Ser(O^{t}Bu)-Thr-Pro-Trp(Boc)-Leu-Asp(Rink-PS-DVB)-Gly-OAllyl (60)*

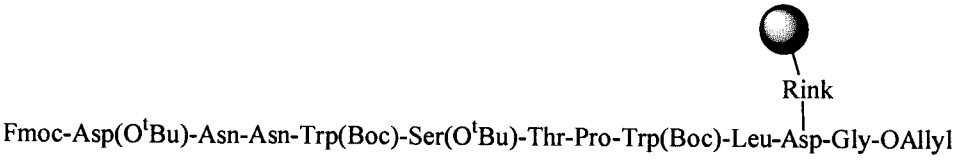

Each resin **(59)** (1 g, 0.5 mmol) was treated with 20% piperidine/ DMF and washed with DMF, DCM, Et_2O (50 mL each), and dried *in vacuo*. To this was added a solution of Fmoc-AA-OH (side chain protected as shown below), DCM:DMF (9:1) (10 mL), DIC (126 mg, 1 mmol) and HOBt (20 mg, 0.1 mmol) using standard DIC/HOBt coupling conditions and monitored for a negative ninhydrin test. The coupling was repeated after the first Fmoc-Trp(Boc)-OH residue. After successful coupling the resin was washed as described above and Fmoc deprotected by suspending the resin in 20% piperidine/ DMF (10 mL) and then washed with DMF (2 x 20 mL), DCM (2 x 20 mL) and Et_2O (2 x 20 mL).

(Amino acids used: Fmoc-Leu-OH, Fmoc-Trp(Boc)-OH, Fmoc-Pro-OH, Fmoc-Thr(O^tBu)-OH, Fmoc-Ser(O^tBu)-OH, Fmoc-Trp(Boc)-OH, Fmoc-Asn-OH, Fmoc-Asn-OH, Fmoc-Asp(O^tBu)-OH).

The *C*-terminal glycine allyl group was deprotected by treatment of the resin (1 g, 0.5 mmol) with, dimedone (70 mg, 0.5 mmol), $Pd(PPh_3)_4$ (614 mg, 0.5 mmol) in DCM (5 mL), THF (5 mL) under N_2 for 16 hours. The *N* terminal Fmoc group was removed as described above and the resins washed with aqueous citric acid (10%) (3 x bed volumes).

A sample of resin (5 mg) was shaken in TFA:DCM:H_2O (95:2.5:2.45) (1 mL) for 2 hours and filtered. The solvent was removed *in vac*uo and the sample analyzed by MS and RP HPLC.

M/z (ES^+): 1302.7 (70%, $[M+H]^+$)
RP HPLC (λ = 220 nm) Gradient 0 – 55% MeCN (55 mins) : 48.5, 50.2 mins.

DIC/HOBt cyclisation was then performed using the standard conditions: To each resin (1 g) was added HOBt (20 mg, 0.1 mmol) in DCM: DMF (9:1) (10 mL) and DIC (126 mg, 1 mmol) and shaken at room temperature for 2 hours.

7.4.6 *Synthesis of cyclo-Asp-Asn-Asn-Trp-Ser-Thr-Pro-Trp-Leu-Asn-Gly- (53)*[188]

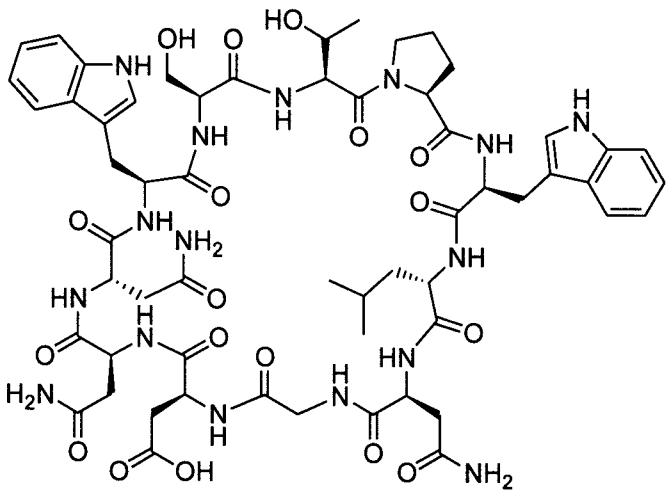

A sample of resin (100 mg) was suspended in TFA:DCM:H_2O (95:2.5:2.45) (1 mL) for 2 hours and filtered. The solvent was removed *in vac*uo to yield the title compound.

M/z (ES^+): 1284.7 (32%, $[M+H]^+$); 1306.6 (44%, $[M+Na]^+$); 1322.6 (10%, $[M+K]^+$).
RP HPLC (λ = 220 nm) Gradient 0 – 50% MeCN (70 min): 58.2 mins.

^{1}H NMR assignment verified by TOCSY and NOESY, (500MHz, 298K, DMSO-d_6): (NH, CH_α, CH_β, other): Trp(I) 7.41, 4.42, 3.16; 2.91, 10.83 (indole NH), 7.56, 6.98, 7.30, 7.05 (Ar-H); Leu 7.80, 4.26; 4.26, 0.85, 1.55;1.48; 1.43; Asn(I) 8.30, 4.63, 2.56; 2.46, 7.47; 7.28 ($CONH_2$); Gly 8.29, 3.82; 3.67; Asp 8.82, 4.56, 2.780; 2.48; Asn(II) 7.91, 4.29, 2.85; 2.40, 7.50; 7.12 ($CONH_2$); Asn(III) 7.90, 4.49, 2.64; 1.85, 7.58; 7.11 ($CONH_2$); Trp(II) 8.54, 4.32, 3.31; 2.93, 7.49 (CH_γ), 10.60 (indole NH), 7.10; 6.97; 7.30; 7.05 (Ar-H); Ser 8.09, 4.34, 3.73; Thr 7.33, 4.60, 3.94, 0.97 (CH_γ); Pro 4.30, 3.52 (CH_δ), 1.35; 1.63; 1.87; 1.52.

7.5 EXPERIMENTAL TO CHAPTER 4

7.5.1 *Synthesis of magnetic chloromethyl resin by suspension polymerization (54b)*

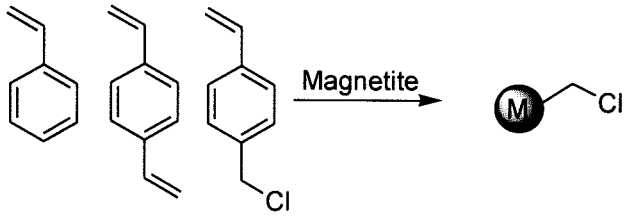

General protocol for the synthesis of magnetic chloromethyl resin

Organic phase was made up as follows: Styrene (13.4 g, 128 mmol), divinyl benzene (0.37 g, 3 mmol) and chloromethyl styrene (2.2 g, 14 mmol) and benzoyl peroxide (0.25 g, 1mmol) were heated at room temperature for 3 hours.

Organic phase (16.2 g) was added to the aqueous phase (2.5 g PVA, (87-89% hydrolysed, Mr 85-150 kDa) in 1000 mL H_2O, at 60°C and bubbled with nitrogen gas for 30 mins) whilst stirring (180 rpm, half-moon stirrer) in a 2.5 L 'Goldfish Bowl'. The suspension equilibrated at 60°C for 25 mins and magnetite (0.69 g, 3 mmol) added. The suspension was heated at 80°C for 16 hours. The heat was removed and the suspension poured into ice (500 mL) and stirred for 16 hours. The beads were filtered using polypropylene filter sheeting and washed sequentially with hot (60°C) solvents: water (1 x 100 mL), dioxane/water (1:1) (1 x 100 mL), dioxane (1 x 100 mL), DMF (1 x 100 mL), and solvents at 20°C: EtOH (1 x 100 mL), MeOH (1 x 100 mL), DCM (1 x 100 mL), Et_2O (1 x 100 mL). The beads were swollen in DCM (30 mL) and placed in an ultrasonic bath for 4 hours to remove loosely bound magnetite and dried *in vacuo* to yield 10.1 g of magnetic chloromethyl resin (62%).

Size distribution: <45 microns 0.06 g (3%); 45-125 microns 1.1 g (54%); 125-250 microns 0.35 g (17%); 250-355 microns 0.05 g (2.2%); 355-500 microns 0.02 g (0.1%); 500+microns 0.45 g (22%).

7.5.2 *Recovery of magnetite from suspension*

The suspension polymerization was carried out as detailed in the general protocol for magnetic chloromethyl resin synthesis adding magnetite (1 g, 0.4 mmol) prior to heating of the suspension at 80°C, as described above. Following the polymerization, unreacted magnetite was separated from the beads by filtration (polypropylene sheeting, average pore diameter 5 - 20 microns). The filtrate was collected and filtered using filter paper to yield 0.7 g of unreacted magnetite.

7.5.3 *Stability and quantification of magnetite in the magnetic chloromethyl resin*

7.5.3.a *Mechanical agitation*

Magnetic chloromethyl PS-DVB resin (100 mg) was suspended in each of DCM (10 mL), MeOH (10 mL), DCM:MeOH (1:1) (10 mL) and shaken for 4 hours after which time no magnetite was observed to have separated from the beads in the suspension.

7.5.3.b *Sonication*

Magnetic chloromethyl PS-DVB resin (100 mg) was suspended in DCM (10 mL) and MeOH (10 mL) and placed in an ultrasonic bath for 10 hours, after which time no magnetite was observed to have separated from the suspension.

7.5.3.c *Colourimetric quantification of Fe in the magnetic chloromethyl beads*

Buffered ferron solution was made up as follows: 8-Hydroxy-7-iodo-5-quinolinesulfonic acid (0.2 g, 0.6 mmol) was dissolved in water (100 mL) and added to sodium acetate solution (1 g, 12 mmol, dissolved in water (100 mL)) and glacial acetic acid (0.2 mL) added dropwise to adjust the pH to 5.

A calibration was performed using 0.08, 0.16 and 0.32 mg of $FeCl_3$ dissolved in buffered ferron solution (25 mL) (table 7.8).

Mass of $FeCl_3$ /mg	Abs 360nm	Abs 600nm
0	0	0
0.08	0.14	0.10
0.16	0.42	0.26
0.32	0.60	0.42

Table 7.8: Calibration of standard $FeCl_3$ solution at 360 and 600 nm.

Magnetic chloromethyl resin (60 mg) was swollen in DCM (0.4 mL) and shaken in HCl (12M) (0.5 mL) for 4 hours until no response to a permanent bar magnet was observed. The resin was filtered and the filtrate diluted to 100 mL with buffered ferron solution, and adjusted to pH 5 with sodium acetate.

Abs (360 nm) = 0.52, Fe = 0.24 mg in 60 mg sample $\rightarrow$ 4 mg Fe^{III}/ g $\rightarrow$ 0.7 μmol/ g.

7.5.3.d *Swelling studies of the magnetic beads*

Swelling studies were conducted using the beads (45 – 125 μm fraction) as described above with chloroform, DCM, dioxane, THF, Toluene, DMF, EtOAc, hexane, MeOH, EtOH and water (table 7.9).

Solvent	2% Commercial Merrifield Resin mL/ g	2% Magnetic Merrifield Resin mL/ g
Chloroform	5.5	5.3
DCM	3.8	3.8
Dioxane	4.0	4.3
THF	4.0	4.1
Toluene	4.1	4.0
DMF	2.7	2.8
EA	2.5	2.5
Hexane	1.9	2.1
Methanol	2.0	2.1
Ethanol	2.0	1.9
Water	1.9	1.9

Table 7.9: Swelling studies performed on magnetic chloromethyl resin, compared to commercially available Merrifield resin of approximately the same diameter size range.

7.5.4 *Synthesis of Phe-Ser-Ala-NH_2 (62) using magnetic resin*

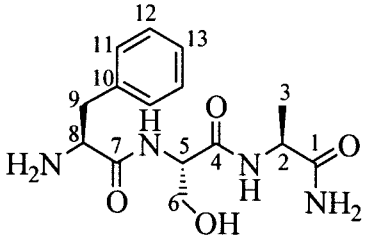

Magnetic chloromethyl resin (1 g, 0.9 mmol) was transformed into magnetic aminomethyl resin by refluxing with potassium phthalimide (1 g, 5.4 mmol) followed by hydrazinolysis with hydrazine hydrate (1 g, 31 mmol) using the standard protocol for aminomethyl resin synthesis.[57] To magnetic aminomethyl resin (1 g, 0.5 mmol) was added a pre-mixed solution of DCM:DMF (9:1) (10 mL) and Fmoc-Rink linker

(4-[(R,S)-α-[1-(9*H*-fluoren-9-yl)-methoxyformido]-2,4-dimethoxybenzyl]-phenoxyacetic acid (540 mg, 1 mmol), DIC (126 mg, 1 mmol) and HOBt (1-hydroxybenzotriazole) (20 mg, 0.1 mmol). The resulting resin suspension was shaken at room temperature for 3 hours. Coupling completion was monitored by the standard ninhydrin test. The magnetic resin was washed with 20% piperidine/DMF (5 mL) (3 mins, 1 min) and then washed with DCM (2 x 20 mL), DMF (2 x 20 mL), DCM (2 x 20 mL) and dried *in vacuo*.

To magnetic Rink loaded PS-DVB resin (1 g) was added a solution of Fmoc-AA-OH (side chain protected as shown below) (1 mmol), DCM:DMF (9:1) (10 mL), DIC (126 mg, 1 mmol) and HOBt (5 mg, 0.04 mmol) using standard DIC/HOBt coupling conditions and monitored for a negative ninhydrin test. After successful coupling the resin was washed as described above (general protocol for DIC/ HOBt coupling) and Fmoc deprotected by treating the resin with 20% piperidine/ DMF (10 mL) and then washing with DMF (2 x 20 mL), DCM (2 x 20 mL), Et_2O (2 x 20 mL) and then dried *in vacuo*.

(Amino acids used: Fmoc-Ala-OH, Fmoc-Ser(O^{t}Bu)-OH and Fmoc-Phe-OH).

The tripeptide **(62)** loaded resin (500 mg) was suspended in TFA:DCM:H_2O (95:2.5:2.45) (10 mL) and shaken at room temperature for 3 hours and filtered through glass wool. The residue was washed with TFA (100%) and the solvent was removed from the filtrate *in vac*uo. The resulting off-white solid was dissolved in TFA (100%) (0.3 mL) and precipitated by the addition of Et_2O (30 mL). The mixture was allowed to stand at room temperature for 3 hours and decanted to yield 95 mg of the title compound.

M/z (ES^+): 323.2 (100%, $[M+H]^+$); 345.3 (30%, $[M+Na]^+$).
RP HPLC (λ = 220 nm) Gradient 0 – 100% MeCN (20 min): 7.3 mins.

δ_H (300MHz, D_2O): 1.35 (3H, d, *J*7, $^3CH_3$); 3.15 (2H, d, *J*7, $^9CH_2$); 3.71 (2H, d, *J*6, $^6CH_2$); 4.22 (1H, q, *J*7, ^2CH); 4.25 (1H, t, *J*7, ^8CH); 4.40 (1H, t, *J*6, ^5CH); 7.27 (5H, pAr-H, $^{11\text{-}13}CH$).

δ_C (75MHz, D_20): 180.1 (^1C); 52.1 (^2C); 19.3 (^3C); 173.0 (^4C); 56.9 (^5C); 63.8 (^6C); 171.2 (^7C); 57.5 (^8C); 39.4 (^9C); 136.3 (^{10}C); 131.8 (^{11}C); 132.0 (^{12}C); 130.6 (^{13}C).

7.5.5 *Array synthesis of sulfonamides using magnetic aminomethyl scavenger resin*

General protocol for synthesis of sulfonamides

Commercially available sulfonyl chlorides (2 mmol) were each dissolved in DCM (3 mL) and commercially available amine compounds (1 mmol) dissolved in DCM (1 mL) added and the reaction shaken at RT for 3 hours. Magnetic aminomethyl resin (1.5 g, 1.35 mmol) was added to the reaction with DCM (3 mL) and shaken gently at RT for 16 hours. A bar magnet was inserted into the reaction and the resin extracted in 3 attempts to capture all of the magnetic resin. The array of sulfonamides were analyzed by MS (ES^+) and HPLC for purity.

N-Cyclohexyl-2,4-dinitro-benzenesulfonamide (67a)

M/z (ES^+): 352.0 (40%, $[M+Na]^+$); 368.0 (19%, $[M+K]^+$)
RP HPLC (λ = 254 nm) Gradient 0 – 100% MeCN (20 min): 11.2 mins (100%).

N-Heptyl-2,4-dinitro-benzenesulfonamide (67b)

M/z (ES^+): 368.0 (16%, $[M+Na]^+$); 384.0 (5%, $[M+K]^+$)
RP HPLC (λ = 254 nm) Gradient 0 – 100% MeCN (20 min): 12.2 mins (97%).

N-Cyclohexyl-4-(4-dimethylamino-phenylazo)-benzenesulfonamide (67c)

M/z (ES^+): 387.1 (80%, $[M+H]^+$)

RP HPLC (λ = 254 nm) Gradient 0 – 100% MeCN (20 min): 12.8 mins (96%).

4-(4-Dimethylamino-phenylazo)-*N*-heptyl-benzenesulfonamide (67d)

M/z (ES^+): 403.1 (86%, $[M+H]^+$)

RP HPLC (λ = 254 nm) Gradient 0 – 100% MeCN (20 min): 13.6 mins (89%).

7.6 EXPERIMENTAL TO CHAPTER 5

7.6.1 *Synthesis of 2-(4-dimethylamino-phenylazo)-benzamide (84)*[252]

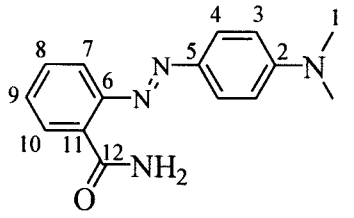

The aminomethyl resins (100 mg, 0.05 mmol) were swollen in DCM (1 x bed volume). Fmoc Rink linker (4-[(R,S)-α-[1-(9H-fluoren-9-yl)-methoxyformido]-2,4-dimethoxybenzyl]-phenoxyacetic acid) (53.6 mg, 0.1 mmol) was dissolved in DCM:DMF (9:1) (3 mL) and HOBt (5 mg) and DIC (12 mg, 0.1 mmol) were added. The solution was allowed to stand for 20 mins and the aminomethyl resin slurry added and the reaction mixture was shaken for 4 hours. The resin **(76)** was washed with DCM (2 x 50 mL), DMF (2 x 50 mL), Et_2O (2 x 5 mL) and dried *in vacuo*. The Fmoc Rink linker was deprotected by treatment of each resin with 20% piperidine/ DMF (5 mL, 2 x 3 mins) and each of the resins was washed and dried as described above. Methyl Red ([2-[4-(dimethylamino)phenyl-azo]benzoic acid]) (135 mg, 0.5 mmol) was dissolved in DCM:DMF (9:1) (3 mL) and DIC (63 mg, 0.5 mmol) and HOBt (10 mg, 0.1 mmol) were added. The solution was allowed to stand for 20 mins and then the swollen aminomethyl resins were added to each solution. The reaction was shaken for 16 hours, and the resin was filtered, washed and dried as described above. Methyl Red-Rink loaded resin (10 mg, 3.7 mmol) was suspended in TFA/ H_2O/ DCM (95:2.5:2.5) (1 mL) and shaken. After 15 s, 30 s, 1 min, 2 mins, 5 mins, 60 mins and 210 mins, 2 μL aliquots (accurate Gilson pipette P20) were withdrawn from each experiment and DCM (1 mL) added. The absorbance of each aliquot (λ = 530 nm) was measured (normalised in table 7.10).

Resin Cross-linking/ % DVB	Time elapsed/ s							
	0	**0.25**	**0.5**	**1**	**2**	**5**	**60**	**90**
0.3	0	10.1	16.6	38.9	56.8	79.4	98.7	100
0.6	0	8	14.2	34.6	53.5	70.0	100	100
0.9	0	3.3	12.7	28.1	36.1	61.0	90.3	100
1.2	0	3.0	7.4	18.4	28.2	24.5	86.1	100
1.5	0	0	10.4	19.5	34.5	39.1	100	100
1.8	0	1.5	2.4	25.2	27.8	31.7	97.5	100
2.1	0	1.2	2.9	5.2	33.5	40.0	100	100
2.4	0	0	2.0	24.3	20.4	32.3	100	100
2.7	0	1.9	5.7	6.6	25.0	25.7	100	100
3.0	0	2.8	6.1	6.9	15.7	28.5	94.9	100
6.0	0	2.1	5.8	7.3	22.8	28.0	93.5	100

Table 7.10: Progress of cleavage reaction of 2-(4-dimethylamino-phenylazo)-benzamide-Rink-PS-DVB resin with cleavage solution.

	Resin Cross-linking/ % DVB										
	0.3	**0.6**	**0.9**	**1.2**	**1.5**	**1.8**	**2.1**	**2.4**	**2.7**	**3.0**	**6.0**
dAbs / min	0.56	0.43	0.29	0.25	0.25	0.21	0.18	0.17	0.15	0.12	0.12

Table 7.11: Initial rates of reaction of 2-(4-dimethylamino-phenylazo)-benzamide-Rink-PS-DVB resin with cleavage solution.

M/z (MS^+): 269.3 ($[M+H]^+$), 559.4 ($[2M+H]^+$).

RP HPLC (λ = 510 nm) Gradient 0 – 100% MeCN (7 min), 100% MeCN (1 min): 7.8 mins (100%).

UV γ_{max}: 530 nm.

R_F: 0.37 (EtOAc).

Mp.: 250-252°C (Lit. 249-250).

δ_H (300MHz, MeOH-d_4): 3.00 (6H, s, $^1CH_3$); 6.76 (2H, d, *J*9, ^3CH); 7.35 (1H, td, *J*8,1, ^9CH); 7.43 (1H, td, *J*8, 1, ^8CH); 7.69 (1H, dd, *J*8, 2, ^7CH); 7.71 (1H, dd, *J*8, 2, ^{10}CH); 7.75 (2H, d, *J*9, ^4CH).

δ_C (75MHz, MeOH): 40.6 (^1C); 148.3 (^2C); 110.5 (^3C); 124.2 (^4C); 141.7 (^5C); 151.8 (^6C); 114.6 (^7C); 132.2 (^8C); 129.6 (^9C); 128.0 (^{10}C); 128.3 (^{11}C); 167.1 (^{12}C).

7.6.2 *Synthesis of biphenyl-4-carboxylic acid amide (93)*[253]

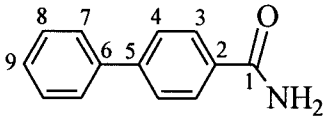

Each Fmoc-Rink loaded resin (0.3%, 0.6%, 0.9%, 1.2%, 1.5%, 1.8%, 2.1%, 2.4%, 2.7%, 3.0% and 6.0%, 100 mg, 0.05 mmol –NH_2) **(76)** was deprotected by suspension in piperidine/ DMF (20%) as described above and suspended in DMF (1.5 mL) and treated with K_2CO_3 (13.8 mg, 0.1 mmol), $PhB(OH)_2$ (phenyl boronic acid) (12.1 mg, 0.1 mmol) and $Pd(PPh_3)_4$ (61.2 mg, 0.05 mmol) (added by way of one 0.5 mL aliquot of stock solution of 1.34 g of catalyst in 11 mL of DMF per tube). The resulting suspension was heated at 80°C and 5 mg aliquots of resin **(92)** were removed from the suspensions at various time intervals. The aliquot of resin (5 mg) was suspended in TFA:DCM:H_2O (95:2.5:2.45) (1 mL) for 2 hours and filtered. The solvent was removed *in vac*uo and the yields shown in table 7.12.

Resin cross-linking	Time/ hours						
	0	1	2	5	10	24	48
0.3	0	60	95	100	100	100	100
0.6	0	43	85	96	98	100	100
0.9	0	28	70	85	95	98	100
1.2	0	14	49	78	92	99	100
1.5	0	5	23	45	73	95	100
1.8	0	16	49	78	93	97	100
2.1	0	16	55	82	95	98	100
2.4	0	10	35	74	90	97	100
2.7	0	5	17	45	76	95	100
3.0	0	4	5	5	5	5	4
6.0	0	3	4	4	3	4	5

Table 7.12: Percentage yields of synthesis of biphenyl-4-carboxylic acid amide with time.

	Resin Cross-linking/ % DVB								
	0.3	**0.6**	**0.9**	**1.2**	**1.5**	**1.8**	**2.1**	**2.4**	**2.7**
Half Life $t_{½}$/ h	1.50	4.25	6.13	6.50	8.00	11.50	9.00	15.50	17.00

Table 7.13: Half-life of Suzuki reaction of resin bound 4-iodobenzoic acid with phenyl boronic acid.

RP HPLC (λ = 254 nm) Gradient 20 – 100% MeCN (9 min): 8.6 mins **(86)**, (cleaved starting material 4-iodobenzoic carboxamide **(87)** (7.4 mins)).

Fmoc deprotected Rink-resin **(76)** (100 mg, 0.05 mmol $-NH_2$) was suspended in the following solvents (1.5 mL) (see below) and treated with K_2CO_3 (13.8 mg, 0.1 mmol), $PhB(OH)_2$ (phenyl boronic acid) (12.1 mg, 0.1 mmol) and $Pd(PPh_3)_4$ (61.2 mg, 0.05 mmol). The resulting suspension was heated at 40°C for 48 hours and the resin

suspended in TFA/ H_2O/ DCM (95:2.5:2.5) (2.5 mL) for 3 hours, filtered and the solvent removed *in vacuo*, to yield the title compound.

R_F: 0.36 (EtOAc).
M/z (APCI$^+$): 198.0 (100%, $[M+H]^+$).
RP HPLC (λ = 254 nm) Gradient 0 – 100% MeCN (20 min): 8.5 mins **(86)**, (cleaved starting material 4-iodobenzoic carboxamide **(87)** (7.3 mins)).

δ_H (300MHz, MeOH): 7.26 (1H, t, *J*7, ^{9}CH); 7.34 (2H, t, *J*7, ^{8}CH); 7.54 (2H, d, *J*7, ^{7}CH); 7.59 (2H, d, *J*7, ^{4}CH); 7.83 (2H, d, *J*7, ^{3}CH)

δ_C (75MHz, MeOH): 169.5 (^{1}C); 130.3 (^{2}C); 129.4 (^{3}C); 128.5 (^{4}C); 146.4 (^{5}C); 142.5 (^{6}C); 128.4 (^{7}C); 129.6 (^{8}C); 128.4 (^{9}C)

Purity (DCM:THF) (1:1) (48 h): 100%
Purity (Dioxane) (48 h): 100%
Purity (DMF) (48 h): 4.9%
Purity (MeOH) (48 h): 1.7%

7.7 EXPERIMENTAL TO CHAPTER 6

7.7.1 *Synthesis of 1-(4-vinyl-benzyl)-1H-imidazole (98)*

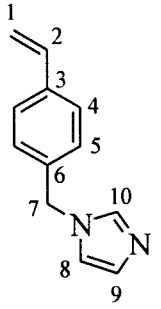

Sodium hydride (NaH) (21.4 g, 60% dispersion in mineral oil, 0.54 mol) was washed by stirring in dry hexane and then decanted. NaH was added portion-wise to a well stirred solution of imidazole (30.6 g, 0.45 mol) in dry THF:DCM (1:1) (100 mL) with catalytic potassium iodide (0.5 g) at 0°C under N_2.

Chloromethyl styrene (68 g, 0.44 mol) in THF (100 mL) was added drop-wise to the mixture over 30 mins and N_2 removed and the solution warmed to room temperature with stirring for 144 hours. Water (20 mL) was added and the solvents removed at 25°C *in vacuo*. EtOAc (400 mL) and water (100 mL) were added and the mixture stirred vigorously overnight. The organic fraction was collected, dried over $MgSO_4$ (10 g) and the solvents removed at 25°C *in vacuo* to yield 76.9 g (93%) of the title compound.

M/z (ES^+): 185 (100%, $[M+H]^+$), 226.1 (8%, $[M+H+MeCN]^+$).
HRMS (EI^+) $C_{12}H_{12}N_2$ Calc. 184.1005, Found 184.1002.
R_F: 0.25 (hexane).
UV γ_{max}: 256 nm.

δ_H (300MHz, DMSO-d_6): 5.29 (2H, s, $^7CH_2$); 5.37 (1H, dd, *J*11, 1, $^1CH_2$); 5.94 (1H, dd, *J*17, 1, ^1CH); 6.83 (1H, m, *J*8, ^2CH); 7.04 (1H, s, ^8CH); 7.30 (1H, s, ^9CH); 7.34 (2H, d, *J*8, ^5CH); 7.57 (1H, d, *J*8, ^4CH); 7.88 (1H, s, ^{10}CH).

δ_C (75MHz, DMSO-d_6): 113.4 (^1C); 135.0 (^2C); 127.8 (^3C); 125.3 (^4C); 126.6 (^5C); 135.0 (^6C); 48.0 (^7C); 127.6 (^8C); 118.4 (^9C); 137.0 (^{10}C).

7.7.2 *Synthesis of poly (styryl-co-DVB-co-1-(4-vinyl-benzyl)-1H-imidazole) resin (92)*

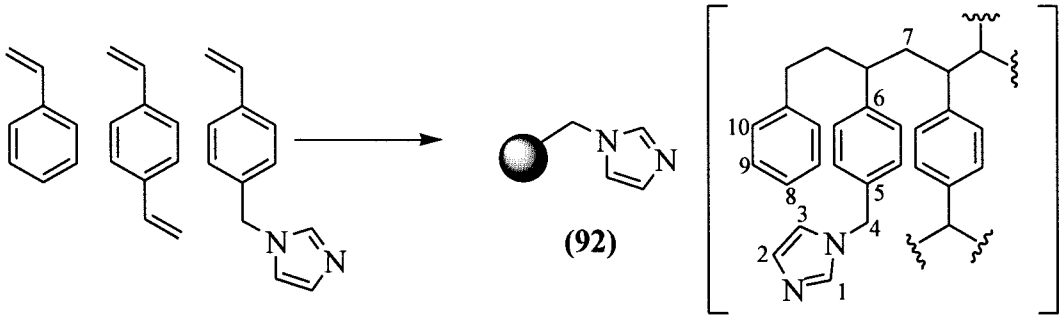

Organic phase (consisting of styrene (44.2 g, 425 mmol), DVB (0.70 g, 5.81 mmol), chloromethyl styrene (27.6 g, 0.15 mol), benzoyl peroxide (0.25 g)) was added to the aqueous phase (2.5 g PVA, (87-89% hydrolysed, Mr 85-150 kDa), 1000 mL H_2O, at 60°C, N_2 degassed for 30 mins) whilst stirring (in a 2.5 L 'Goldfish Bowl'). The suspension was allowed to equilibrate for 60 mins. The heat was removed and the suspension poured into ice and stirred slowly in an open atmosphere for 16 hours. The beaded resin product was filtered using polypropylene filter sheeting and the beads were washed with hot DMF (2 x 50 mL), DMF/ water (1:1) (2 x 50 mL), water (2 x 50 mL), dioxane (2 x 50 mL), MeOH (2 x 50 mL), DCM (2 x 50 mL), Et_2O (50 mL) and dried *in vacuo* to yield 51.4g (76%) of the title compound.

Size distribution: <45 microns 1.0 g; 45-125 microns 4.6 g; 125-250 microns 26.1 g; 250-355 microns 10.2 g; 500+ microns 7.8 g.

Combustion analysis: C (87.44%), H (7.85%), N (3.09%).

Loading : 1.12 mmol/ g.

δ_C (75MHz, benzene-d_6, Gel Phase): 146.0 (^{1}C); 119.4 (^{2}C); 126.5 (^{3}C); 50.5 (^{4}C); 134.7 (^{5}C); 138.0 (^{6}C); 41.4 (^{7}C); 126.5-130.7 ($^{8\text{-}10}$C).

7.7.3 *Binding of copper to poly (styrene-co-DVB-co-1-(4-vinyl-benzyl)-1H-imidazole) resin*

Poly (styrene-co-DVB-co-1-(4-vinyl-benzyl)-1*H*-imidazole) resin (100 mg) was swollen in THF and added to a solution of $CuSO_4$ (0.2M, 5 mL) and glycine (75 mg, 1 mmol) in THF (5 mL) and shaken at room temperature for 72 hours. The beads were filtered and washed with water (2 x 50 mL), DMF (2 x 50 mL) and Et_2O (50 mL) and dried *in vacuo*. The beads were observed to change from off-white to a turquoise/blue colour, which remained following the wash protocol.

7.7.4 *Colourimetric estimation of binding of copper to poly (styrene-co-DVB-co-1-(4-vinyl-benzyl)-1H-imidazole) resin*

Poly (styrene-co-DVB-co-1-(4-vinyl-benzyl)-1*H*-imidazole) resin (3 x 1 g) was suspended in increasing concentrations of $CuSO_4$ in DMF (0.05M, 0.10M and 0.20M) and shaken gently at room temperature for 36 hours. The resin was washed with DMF and the filtrates volume reduced *in vacuo* and diluted to 10 mL with DMF.

	Concentration of $CuSO_4$ in DMF / mmol						
	0.6708	0.3354	0.1677	0.08386	0.04193	0.02096	0.01048
Absorbance	1.9379	1.0603	0.5513	0.35246	0.12022	0.08055	0.04428

Table 7.14: Calibration with known concentrations of $CuSO_4$ in DMF.

The absorbances of the supernatants were measured (270 nm) and their concentrations calculated (table 7.15). The mass of $CuSO_4$ bound in the beads and therefore the binding ratios were thus calculated for the three sets of beads (table 7.16).

Total mass of $CuSO_4$ in DMF/ mg	**Sample Abs**	**Dilution of sample**	**Supernatant concentration/ mol/ dm^3**	**Mass of $CuSO_4$ in supernatant/ mg**
80	0.3879	25	0.003	5
160	0.3446	400	0.043	68
320	0.4539	100	0.140	223

Table 7.15: Calculation of $CuSO_4$ in supernatant.

Total mass of $CuSO_4$ in DMF/ mg	**Mass of $CuSO_4$ bound by beads/ mg**	**$CuSO_4$ bound in beads/ mmol**	**Molar ratio of imidazole groups: Cu bound by resin**
80mg	75	0.470	2.38
160mg	92	0.577	1.94
320mg	96	0.602	1.86

Table 7.16: Calculation of $CuSO_4$ bound by the beads.

The molar ratio of imidazole groups in the resin: molar amount of $CuSO_4$ bound by the beads was 2.06.

7.7.5 *Synthesis of isocyanate bound PS-DVB resin*

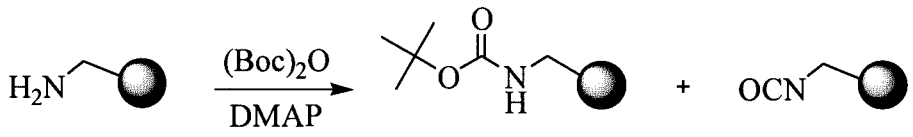

General protocol for synthesis of isocyanate bound PS-DVB resin

Boc_2O (1.4 eq. Mr 218) and DMAP (2 eq. Mr 122) were dissolved in DCM (2 mL) and the mixture allowed to stand at room temperature for 4 mins. Aminomethyl PS-DVB resin (100 mg, 0.14 mmol) was swollen in DCM (1 x bed volume) and the suspension shaken according to the conditions listed in table 7.17.

Entry	Temp/ °C	Solvent	Resin	Time/ min	Eq. Boc_2O	IR yield (%)
A	-78	DCM	PS	45	1.4	0
B	0	DCM	PS	45	1.4	50
C	20	DCM	PS	45	1.4	50
D	-78 → 20	DCM	PS	90	1.4	60
E	-78	DCM	PS	135	1.4	40
F	20	DCM	PS	45	1.4 (-DMAP)	0
G	20	DCM	MPA	45	2	0
H	20	MeCN	PS	22.5	2	0
I	20	MeCN	PS	45	2	0
J	20	MeCN	MPA	22.5	2	0
K	20	DCM	PS	22.5	2	50
L	20	DCM	PS	82.5	2	33
M	20	DCM	MPA	22.5	2	50
N	20	DCM	MPS-80	22.5	2	0

Table 7.17: Synthesis of isocyanate bound PS-DVB resin. MPA = macroporous polystyrene resin (loading 5.6 mmol/ g), MPS = macroporous polystyrene resin (loading 0.5 mmol/ g).

IR (υ_{max}/ cm^{-1}): 2250 cm^{-1} N=C=O (m), 1710 cm^{-1} C=O (s), 1160 cm^{-1} C-O (s).

7.7.6 *Synthesis of ethyl benzoate*[254]

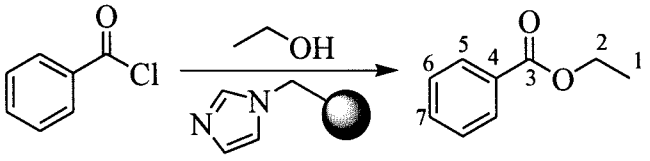

Three experiments were carried out as follows:

Experiment 1: Benzoyl chloride (140 mg, 1 mmol) was treated with EtOH (230 mg, 5 mmol) in DCM (2 mL) and 20 μL aliquots withdrawn and quenched with time (table 7.18).

Experiment 2: Benzoyl chloride (140 mg, 1 mmol) was treated with EtOH (230 mg, 5 mmol) in a suspension of poly (styrene-co-DVB-co-1-(4-vinyl-benzyl)-1*H*-imidazole) resin (50 mg, 70 μmol) in DCM (2 mL) and 20 μL aliquots withdrawn and quenched with time (table 7.18).

Experiment 3: Benzoyl chloride (140 mg, 1 mmol) was treated with EtOH (1.64 g, 35.6 mmol) in a suspension of poly (styrene-co-DVB-co-1-(4-vinyl-benzyl)-1*H*-imidazole) resin (50 mg, 70 μmol) in DCM (2 mL) and 20 μL aliquots withdrawn and quenched with time (table 7.18).

Experiment	Time/ min									
	1	2	3	4	5	10	25	40	80	160
1	4.8	5.1	8.2	10.1	12.1	13.1	40.7	56.0	74.0	89.6
2	6.1	9.0	12.5	15.5	18.7	30.6	51.7	65.7	76.3	95.3
3	6.2	8.5	11.2	13.6	16.1	27.1	48.8	63.2	83.9	96.6

Table 7.18: Progress of the reaction of benzoyl chloride with ethanol. The data in the table represents the ratio of hydrolyzed benzoyl chloride: ethyl benzoate.

The reaction volumes in experiments 1 – 3 above were filtered and the filtrate (0.025 mL) added to diisopropyl-ethylamine (13 mg, 0.1 mmol) and PS-DVB resin (600 mg, approx 0.4 mmol, entry K, table 7.17) in DCM (7 mL) added. The mixture was shaken at room temperature for 16 hours and filtered. To the filtrate was added Amberlite® IR-120 ion exchange resin and the suspension shaken at room temperature for a further 6 hours. The reaction was filtered and the ethyl benzoate (6 mg) isolated in 82% purity and 78% yield.

RP HPLC (λ = 254 nm) Gradient 0 – 100% MeCN (9 min), 100% MeCN (4 min): 10.0 mins (ethyl benzoate); 7.3mins (benzoic acid).

R_F: 0.75 (EtOAc).

IR (υ_{max}/ cm^{-1}): 1714 C=O (s), 1270 C-O (s).

UV γ_{max}: 236 nm.

δ_H (300MHz, $CDCl_3$): 1.29 (3H, t, *J*7, $^1CH_3$); 4.34 (2H, q, *J*7, $^2CH_2$); 7.50 (2H, t, *J*10, ^6CH); 7.72 (1H, t, *J*10, ^7CH); 7.74 (2H, d, *J*10, ^5CH).

δ_C (75MHz, $CDCl_3$): 14.3 (^1C); 60.8 (^2C); 165.8 (^3C); 129.1 (^4C); 129.9 (^5C); 128.2 (^6C); 133.3 (^7C).

References

1. Sucholeiki, I. *Mol. Divers.* **1998**, *4*, 25-30.
2. Griessbach, R. *Angew. Chem.* **1939**, *52*, 215-217.
3. Kun, K. A.; Kunin, R. *J. Polym. Sci.* **1964**, *82*, 839-843.
4. Moore, S.; Stein, W. H. *J. Biol. Chem.* **1951**, *192*, 663-664.
5. Bendich, A. *J. Am. Chem. Soc.* **1955**, *77*, 3671-3673.
6. Shuttleworth, S. J.; Allin, S. M.; Sharma, P. K. *Synthesis* **1997**, 1217-1239.
7. C. U. Pittman Jr. *Comprehensive Organometallic Chemistry*; G. W. Wilkinson Ed.; Pergamon Press, 1982; Vol. 8, p553-611.
8. Simon, E. *Ann. Pharm.* **1839**, *31*, 258-265.
9. Calmon, C. *React. Polym.* **1982**, *1*, 3-19.
10. Sarkenstein, E. *Biochem. Z.* **1910**, *24*, 210-218.
11. Staudinger, H.; Heuer, W. *Ber. Deut. Chem. Ger.* **1934**, *67*, 1164-1172.
12. Storey, B. T. *J. Polym. Sci.* **1965**, *3*, 265-282.
13. Adams, B. A.; Leighton Holmes, E. *J. Soc. Chem. Ind.* **1935**, *54*, 1-6.
14. Bolto, B. A.; Jackson, M. B. *React. Polym.* **1983**, *1*, 119-128.
15. Bolto, B. A.; Siudak, R. V. *Poly. Sci. Polym. Symp. Ed.* **1976**, *55*, 87-94.
16. Bolto, B. A.; Eppinger, K. H.; Macpherson, A. S.; Siudak, R. V.; Weiss, D. E.; Willis, D. *Desalination* **1973**, *13*, 269-270.
17. Merrifield, R. B. *J. Am. Chem. Soc.* **1963**, *85*, 2149-2154.
18. Gutte, B.; Merrifield, R. B. *J. Biol. Chem.* **1971**, *246*, 1922-1941.
19. Büttner, K.; Zahn, H.; Fischer, W. H. *Peptides: Chemistry and biology, Proceedings of the Tenth American Peptide Symposium*; Marshall, G. R., Ed.; Escom Science Publishers: Leiden, The Netherlands; 1988; p210-211.
20. Bolm, C.; Maischak, A.; Gerlach, A. *Chem. Commun.* **1997**, 2353-2354.
21. Gao, H.; Angelici, R. J. *J. Am. Chem. Soc.* **1997**, *119*, 6937-6938.
22. Atherton, E.; Clive, D. L. J.; Sheppard, R. C. *J. Am. Chem. Soc.* **1975**, *97*, 6584-6585.
23. Eichler, J.; Bienert, M.; Stierandova, A.; Lebl, M. *J. Peptide Res.* **1991**, *4*, 296-307.
24. Englebretsen, D. R.; Harding, D. R. K. *Int. J. Peptide Protein Res.* **1994**, *43*, 546-554.

25. Geysen, H. M.; Meloen, R. H.; Barteling, S. J. *Proc. Nat. Acad. Sci. USA.* **1984**, *81*, 3998-4002.
26. Maeji, N. J.; Valerio, R. M.; Bray, A. M.; Campbell, R. A.; Geysen, H. M. *Reactive Funct. Polym.* **1994**, *22*, 203-212.
27. Houghten, R. A. *Proc. Natl. Acad. Sci. USA* **1985**, **82**, 5131-5135.
28. Atrash, B.; Bradley, M.; Kobyleiki, R.; Cowell, D.; Reader, J. *Angew. Chem. Int. Ed.* **2001**, *in press*.
29. MacDonald, A. A.; Dewitt, S. H.; Ghosh, S.; Hogan, E. M.; Kieras, L.; Czarnik, A. W.; Ramage, R. *Mol. Divers.* **1996**, *1*, 183-186.
30. Larhed, M.; Lindeberg, G.; Hallberg, A. *Tetrahedron Lett.* **1996**, *37*, 8219-8222.
31. Labadie, J. W. *Curr. Op. Chem. Biol.* **1998**, *2*, 346-352.
32. Gooding, O. W.; Baudart, S.; Deegan, T. L.; Heisler, K.; Labadie. J. W.; Newcomb, W. S.; Porco Jr., J. A.; van Eikeren, P. *J. Comb. Chem.* **1999**, *1*, 113-122.
33. Labadie, J. W.; Deegan, T. L.; Gooding, O. W.; Heisler, K.; Newcomb, W. S.; Porco, J. A.; Tran, T. H.; van Eikeren, P. *Polym. Mater. Sci. Eng.* **1996**, *75*, 389-390.
34. Cho, J. K.; Park, B. D.; Lee, Y. S. *Tetrahedron Lett.* **2000**, *41*, 7481-7485.
35. Meldal, M. *Tetrahedron Lett.* **1992**, *33*, 3077-3080.
36. Li, W. B.; Yan, B. *J. Org. Chem.* **1998**, *63*, 4092-4097.
37. Bui, C. T.; Rasoul, F. A.; Ercole, F.; Pham, Y.; Maeji, N. J. *Tetrahedron Lett.* **1998**, *39*, 9279-9282.
38. Li, W. B.; Xiao, X. Y.; Czarnik, A. W. *J. Comb. Chem.* **1999**, *1*, 127-129.
39. Toy, P. H.; Janda, K. D. *Tetrahedron Lett.* **1999**, *40*, 6329-6332.
40. Kempe, M.; Barany, G. *J. Am. Chem. Soc.* **1996**, *118*, 7083-7093.
41. Bayer, E.; Rapp, W. *Poly(ethylene Glycol) Chemistry : Biotechnical and Biomedical Applications*; J. Milton Harris Ed.; Plenum Press: New York, **1992**, 325-345.
42. Amos, J. L. *Polym. Eng. Sci.* **1974**, *14*, 1-7.
43. R. H. M. Simon; D. C. Chappelear *Polymerization Reactions and Processes, ACS Symposium Series;* Henderson, J. N.; T. C. Bonton, Eds.; American Chemical Society: Washington DC, **1979; Vol.** *104*, p71-112.

44. Durst, H. D. *Tetrahedron Lett.* **1974**, *28*, 2421-2424.
45. Ugelstad, J.; Mørk, P. C. *Adv. Coll. Int. Sci.* **1980**, *13*, 101-140.
46. Carothers, W. H. *J. Am. Chem. Soc.* **1929**, *51*, 2548-2559.
47. Cameron, G. G.; Law, K. S. *Polymer* **1981**, *22*, 272-273.
48. Yuan, H. G.; Kalfas, G, Ray, W. H. J. *Macromol. Sci. Rev. Macromol. Chem. Phys.* **1991**, *C31*, 215-299.
49. Vivaldo-Lima, E.; Wood, P. E.; Hamielec, A. E.; Penlidis, A. *Ind. Eng. Chem. Res.* **1997**, *36*, 939-965.
50. Arshady, R. *Makromol. Chem.* **1984**, *185*, 2387-2400.
51. Cooper, A. I. *J. Mater. Chem.* **2000**, *10*, 207-234.
52. Wulff, G. *Angew. Chem. Int. Ed Engl.* **1995**, *34*, 1812-1832.
53. Arshady, R. *Colloid. Polym. Sci.* **1992**, *270*, 717-732.
54. Renneberg, B.; Labadie, J. W. *Chemistry Today* **1999**, *17*, 7-9.
55. Mitchell, A. R.; Kent, S. B. H.; Erickson, B. W.; Merrifield, R. B. *Tetrahedron Lett.* **1976**, *42*, 3795-3798.
56. Wang, S. S. *J. Org. Chem.* **1975**, *40*, 1235-1239.
57. Carpino, L. A.; Cohen, B. J.; Stephens Jr., K. E.; Sadataalaee, S. Y.; Tien, J. H.; Langridge, D. C. *J. Org Chem.* **1986**, *51*, 3732-3734.
58. Yamashiro, D.; Noble, R. L.; Li, C. H. *J. Org. Chem.* **1973**, *38*, 3561-3565.
59. Noble, R. L.; Yamashiro, D.; Li, C. H. *Int. J. Peptide Protein Res.* **1977**, *10*, 385-393.
60. Chaturvedi, N.; Sigler, G.; Fuller, W.; Verlander, M.; Goodman, M. *Chemical Synthesis and Sequencing of Peptides and Proteins;* Liu, T. Y.; Schechter, A. N.; Heinrikson, R. L.; Condliffe, P. G. Eds.; American Chemical Society, **1981**.
61. Fields, C. G.; Fields, G. B.; Noble, R. L.; Cross, T. A. *Int. J. Peptide Protein Res.* **1989**, *33*, 298-303.
62. Eritja, R.; Ziehler-Martin, J. P.; Walker, P. A.; Lee, T. D.; Legesse, K.; Albericio, F.; Kaplan, B. E. *Tetrahedron* **1987**, *43*, 2675-2680.
63. Kisfaludy, L.; Schőn, I. *Synthesis* **1983**, 325-327.
64. Kisfaludy, L.; Otros Jr., L.; Schőn, I.; Low. M. *Peptides: Structure and Function;* Deber, C. M.; Hruby, V. J.; Kopple, K. D. Eds., **1985,** p221-224.

65. Bodanszky, M.; Bodanszky, A.; Tolle, J. C.; Bednarek, M. A. *Chemical Synthesis and Sequencing of Peptides and Proteins*; Liu. T, Y.; Schechter, A. N.; Heinrikson, R. L.; Condliffe, P. G. Eds.; Elsevier North Holland, Amsterdam, **1981,** p165-167.
66. Atherton, E.; Logan, C. J.; Sheppard, R. C. *J. Chem. Soc. Perkin Trans. 1* **1981**, 538-546.
67. Hudson, D. *J. Org. Chem.* **1988**, *53*, 617-624.
68. Atherton, E.; Cameron, L. R.; Sheppard, R. C. *Tetrahedron* **1988**, *44*, 843-857.
69. Dryland, A.; Sheppard, R. C. *Tetrahedron* **1988**, *44*, 859-876.
70. Atherton, E.; Sheppard, R. C. *J. Chem. Soc. Chem. Commun.* **1985**, 165-166.
71. Pedroso, E.; Grandas, A.; Saralegui, M. A.; Giralt, E.; Granier, C.; Van Rietschoten, J. *Tetrahedron* **1982**, *38*, 1183-1192.
72. Guillier, F.; Orain, D.; Bradley, M. *Chem. Rev.* **2000**, *100*, 2091-2157.
73. Rink, H. *Tetrahedron Lett.* **1987**, *28*, 3787-3790.
74. Morphy, J. R.; Rankovic, Z.; Rees, D. C. *Tetrahedron Lett.* **1996**, *37*, 3209-3212.
75. Holmes, C. P.; Jones, D. G. *J. Org. Chem.* **1995**, *60*, 2318-2319.
76. Sternson, S. M.; Schreiber, S. L. *Tetrahedron Lett.* **1998**, *39*, 7451-7454.
77. Kenner, G. W.; McDermott, J. R.; Sheppard, R. C. *J. Chem. Soc. Commun.* **1971**, 636-637.
78. Brase, S.; Enders, D.; Kobberling, J.; Avemaria, F. *Angew. Chem. Int. Ed. Engl.* **1998**, *37*, 3413-3415.
79. Siuzdak, G.; Lewis, J. K. *Biotech. Bioeng. (Comb. Chem.)* **1998**, *61*, 127-134.
80. Metzger, J. W.; Wiesmuller, K. H.; Gnau, V.; Brunjes, J.; Jung, G. *Angew. Chem. Int. Ed. Engl.* **1993**, *32*, 894-896.
81. Karas, M.; Bachmann, D.; Bahr, U.; Hillenkamp, F. *Int. J. Mass Spectrom. Ion. Proc.* **1987**, *78*, 53-68.
82. Karas, M.; Bahr, U.; Hillenkamp, F. *Int. J. Mass Spectrom. Ion. Proc.* **1989**, *92*, 231-242.
83. Egner, B. J.; Langley, G. J.; Bradley, M. *J. Org. Chem.* **1995**, *60*, 2652-2653.
84. Look, G. C.; Holmes, C. P.; Chinn, J. P.; Gallop, M. A. *J. Org. Chem.* **1994**, *59*, 7588-7590.
85. Fitch, W. L.; Detre, G.; Holmes, C. P.; Shoolery, J. N.; Keifer, P. A. *J. Org. Chem.* **1994**, *59*, 7955-7956.

86. Wehler, T.; Westman, J. *Tetrahedron Lett.* **1996**, *37*, 4771-4774.

87. Moore, S.; Stein, W. H. *J. Biol. Chem.* **1948**, *176*, 367.

88. Kaiser, E.; Colescott, R. L.; Bossinger, C. D.; Cook, P. I. *Anal. Biochem.* **1970**, *34*, 595-598.

89. Sarin, V. K.; Kent, S. B. H.; Tam, J. P.; Merrifield, R. B. *Anal. Biochem.* **1981**, *117*, 147-157.

90. Chang, C. D.; Waki, M.; Ahmad, M.; Meienhofer, J.; Lundell, E. O.; Haug, J. D. *Int. J. Peptide Protein Res.* **1980**, *15*, 59-66.

91. Heimer, E. P.; Chang, C. D.; Lambros, T. L.; Meienhofer, J. *Int. J. Peptide Protein Res.* **1981**, *18*, 237-241.

92. Meienhofer, J.; Waki, M.; Heimer, E. P.; Lambros, T. J.; Makofske, R. C.; Chang, C. D. *Int. J. Peptide Protein Res.* **1979**, *13*, 35-42.

93. Krchnak, V.; Vagner, J.; Eichler, J.; Lebl, M. *Peptides 1988*; Jung, G.; Bayer, E. Eds.; Walter de Gruyter and Company: Berlin, **1989** p232-234.

94. Krchnak, V.; Vagner, J.; Lebl, M. *Int. J. Peptide Protein Res.* **1988**, *32*, 415-416.

95. Krchnak, V.; Vagner, J.; Safar, P.; Lebl, M. *Coll. Czech. Chem. Commun.* **1988**, *53*, 2542-2548.

96. Christensen, T. *Peptides: Structure and Biological Function*; Gross, E.; Meienhofer, J. Eds.; Pierce Chemical Company: Rockford, IL, **1979** p385-388.

97. Christensen, T.; Villemoes, P.; Brunfeldt, K. *Peptides: Proceedings of the 5th American Peptide Symposium;* Goodman, M.; Meinhofer, J. Eds.; Halsted Press: New York **1977**, p569-571.

98. Edman, P. *Acta Chem. Scand.* **1950**, *4*, 283-293.

99. Edman, P. *Acta Chem. Scand.* **1956**, *10*, 761-768.

100. Edman, P.; Begg, G. *European J. Biochem.* **1967**, *1*, 80-91.

101. Terrett, N. K.; Gardner, M.; Gordon, D. W.; Kobylecki, R. J.; Steele, J. *Tetrahedron* **1995**, *51*, 8135-8173.

102. Furka, A.; Sebestyén, F.; Asgedom, M.; Dibó, G. *Int. J. Peptide Protein Res.* **1991**, *37*, 487-493.

103. Früchtel. J. S.; Jung, G. *Angew. Chem. Int. Ed. Engl.* **1996**, *35*, 17-42.

104. Thompson, L. A.; Ellman, J. A. *Chem. Rev.* **1996**, *96*, 555-600.

105. Wyatt, J. R.; Vickers, T. A.; Roberson, J. L.; Buckheit Jr, R. W.; Klimkait, T.; DeBaets, E.; Davis, P. W.; Rayner, B.; Imbach, J. L.; Ecker, D. J. *Proc. Natl. Acad. Sci.* **1994**, *91*, 1356-1360.

106. Flynn, D. J.; Crich, J. Z.; Devraj, R. V.; Hockerman, S. L.; Parlow, J. J.; South, M. S.; Woodard, S. *J. Am. Chem. Soc.* **1997**, *119*, 4874-4881.

107. Simon, R. J.; Kania, R. S.; Zuckermann, R. N.; Huebner, V. D.; Jewell, D. A.; Banville, S.; Ng, S.; Wang, L.; Rosenberg, S.; Marlowe, C. K.; Spellmeyer, D. C.; Tan, R. Y.; Frankel, A. D.; Santi, D. V.; Cohen, F. E.; Bartlett, P. A. *Proc. Natl. Acad. Sci.* **1992**, *89*, 9367-9371.

108. Zuckermann, R. N,; Kerr, J. M.; Kent, S. B. H.; Moos, W. H. *J. Am. Chem. Soc.* **1992**, *114*, 10646-10647.

109. Cho, C. Y.; Moran, E. J.; Cherry, S. R.; Stephans, J. C.; Fodor, S. P. A.; Adams, C. L.; Sundaram, A.; Jacobs, J. W.; Schultz, P. G. *Science* **1993**, *261*, 1303-1305.

110. Bunin, B. A.; Ellman, J. A. *J. Am. Chem. Soc.* **1992**, *114*, 10997-10998.

111. Ordon, D. W.; Steale, J. *BioMed. Chem. Lett.* **1995**, *5*, 47-50.

112. Beebe, X.; Schore, N. E.; Kurth, M. J. *J. Am. Chem. Soc.* **1992**, *114*, 10061-10062.

113. Kurth, M. J.; Randall, L. A. A.; Chen, C. X.; Melander, C.; Miller, R. B.; McAlister, K.; Reitz, G.; Kang, R.; Nakatsu, T.; Green, C. *J. Org. Chem.* **1994**, *59*, 5862-5864.

114. Floyd, C. D.; Lewis, C. N.; Whittaker, M. *Chemistry in Britain* **1996**, *32*, 31-35.

115. Gallop, M. A.; Barrett, R. W.; Dower, W. J.; Fodor, S. P. A.; Gordon, E. M. *J. Med Chem.* **1994**, *37*, 1233-1251.

116. In synthesis notes, CN Biosciences UK, NovaBiochem product catalogue, Eds.; Dőrner, B.; White, P., 2000.

117. Kim, D.Y.; Suh, K. H. *Synthetic Commun.* **1999**, *29*, 1271-1275.

118. Yim, A. M.; Vidal, Y.; Viallefont, P.; Martinez, J. *Tetrahedron Lett.* **1999**, *40*, 4535-4538.

119. Bonnet, D.; Rommens, C.; Gras-Masse, H.; Melnyk, O. *Tetrahedron Lett.* **1999**, *40*, 7315-7318.

120. Arsequell, G.; Espuna, G.; Valencia, G.; Barluenga, J.; Carlon, R. P.; Gonzalez, J. M.; *Tetrahedron Lett.* **1999**, *40*, 7279-7282.

121. Richter, H.; Walk, T.; Holtzel, A.; Jung, G. *J. Org. Chem.* **1999**, *64*, 1362-1365.

122. Hébert, N.; Hannah, A. L.; Sutton, S. C. *Tetrahedron Lett.* **1999**, *40*, 8547-8550.

123. Katritzky, A. R.; Qi, M.; Feng, D. M.; Zhang, G. F.; Griffith, M. C.; Watson, K. *Org. Lett.* **1999**, *1*, 1189-1191.

124. Combs, A. P.; Saubern, S.; Rafalski, M.; Lam, P. Y. S. *Tetrahedron Lett.* **1999**, *40*, 1623-1626.

125. Goff, D. A. *Tetrahedron Lett.* **1999**, *40*, 8741-8745.

126. Peng,G.; Sohn, A.; Gallop, M. A. *J. Org. Chem.* **1999**, *64*, 8342-8349.

127. Cavallaro, C. L.; Herpin, T.; McGuinness, B. F.; Shimshock, Y. C.; Dolle, R. E. *Tetrahedron Lett.* **1999**, *40*, 2711-2714.

128. Caddick, S.; Hamza, D.; Wadman, S. N. *Tetrahedron Lett.* **1999**, *40*, 7285-7288.

129. Rossé, G.; Ouertani, F.; Schroder, H. *J. Comb. Chem.* **1999**, *1*, 397-401.

130. Karoyan, P.; Triolo, A.; Nannicini, R.; Giannotti, D.; Altamura, M.; Chassaing, G.; Perrotta, E. *Tetrahedron Lett.* **1999**, *40*, 71-74.

131. Tremblay, M. R.; Simard, J.; Poirier, D. *Bioorg. Med. Chem. Lett.* **1999**, *9*, 2827-2832.

132. Grubbs, R. H.; Kroll, L. C. *J. Am. Chem. Soc.* **1971**, *93*, 3062-3063.

133. Trost, B. M.; Keinan, E. *J. Am. Chem. Soc.* **1978**, *100*, 7779-7781.

134. McQuillin, J. F.; Ord, W. O.; Simpson, P. L. *J. Chem. Soc.* **1996**, 5996-6001

135. Nicewonger, R. B.; Ditto, L.; Varady, L. *Tetrahedron Lett.* **2000**, *41*, 2323-2326.

136. Booth, R. J.; Hodges, J. C. *J. Am. Chem. Soc.* **1997**, *119*, 4882-4886.

137. Ault-Justus, S. E.; Hodges, J. C.; Wilson, M. W. *Biotech. Bioeng. (Comb. Chem.)* **1998**, *61*, 17-22.

138. Schlenk, W.; Appenrodt, J.; Michael, A.; Thal, A. *Ber. Deut. Chem. Ger.* **1914**, *47*, 473-490.

139. Priddy, D. B. US Patent 4647632, 1987.

140. Priddy, D. B.; Piro, M. US Patent 4572819, 1986.

141. D. R. Lyengar,; T. J. McCarthy *ACS Polymer Preprints*; ACS meeting: Miami Beach, Florida, 1989, 30, p154.

142. Whitmore, F. C. *Ind. Eng. Chem.* **1964**, *26*, 94.

143. Sandler, S. R.; Karo, W.; Bonesteel, J.; Pearce, E. M. *Polymer Synthesis and Characterisation – A Laboratory Manual*; Academic Press, Harcourt Brace and Company (Publishers); **1998**, p9-12.

144. Church, J. M. *Chem. Eng.* **1966**, 79-82.

145. Coffey D.; *Lecture Notes, Developing new solid supports to improve synthesis in combinatorial chemistry libraries*; Solid Phase Support Product Manager, Polymer Laboratories, Essex Road, Church Stretton, Shropshire, SY6 6AX, UK.

146. Zaugg, H. E.; Martin, W. B. *Org. React.* **1965**, *14*, 52-269.

147. McAlpine, S. R.; Schreiber, S. L. *Chem. Eur. J.* **1999**, *5*, 3528-3532.

148. Sarin, V. K.; Kent, S. B. H.; Merrfield, R. B. *J. Am. Chem. Soc.* **1980**, *102*, 5463-5470.

149. Arshady, R.; Ledwith, A. *React. Polym.* **1983**, *1*, 159-174.

150. Erbay, E.; Bilgiç, T.; Karali, M.; Savaşçi, Ő, T. *Polym. Plast. Technol. Eng.* **1992**, *31*, 589-605.

151. European Patent 87118837.1.

152. Borhan, B.; Wilson, J. A.; Gasch, M. J.; Ko, Y.; Kurth, D. M.; Kurth, M. J. *J. Org. Chem.* **1995**, *60*, 7375-7378.

153. Arshady, R.; Kenner, G. W.; Ledwith, A. *J. Polym. Sci. Polym. Chem. Edn.* **1974**, *12*, 2017-2025.

154. Christian, P.; Giles, M. R.; Howdle, S. M.; Major, R. C.; Hay, J. N. *Polymer* **2000**, *41*, 1251-1256.

155. Stranix, B. R.; Gao, J. P.; Barghi, R.; Salha, J. *J. Org. Chem. Soc.* **1997**, *62*, 8987-8993.

156. Wyeth P.; *Lecture Notes*, University of Southampton, Post Graduate Lecture Course PG313, 1999.

157. Bayer, E.; Hagenmaier, H.; Jung, G.; König, W. *Peptides 1968*; North-Holland Publishing Group: Amsterdam 1968.

158. Tanaka, M.; Nakshima, T.; Benson, A.; Mower, H.; Tasunobu, K. T. *Biochemistry* **1996**, *5*, 1666-1668.

159. Consden, J. R.; Gordon, A. H.; Martin, A. J. P.; Synge, R. D. M. *Biochem. J.* **1947**, *28*, 596-602.

160. Marsh, I. R.; Bradley, M.; Teague, S. J. *J. Org. Chem.* **1997**, *62*, 6199-6203.

161. Abstract; *Advance ACS Abstracts*, August 1, 1997.

162. Trzeciak, A.; Bannwarth, W. *Tetrahedron Lett.* **1992**, *33*, 4557-4560.

163. Kopple, D. D. *J. Pharm. Sci.* **1972**, *61*, 1345-1356.

164. Alsina, J.; Rabanal, F.; Giralt, E.; Albericio, F. *Tetrahedron Lett.* **1994**, *35*, 9633-9636.

165. Fields, G. B.; Noble, R. L. *Int. J. Peptide Protein Res.* **1990**, *35*, 161-214.

166. Kates, S. A.; Sole, N. A.; Johnson, C. R.; Hudson. D.; Barany, G.; Albericio, F. *Tetrahedron Lett.* **1993**, *34*, 1549-1552.

167. Isied, S. S.; Kuehn, G. G.; Lyon, J. M.; Merrifield, R. B. *J. Am. Chem. Soc.* **1982**, *104*, 2632-2634.

168. Rovero, P.; Quartara, L.; Fabbri, G. *Tetrahedron Lett.* **1991**, *32*, 2639-2642.

169. McMurray, J. S. *Tetrahedron Lett.* **1991**, *32*, 7679-7682.

170. Egner, B. J.; Bradley, M. *Tetrahedron* **1997**, *53*, 14021-14030.

171. Botti, P.; Pallin, T. D.; Tam, J. P. *J. Am. Chem. Soc.* **1996**, *118*, 10018-10024.

172. Felix, A. M.; Wang, C. T.; Heimer, E. P.; Fournier, A. *Int. J. Peptide Protein Res.* **1988**, *31*, 231-238.

173. Mazur, S.; Jayalekshmy, P. *J. Am. Chem. Soc.* **1979**, *101*, 677-683.

174. Leznoff, C. C. *Chem. Soc. Rev.* **1974**, *3*, 65-85.

175. Overberger, C. G.; Sannes, K. N. *Angew. Chem. Int. d. Engl.* **1974**, *13*, 99-104.

176. Crowley, J. I.; Harvey III, T. B.; Rapoport, H. J. *Macromol. Sci. Chem.* **1973**, *7*, 1118.

177. Crowley, J. I.; Rapoport, H. *Acc. Chem. Res.* **1976**, *9*, 135-144.

178. Scott, L. T.; Rebek, J.; Ovsyanko, L.; Sims, C. L. *J. Am. Chem. Soc.* **1977**, *99*, 625-626.

179. Patchornik, A.; Kraus, M. A. *J. Am. Chem. Soc.* **1970**, *92*, 7587-7589.

180. Kraus, M. A.; Patchornik, A. *J. Am. Chem. Soc.* **1971**, *93*, 7325-7327.

181. Grubbs, R. H.; Gibbons, C.; Kroll, L. C.; Bonds Jr., W. D.; Brubaker Jr., C. H. *J. Am. Chem. Soc.* **1973**, *95*, 2373-2375.

182. Regen, S. L. *J. Am. Chem. Soc.* **1974**, *96*, 5275-5276.

183. Fridkin, M.; Patchornik, A.; Katchalski, E. *J. Am. Chem. Soc.* **1965**, *87*, 4646-4648.

184. Hodge, P.; Ji-Long, J.; Owen, G. J.; Houghton, M. P. *Polymer* **1996**, *37*, 5059-5067.

185. Rao, M. H.; Yang, W.; Joshua, H.; Becker, J. M.; Naider, F. *Int. J. Peptide Protein Res.* **1995**, *45*, 418-429.

186. Mutter, M. *J. Am. Chem. Soc.* **1977**, *99*, 8307-8314.

187. Merrifield, R. B.; Littau, V. *Peptides 1968*; North-Holland Publishing Group: Amsterdam 1968.

188. Ishida, K.; Matsuda, H.; Murakami, M.; Yamaguchi, K. *J. Nat. Prod.* **1997**, *60*, 724-726.

189. Kates, S. A.; Solé, N. A.; Albericio, F.; Barany, G. *Peptides: Design, Synthesis and Biological Activity*; Basava, C.; Anantharamaiah, G. M. Eds.; Birlchäuser: Boston 1994, p39-58.

190. Kimbonguila, A. M.; Merzouk, A.; Guibé, F.; Loffet, A. *Tetrahedron Lett.* **1994**, *35*, 9035-9038.

191. Greenberg, M. M.; Matray, T. J.; Kahl, J. D.; Yoo, D. J.; McMinn, D. L. *J. Org. Chem.* **1998**, *63*, 4062-4068.

192. Guibé, F. *Tetrahedron* **1998**, *54*, 2967-3042.

193. Waldmann, H.; Kunz, H. *Liebigs Ann. Chem.* **1983**, 1712-1725.

194. Trost, B. M. *Acc. Chem. Res.* **1980**, *13*, 385-393.

195. Friedrichbochnitschek, S.; Waldmann, H.; Kunz, H. *J. Org. Chem.* **1989**, *54*, 751-756.

196. Hayakawa, Y.; Kato, H.; Uchiyama, M.; Kajino, H.; Noyori, R. *J. Org. Chem.* **1986**, *51*, 2400-2402.

197. Khng, H. P.; Cunliffe, D.; Davies, S.; Turner, N. A.; Vulfson, E. N. *Biotechnol. Bioeng.* **1998**, *60*, 419-424.

198. Shiho, H.; Manabe, Y.; Kawahashi, N. *J. Mater. Chem.* **2000**, *10*, 333-336.

199. Lee, R. A.; Donald, D. S. *Tetrahedron Lett.* **1997**, *38*, 3857-3860.

200. Szymonifka, M. J.; Chapman, K. T. *Tetrahedron Lett.* **1995**, *36*, 1597-1600.

201. Sasaki, S.; Takagi, M.; Tanaka, Y.; Maeda, M. *Tetrahedron Lett.* **1996**, 37, 85-88.

202. Sucholeiki, I.; Perez, J. M. *Tetrahedron Lett.* **1999**, *40*, 3531-3534.

203. Dynabeads™ from the Dynal Corporation, PO Box 158, SilØyen, N0212 OSLO, Norway.

204. Dynal product information sheets, obtained from Dynal UK Ltd.

205. Hewett, P. W.; Murray, J. C. *Eur. J. Cell Biol.* **1993**, *62*, 451-454.

206. Jackson, C. J.; Garbett, P. K.; Nissen, B.; Schrieber, L. *J. Cell Sci.* **1990**, *96*, 257-262.

207. Bukhari, Z.; McCuin, R. M..; Fricker, C. R.; Clancy, J. L. *Appl. Environ. Microbiol.* **1998**, *64*, 4495-4499.

208. Christenson, L. K.; Stouffer, R. L. *Biol. Reprod.* **1996**, *55*, 1397-1404.

209. Drake, B. L.; Loke, Y. W. *Human Reprod.* **1991**, *6*, 1156-1159.

210. Partington, K. M.; Jenkinson, E. J.; Anderson, G. *J. Immunol. Methods* **1999**, *223*, 195-205.

211. Mosbach, K.; Andersson, L. *Nature* **1977**, *270*, 259-261.

212. Jakobsen, K. S.; Breivold, E.; Hornes, E. *Nucl. Acids Res.* **1990**, *18*, 3669-3669.

213. Gabrielsen, O. S.; Huet, J. *Methods Enzymol.* **1993**, *218*, 508-525.

214. Bäckman, A.; Lantz, P.-G.; Rådström, P.; Olcén, P. *Mol. Cell. Probe.* **1999**, *13*, 49-60.

215. Swank, H. W.; Mellon, M. G. *Ind Eng. Chem.* **1937**, *9*, 406-409.

216. Yoe, J. H. *J. Am. Chem. Soc.* **1932**, *54*, 4139-4143.

217. Rana, S.; White, P.; Bradley, M. *Tetrahedron Lett.* **1999**, *40*, 8137-8140.

218. Bell, R. P. *Advanc. Catal.* **1952**, *4*, 151-207.

219. Rodriguez, O.; Setínek, K. *J. Catal.* **1975**, *39*, 449-455.

220. Andrianova, T. I. *Kinet. Katal.* **1964**, *5*, 927-929.

221. Prokop, Z.; Setínek, K. *Collect. Czechosl. Chem. Commun.* **1974**, *39*, 1253-1263.

222. Ševčik, S.; Štamberg, J.; Procházka, M. *Collect. Czechosl. Chem. Commun.* **1968**, *33*, 1327-1332.

223. Setínek, K. *Collect. Czechosl. Chem. Commun.* **1977**, *42*, 979-986.

224. Beránek, L.; Setínek, K.; Kraus, M. *Collect. Czechosl. Chem. Commun.* **1972**, *37*, 2265-2268.

225. Sung, D. W. L.; Hodge, P.; Stratford, P. W. *J. Chem. Soc. Perkin Trans. 1* **1999**, 1463-1472.

226. Gut, V.; Rudinger, J. *Peptides 1968*; North-Holland Publishing Company: Amsterdam, 1968; p185-188.

227. Kuruso, Y. *Bull. Chem. Soc. Japan* **1972**, *45*, 2211-2212.

228. Collman, J. P.; Hegedus, L. S.; Cooke, M. P.; Norton, J. R.; Dolcetti, G.; Marquardt, D. N. *J. Am. Chem. Soc.* **1972**, *94*, 1789-1790.

229. Takaishi, N.; Imai, H.; Bertelo, C. A.; Stille, J. K. *J. Am. Chem. Soc.* **1976**, *98*, 5400-5402.

230. Dumont, W.; Poulin, J. C.; Dang, T. P.; Kagan, H. B. *J. Am. Chem. Soc.* **1973**, *95*, 8295-8299.

231. Yan, B.; Sun, Q. *J. Org. Chem.* **1998**, *63*, 55-58.

232. Yan, B.; Sun, Q.; Wareing, J. R.; Jewell, C. F. *J. Org. Chem.* **1996**, *61*, 8765-8770.

233. Yan, B.; Fell, J. B.; Kumaravel, G. *J. Org. Chem.* **1996**, *61*, 7467-7472.

234. Suzuki, A.; Miyaura, N. *J. Chem. Soc. Chem. Commun.* **1979**, 866-867.

235. Miyaura, N.; Suzuki, A. *Chem. Rev.* **1995**, *95*, 2457-2483.

236. Martin, A. R.; Yang, Y. H. *Acta Chem. Scand.* **1993**, *47*, 221-230.

237. Laue, T.; Plagens, A.; *Named Organic Reactions*; John Wiley and Sons: New York, 1999, 4th Edn.; p262.

238. Milstein, D.; Stille, J. K. *J. Am. Chem. Soc.* **1978**, *100*, 3636-3638.

239. Stille, J. K. *Angew. Chem. Int. Ed.* **1986**, *25*, 508-523.

240. Nicolaou, K. C.; Sorensen, E. J.; *Classics in Total Synthesis – Targets, Strategies, Methods*; VCH Verlagsgesellschaft: Weinheim, 1996.

241. *Biochemistry, International Edition*, J. D. Rawn; Neil Patterson publishers; Carolina Biological Supply Company: Burlington, North Carolina; **1989**.

242. Collman, J. P.; Reed, C. A. *J. Am. Chem. Soc.* **1973**, *95*, 2048-2049.

243. Verweij, P. D.; Driessen, W. L.; Reedijk, J.; Rowatt, B.; Sherington, D. C. *React. Polymer* **1990**, *13*, 83-92.

244. Bergbreiter, D. E.; Koshti, N.; Franchina, J. G.; Frels, J. D. *Angew. Chem. Int. Ed.* **2000**, *39*, 1040-1042.

245. Booth, R. J.; Hodges, J. C. *Acc. Chem. Res.* **1999**, *32*, 18-26.

246. Rebek, J.; Brown, D.; Zimmerman, S. *J. Am. Chem. Soc.* **1975**, *97*, 4407-4408.

247. Dressman, B. A.; Singh, U.; Kaldor, S. W. *Tetrahedron Lett.* **1998**, *39*, 3631-3634.

248. Creswell, M. W.; Bolton, G. L.; Hodges, J. C.; Meppen, M. *Tetrahedron* **1998**, *54*, 3983-3998.

249. Hulme, C.; Ma, L.; Romano, J.; Morrissette, M. *Tetrahedron Lett.* **1999**, *40*, 7925-7928.

250. Chong, P. Y.; Janicki, S. Z.; Petillo, P. A. J. Org. Chem. 1998, 63, 8515-8521.

251. Knolker, H.J.; Braxmeier, T.; Schlechtingen, G. *Angew. Chem. Int. Ed. Engl.* **1995**, *34*, 2497-2499.

252. Zhmurova, J. *J. Gen. Chem. USSR (Engl. Transl.)*, **1972**, *42*, 1947-1954.

253. Larhed, M.; Lindeberg, G.; Halberg, A. *Tetrahedron Lett.* **1996**, *37*, 8219-8222.

254. Meerwein, G. *Angew. Chem.* **1958**, *70*, 211-213.

APPENDIX - SKETCH OF GOLDFISH BOWL/ POLYMERISATION REACTOR

GOLDFISH BOWL (1L)

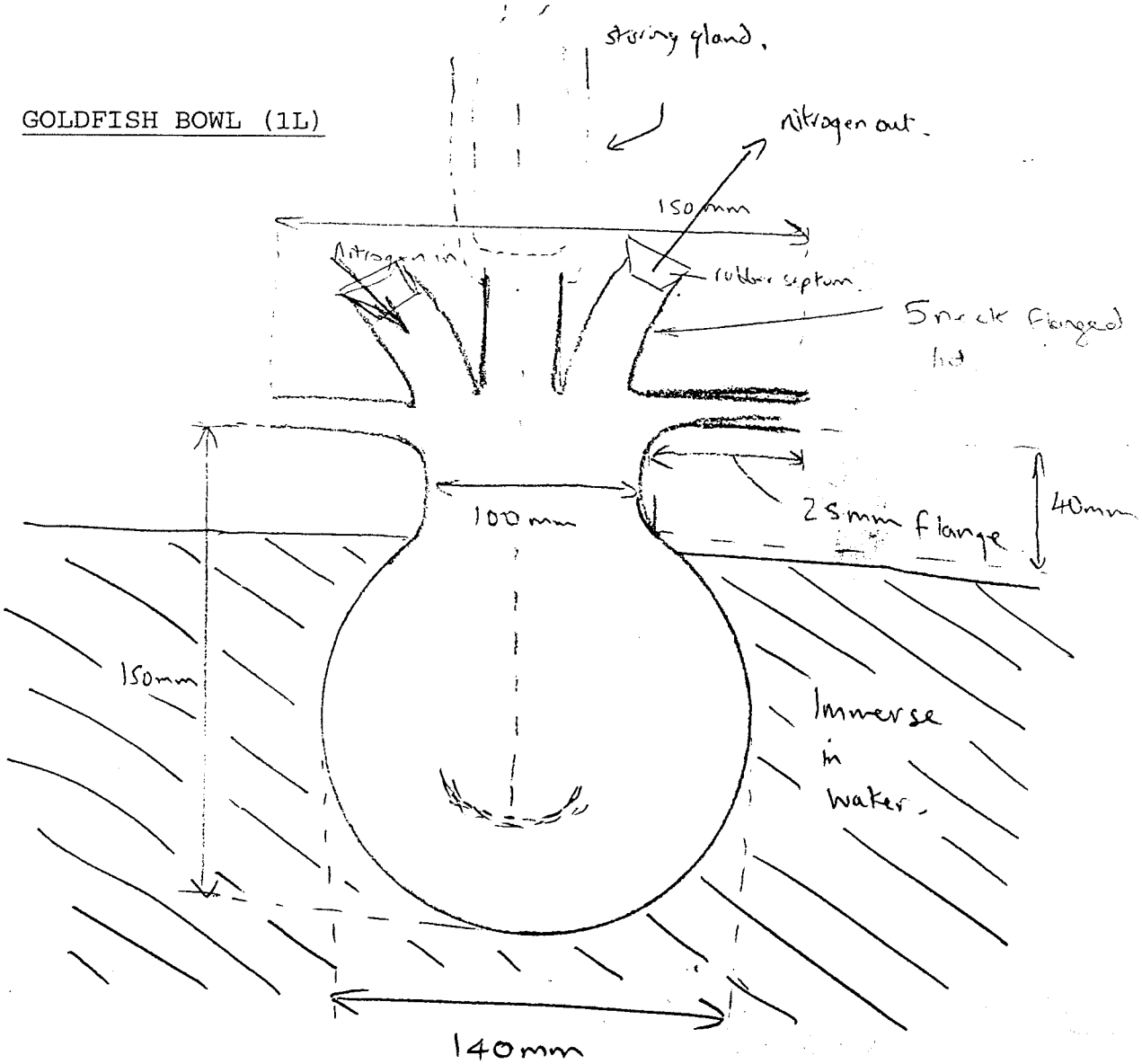

Composition: Heat-resistant glass.

NB: Not to scale.

APPENDIX - SKETCH OF GOLDFISH BOWL/ POLYMERISATION REACTOR

'HALF-MOON SHAPED STIRRER'

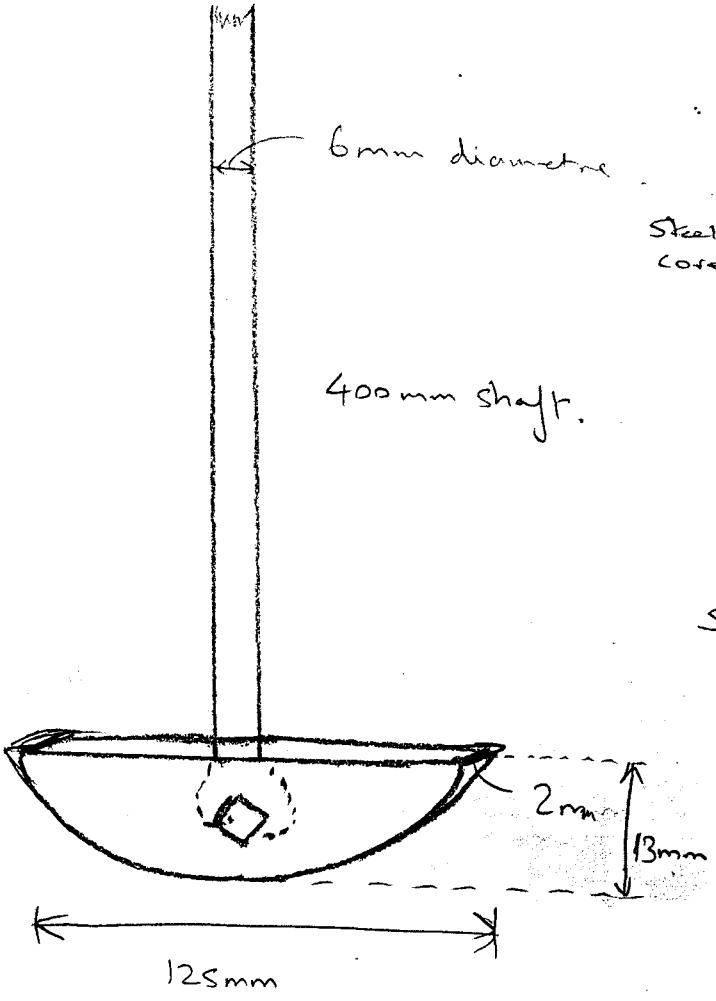

'ANCHOR STIRRER'

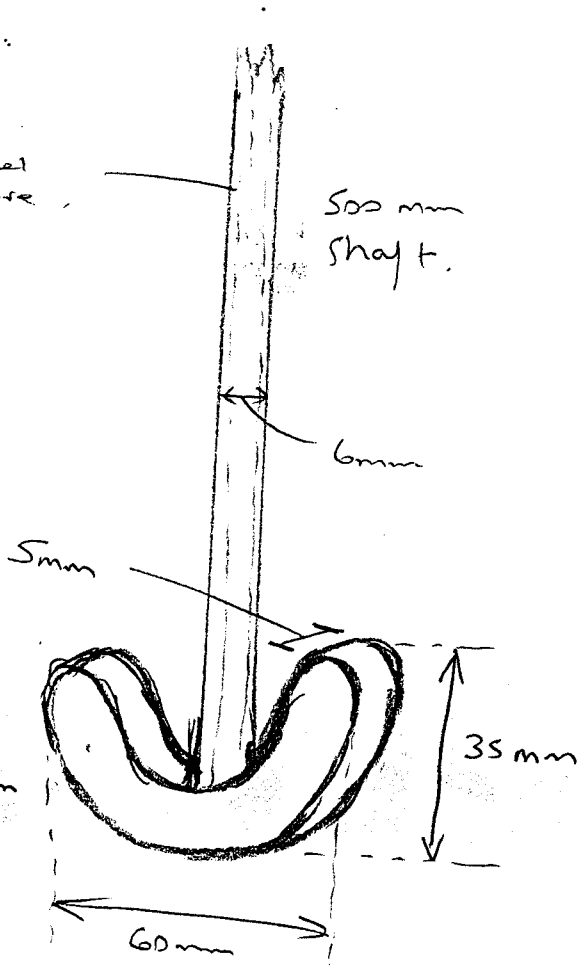

Composition: Teflon coated steel.

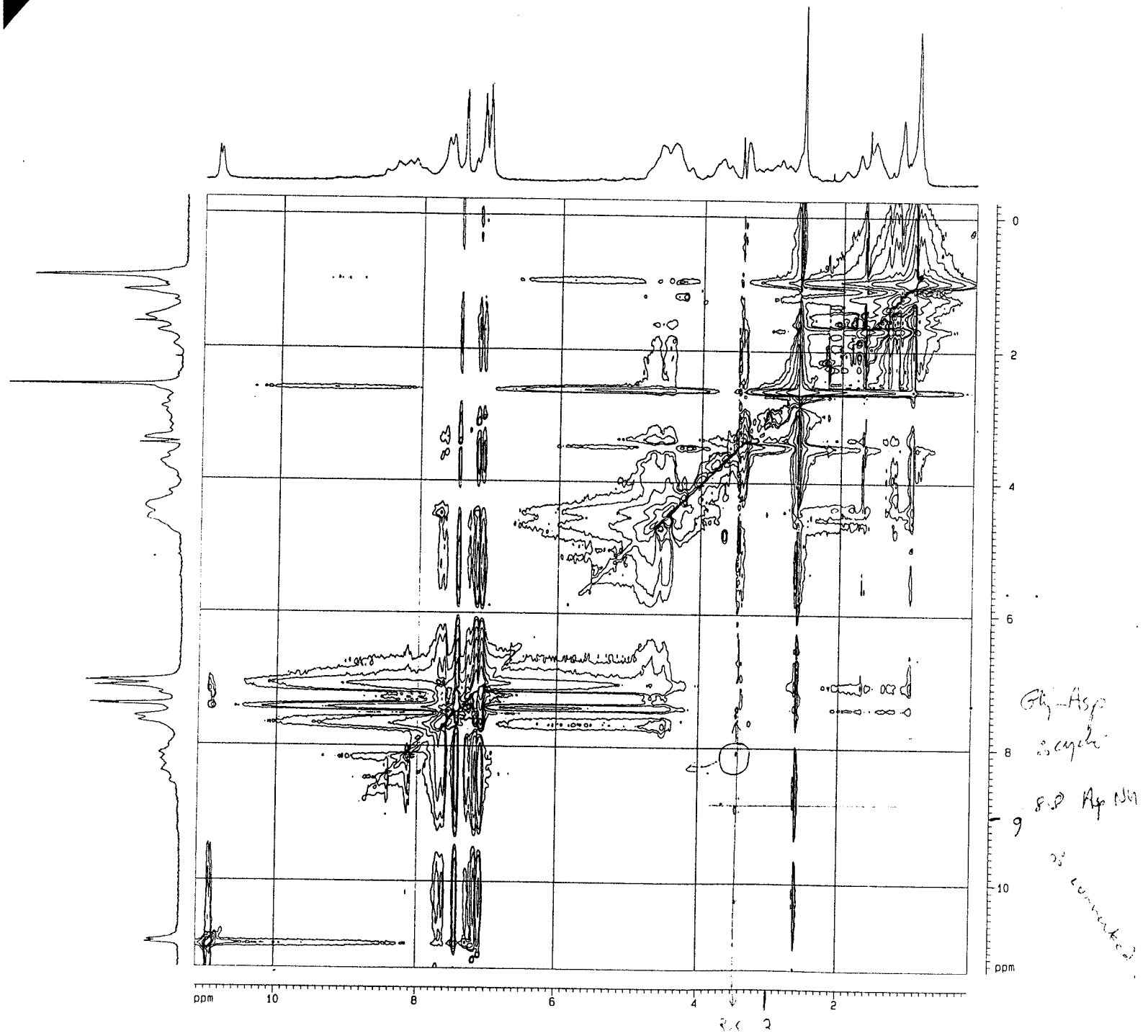

H2O Supp ROESY

MC2 - TPPI

INV4

Current Data Parameters

NAME	oc06jmssr1
EXPNO	5
PROCNO	1

F2 - Acquisition Parameters

Date_	991007
Time	16.50
INSTRUM	spect
PROBHD	5 mm Dual 13
PULPROG	roesyprtp
TD	2048
SOLVENT	DMSO
NS	100
DS	4
SWH	6410.256 Hz
FIDRES	3.130008 Hz
AQ	0.1597940 sec
RG	800
DW	78.000 usec
DE	6.00 usec
TE	300.0 K
d0	0.00000300 sec
d11	0.03000000 sec
d12	0.00002000 sec
d13	0.00000300 sec
PL9	60.00 dB
D1	1.50000000 sec
SFO1	400.1313893 MHz
NUC1	1H
PL1	0.00 dB
P1	10.30 usec
PL11	21.00 dB
P15	300000.00 usec
INO	0.00007800 sec

F1 - Acquisition parameters

ND0	2
TD	256
SFO1	400.1314 MHz
FIDRES	25.040064 Hz
SW	16.020 ppm

F2 - Processing parameters

SI	1024
SF	400.1300000 MHz
WDW	QSINE
SSB	2
LB	0.00 Hz
GB	0
PC	1.00

F1 - Processing parameters

SI	1024
MC2	TPPI
SF	400.1300000 MHz
WDW	QSINE
SSB	2
LB	0.00 Hz
GB	0

2D NMR plot parameters

CX2	20.00 cm
CX1	20.00 cm
F2PLO	11.122 ppm
F2LO	4450.40 Hz
F2PHI	0.124 ppm
F2HI	49.61 Hz
F1PLO	11.294 ppm
F1LO	4519.26 Hz
F1PHI	-0.236 ppm
F1HI	-94.37 Hz
F2PPMCM	0.54992 ppm/cm
F2HZCM	220.03957 Hz/cm
F1PPMCM	0.57652 ppm/cm
F1HZCM	230.68159 Hz/cm

The following published papers were included in the bound thesis. These have not been digitised due to copyright restrictions, but their doi are provided.

Rana, S., White, P. & Bradley, M., 1999. Synthesis of magnetic beads for solid phase synthesis and reaction scavenging. Tetrahedron Letters, 40(46), pp.8137–8140. Available at: http://dx.doi.org/10.1016/s0040-4039(99)01572-5.

Rana, S. et al., 2000. The synthesis of the cyclic antibacterial peptide Kawaguchipeptin B on 11 different DVB cross-linked PS resins. Tetrahedron Letters, 41(26), pp.5135–5139. Available at: http://dx.doi.org/10.1016/s0040-4039(00)00754-1

Rana, S., White, P. & Bradley, M., 2001. Influence of Resin Cross-Linking on Solid-Phase Chemistry. Journal of Combinatorial Chemistry, 3(1), pp.9–15. Available at: http://dx.doi.org/10.1021/cc0000592